Chemical studies on Meliaceous plants (*Dysoxylum cumingianum*, *Azadirachta indica*) and a Lamiaceous plant (*Scutellaria coleifolia*)

2014

Shin-ichiro Kurimoto

Abbreviations

NMR: nuclear magnetic resonance

^{1}H NMR: proton nuclear magnetic resonance

^{13}C NMR: carbon-13 nuclear magnetic resonance

DEPT: distortionless enhancement by polarization transfer

COSY: correlation spectroscopy

HSQC: heteronuclear single-quantum coherrence spectrum

HMBC: heteronuclear multiple bond coherrence spectrum

NOEDS: nuclear Overhauser enhancement difference spectrum

NOESY: nuclear Overhauser enhancement and exchange spectroscopy

ROESY: Rotating-frame Overhauser enhancement and exchange spectroscopy

MS: mass spectrometry

HRESIMS: high-resolution electro-spray ionization mass spectrometry

UV: ultraviolet spectroscopy

CD: circular dichroism

IR: Infrared spectroscopy

TLC: thin-layer chromatography

HPLC: high-performance liquid chromatography

UPLC: ultra-performance liquid chromatography

GC: gas chromatography

DMAP: 4-dimethylamino pyridine

EDC: 1-(3-dimethylaminopropyl)-3-ethylcarbodiimide

DMSO: dimethyl sulfoxide

General Introduction

Natural resources produce a large number of secondary metabolites, possessing diverse structures and various biological activities. Therefore, natural products have been playing an important role in developments of new therapeutic agents as a source of lead compounds. Although new techniques such as combinatorial chemistry and computer drug design have been developed, more than 60% of small-molecule drugs approved by the US Food and Drug Administration (FDA) from 1981 to 2010 contain structures derived from natural products [1], strongly indicating the importance of natural products in drug discovery.

Nowadays, many research groups have been exploring natural resources for finding new drug seeds, so that a variety of novel bioactive compounds have been isolated and characterized. We owe it to the progress of spectroscopic techniques (NMR, MS, UV, IR, CD, etc.), separation techniques (HPLC, UPLC, GC, etc.) and invention of new bioassay methods. However, plenty of unexplored natural resources have still remained.

On the other hand, preclinical strategies that are used to identify potential drug candidates include target-based screening, phenotypic screening, modification of natural substances and biologic-based approaches. Regarding two different approaches of target-based screening and phenotypic screening, Swinney *et al*. analyzed the discovery strategies and the molecular mechanism of action (MMOA) for new molecular entities and new biologics that were approved by FDA between 1999 and 2008, and reported that the contribution of phenotypic screening to the discovery of first-in-class small-molecule drugs exceeded that of target-based approaches [2]. Considering that natural resources produce a wide variety of secondary metabolites, which might show biological activity by unknown mechanisms of action, the phenotypic screening is still useful for searching potential bioactive natural product seeds.

In this study, the chemical studies on two Meliaceous plants (*Dysoxylum cumingianum* C. DC. and *Azadirachta indica* A. Juss) and a Lamiaceous plant (*Scutellaria coleifolia* Levl.) were carried out to discover new drug seeds, and have resulted in the isolation of seventy-four compounds, including forty-five new terpenoids.

From the MeOH extract of the leaves of *D*. *cumingianum*, six new triterpenoids, a new triterpenoid glucoside and three steroids, together with fifteen known compounds were isolated and characterized.

Chemical study on the MeOH extract of the fruits of *A*. *indica* has resulted in the isolation and characterization of four new triterpenoids as well as eight known compounds.

Thirty-one new terpenoids, including two sesterterpenoids, three *nor*-diterpenoids and twenty-six diterpenoids, together with six known compounds, were isolated from the 70% aqueous acetone extract of the aerial parts of *S.coleifolia*.

As a biological activity evaluation, cytotoxicities of thirty-four isolated compounds against several human cancer cell lines, including multi-drug resistant (MDR) cells, were examined.

Chapter 1
Study on the constituents of *Dysoxylum cumingianum* C. DC.

1.1. Introduction

Dysoxylum cumingianum C. DC. (Meliaceae), known as "Lanyu Kung Mu", is an evergreen tree, only found in Taiwan and Philippines [3]. Previous study on the MeOH extract of the leaves of *D. cumingianum* led to the isolation and characterization of a series of 14,18-cycloapotirucallane glucosides, cumingianosides A-O [4, 5], and apotirucallane glucosides, cumingianosides P and Q [6] as well as trisnor- and tetranortriteroenoid glucosides, cumindysosides A and B [4]. Among these compounds, cumingianosides A and C (Fig. 1.1) were selective potent cytotoxic triterpenoids against MOLT-4 human leukemia cells with ED_{50} values of <0.00625 and <0.0045 μM, respectively [4]. In addition, a pentacyclic triterpenoid with an unnatural skeleton was obtained by the treatment of cumingianoside E with *p*-toluenesulfonic acid in CH_2Cl_2 [7]. This was selected as a candidate compound of *in vivo* testing by National Cancer Institute because of its selective cytotoxic profile especially against colon cancer cell lines.

The continuation of this study aimed at searching novel antitumor agents resulted in the isolation of six new triterpenoids, a new triterpenoid glucoside, a new stigmastane and two new pregnanes together with fifteen known compounds.

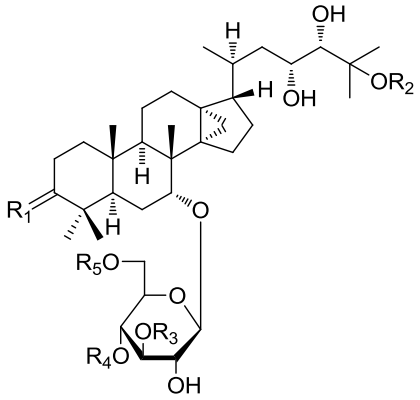

	R_1	R_2	R_3	R_4	R_5
cumingianoside A	α-OAc, β-H	H	H	H	Ac
cumingianoside B	α-OAc, β-H	H	H	H	H
cumingianoside C	α-OAc, β-H	Me	H	H	Ac
cumingianoside G	α-OH, β-H	H	H	H	H
cumingianoside H	α-OH, β-H	H	H	H	Ac
cumingianoside I	α-OAc, β-H	H	Ac	H	H
cumingianoside J	α-OAc, β-H	H	H	Ac	H
cumingianoside L	O	H	H	H	H
cumingianoside M	O	H	H	H	Ac

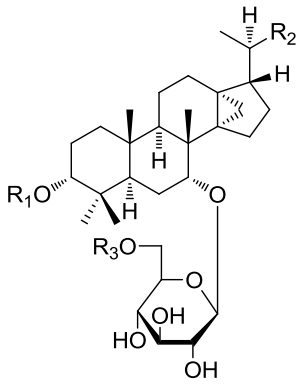

	R_1	R_2	R_3
cumingianoside D	Ac	I	Ac
cumingianoside E	Ac	II	Ac
cumingianoside F	H	II	Ac
cumingianoside K	Ac	III	Ac
cumingianoside N	Ac	I	H
cumingianoside O	Ac	IV	Ac

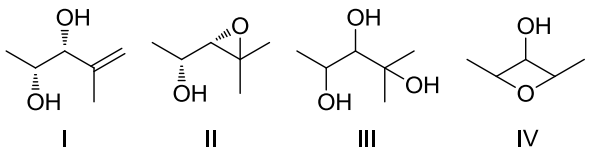

Figure 1.1. Cumingianosides, cumindysosides and their derivatives.

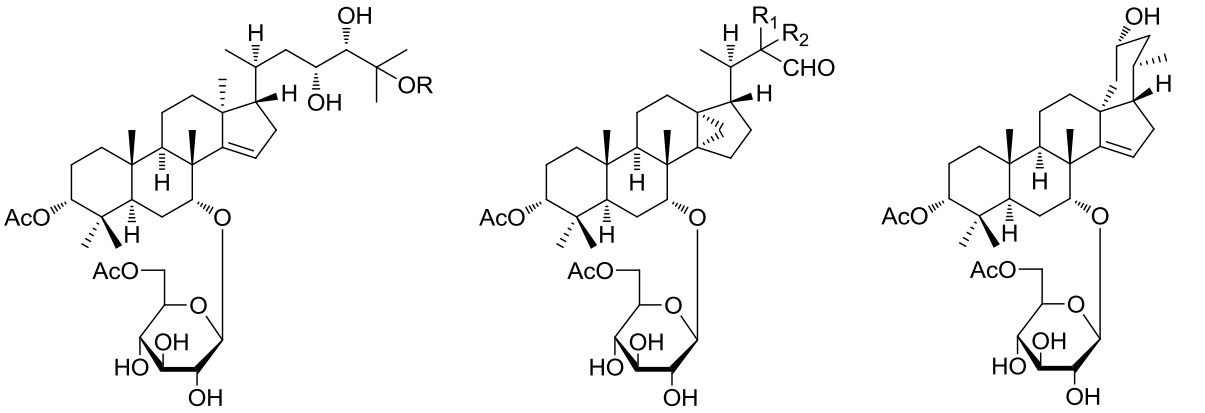

Figure 1.1. continued.

1.2. Extraction and isolation

Air-dried leaves of *D. cumingianum* (8.7 kg) were extracted with MeOH (3×20 L) at room temperature. After concentration, an aliquot (580 g) was partitioned between $CHCl_3$ and H_2O. The $CHCl_3$-soluble fraction was further partitioned with *n*-hexane and MeOH-H_2O (9:1, v/v) to give *n*-hexane-soluble fraction (50 g) and 90% MeOH-soluble fraction (228.5 g). The 90% MeOH-soluble fraction was repeatedly separated as shown in scheme 1 to afford ten new compounds (**1-3**, **7**, **11**, **12**, **15**, **20**, **22**, **24**), together with fifteen known compounds (**4-6**, **8-10**, **13**, **14**, **16-19**, **21**, **23**, **25**).

Scheme 1

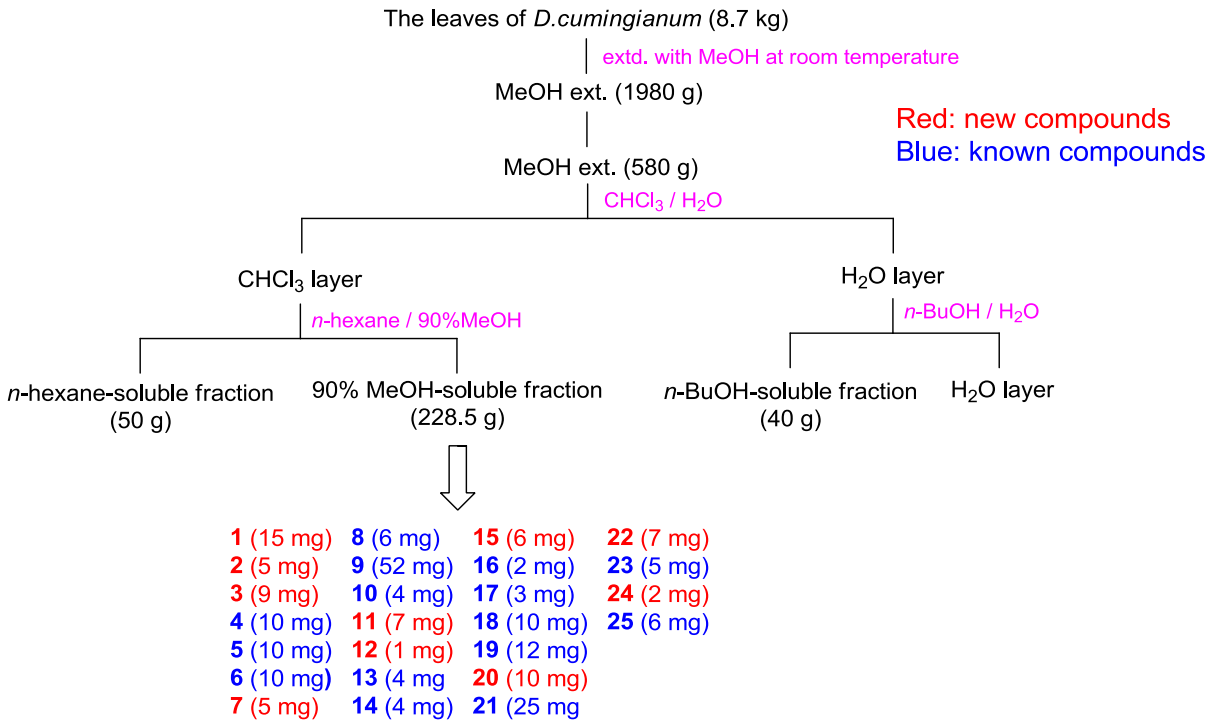

1.3. Identification of known compounds

Compounds **4-6**, **8-10**, **13**, **14**, **16-19**, **21**, **23** and **25** were identified as cumingianoside A (**4**) [4], cumingianoside B (**5**) [4], cumingianoside H (**6**) [5], cumingianoside N (**8**) [5], cumindysoside A (**9**) [4], cumindysoside B (**10**) [4], agladupol A (**13**) [8], 21-*O*-methyltoosendanpentol (**14**) [8], hispidiol A (**16**) [9], hispidiol B (**17**) [9], cabraleadiol (**18**) [10], 3-epi-cabraleahydroxylactone (**19**) [11], (-)-(3*S*,4*R*,22*R*,24*R*)-ethylcholest-5-en-3,4,22-triol (**21**) [12], meliavosin (**23**) [13] and ribenone (**25**) [14], respectively, by comparison of their spectroscopic data with those described in the literature.

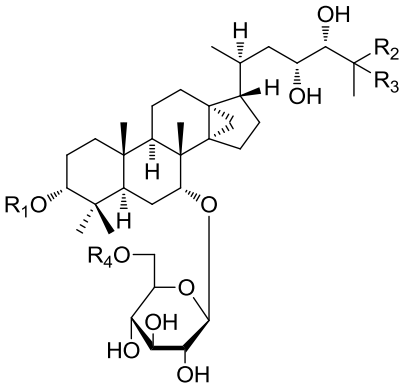

	R_1	R_2	R_3	R_2
4	Ac	Me	OH	Ac
5	Ac	Me	OH	H
6	H	Me	OH	Ac
8	Ac	$-CH_2-$		Ac

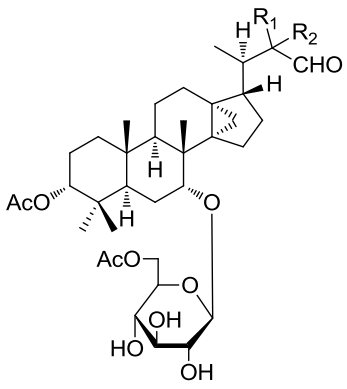

9 $R_1-R_2 = CH_2$
10 $R_1 = R_2 = H$

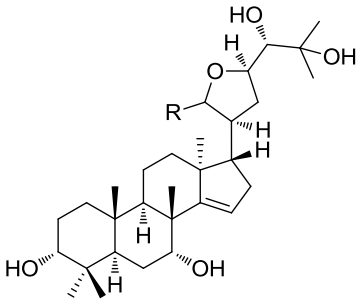

	R
13	β-OMe
14	α-OMe

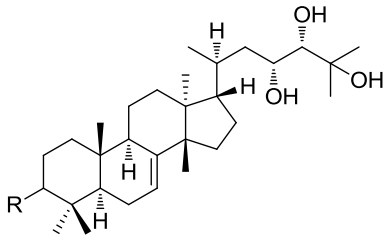

	R
16	α-OH
17	β-OH

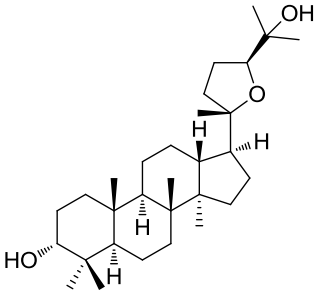

18

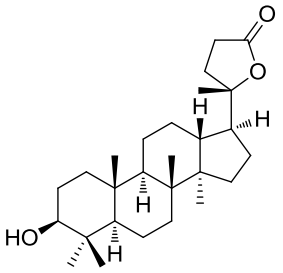

19

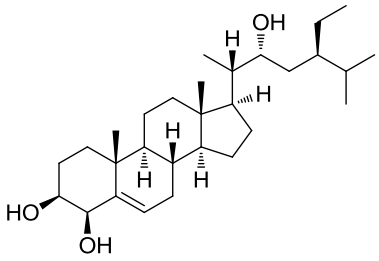

21

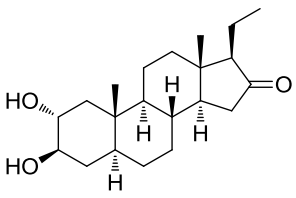

23

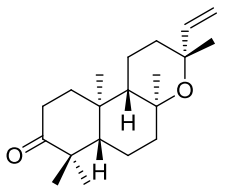

25

Figure 1.2. Known compounds from the 90% MeOH-soluble fraction of *D. cumingianum*.

1.4. Structure elucidation

1.4.1. Compounds **1** and **2**

The molecular formula of **1** was assigned as $C_{32}H_{54}O_6$ by HRESIMS (*m/z* 557.3803 $[M+Na]^+$). The ^1H NMR spectrum showed the presence of six tertiary methyl groups (δ_H 0.85, 0.90, 1.07, 1.12, 1.64 and 1.68), a secondary methyl group [δ_H 1.13 (d, J = 6.4 Hz)], four oxygenated methine groups [δ_H 3.62 (br s), 3.67 (s), 4.57 (br t, J = 6.8 Hz) and 5.20 (br s)] and an acetyl group (δ_H 2.02) together with a cyclopropyl methylene signals [δ_H 0.48 and 0.70 (each 1H, d, J = 5.2 Hz)] characteristic of 14,18-cycloapotirucallane-type triterpenoids. The ^{13}C NMR spectrum with a DEPT experiment revealed the existence of 32 carbons including five sp^3 quaternary carbons (δ_C 27.3, 34.8, 37.0, 37.1 and 38.0), an oxygen-bearing sp^3 quaternary carbon (δ_C 73.4) and an acetyl carbonyl group (δ_C 21.1 and 170.1). These data were similar to those of cumingianoside A [4] except for the absence of signals due to the 6-*O*-acetyl glucosyl moiety, indicating that **1** was a 14,18-cycloapotirucallane-type triterpenoid. The locations of the hydroxyl groups were determined to be at C-3, C-7, C-23, C-24 and C-25 from the ^1H-^1H COSY correlations of H_2-1–H_2-2–H-3, H-5–H_2-6–H-7, and H-20–(Me-21)–H_2-22–H-23–H-24, coupled with the HMBC correlations of Me-28 and Me-29 with C-3 (δ_C 74.6), Me-30 with C-7 (δ_C 76.3) and of Me-26 and Me-27 with C-24 (δ_C 76.5) and C-25 (δ_C 73.4). The acetyl group was concluded to be attached at the C-7 hydroxyl group from the down-field shift of the H-7 [δ_H 5.20 (br s)] signal as well as the HMBC correlation of H-7 with the acetyl carbonyl carbon (δ_C 170.1). The small coupling constant values of H-3 and H-7 [δ_H 3.62 (br s) and 5.20 (br s), respectively] indicated both hydroxyl groups to be α-oriented, which were further supported by the NOE correlations of H-3 with Me-28 and Me-29 and of H-7 with Me-30. The α configuration of H_2-18 was assigned by the NOE correlations of H-5 with H-9 and H-9 with H-18. The β configuration of H-17 and the *S** configuration of C-20 were elucidated from the NOESY correlation of H-17 with Me-21 and the NOE enhancement of H-20 on irradiation of H-18 (δ_H 0.48) in the NOE difference spectrum (Fig. 1.4). The *threo* relationship between H-23 and H-24 was deduced from their *J*-value ($J_{23,24}$ = 0 Hz) [9, 15-17], being similar to that of cumingianoside A whose absolute configuration was determined as 23*R*, 24*S* by X-ray crystallographic analysis of its derivative [18]. Thus, the structure of **1** was elucidated as shown in Figure 1.5.

Compound **2** possessed the same molecular formula ($C_{32}H_{54}O_6$) as **1**. The ^1H and ^{13}C NMR spectral data were quite similar to those of **1** showing the presence of the same 14,18-cycloapotirucallane-structure. However, the signal assignable to H-3 was appeared at lower field [δ_H 4.86 (1H, br s)], whereas H-7 signal was shifted to higher field [δ_H 3.87 (1H,

br s)] in the ^{1}H NMR spectrum as compared with those of **1**. The ^{1}H-^{1}H COSY and HMBC correlations (Fig. 1.3) were quite similar to those of **1** except for the HMBC correlation of H-3 [δ_H 4.86 (1H, br s)] with the acetyl carbonyl carbon (δ_C 170.5), indicating that the acetyl group was connected to C-3. The relative configuration of **2** was concluded to be the same as that of **1** from the coupling constant values and the NOESY examinations (Fig. 1.4). On the basis of these observations, the structure of **2** was assigned as shown (Fig. 1.5).

1.4.2. Compound **3**

Compound **3** gave a pseudo-molecular ion peak at *m/z* 691.4398 (calcd for 691.4397 $[M+Na]^{+}$) in the positive-ion HRESIMS, indicating the molecular formula $C_{37}H_{64}O_{10}$. The glycosidic nature of **3** was indicated by anomeric resonances [δ_H 4.85 (1H, d, J = 7.6 Hz); δ_C 100.1]. The ^{1}H and ^{13}C NMR spectra were very similar to those of cumingianoside C [4] except for the absence of two acetyl signals, indicating that **3** was a deacetyl cumingianoside C. Acetylation of **3** with acetic anhydride and pyridine gave a heptaacetate, whose 1D NMR spectral data was found to be identical with those of cumingianoside C peracetate [4]. From these findings, the structure of **3** was characterized as shown in Figure 1.5.

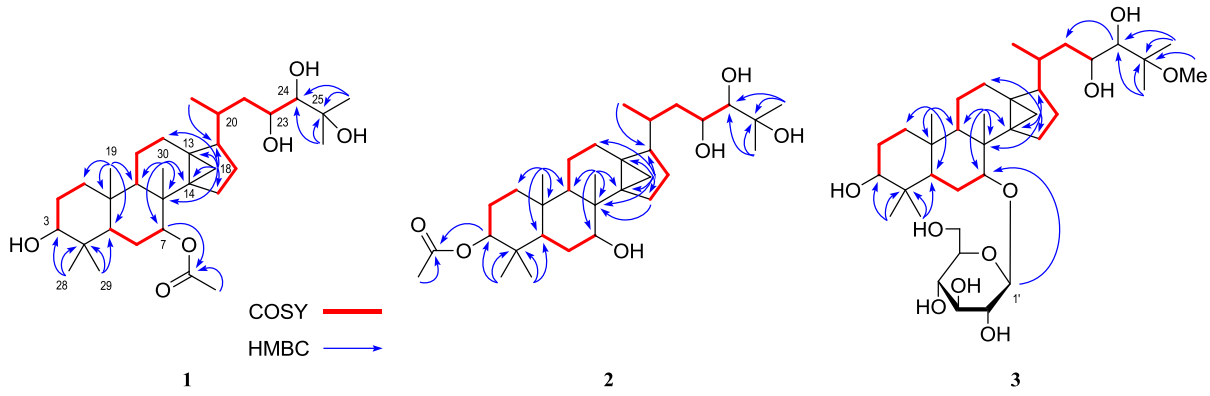

Figure 1.3. Key COSY and HMBC correlations of **1**-**3**.

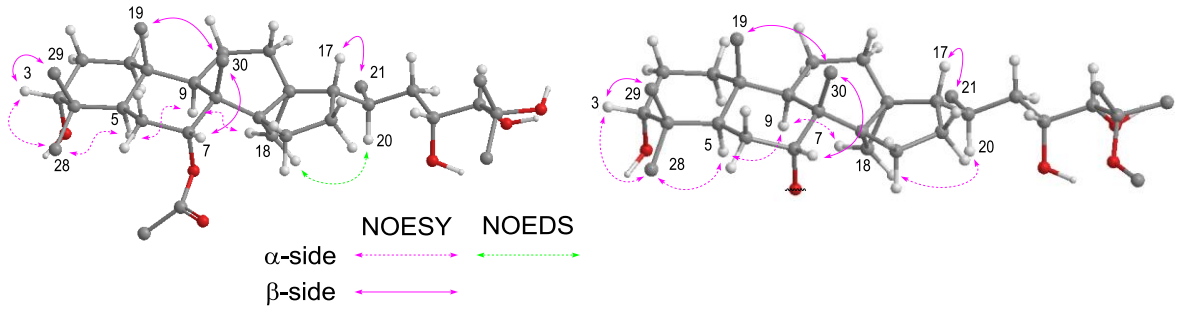

Figure 1.4. Key NOE correlations of **1** and **3**.

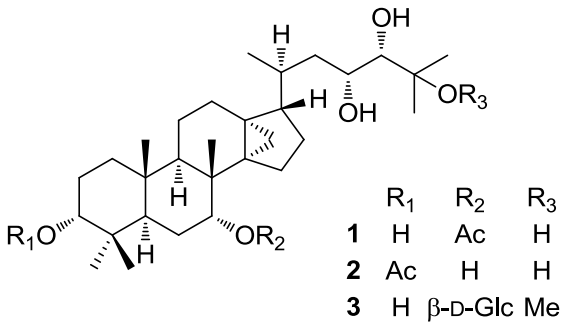

Figure 1.5. The structures of **1-3**.

1.4.3. Compound **7**

Compound **7** gave a pseudo-molecular ion peak at *m/z* 539.3704 (calcd for 539.3712 $[M+Na]^+$) in the positive-ion HRESIMS, indicating the molecular formula $C_{32}H_{52}O_5$, which was 18 mass units less than that of **1**. The ^1H and ^{13}C NMR spectra were closely correlated with those of **1**, but differed in the observation of signals of an exo-olefin [δ_H 5.07, 5.32 (each 1H, br s); δ_C 112.1, 147.2] and the disappearance of an oxygen-bearing sp^3 quaternary carbon seen in **1**. The presence of the exo-olefin group at C-25 was shown by the HMBC cross peaks of the exo-olefin signals with C-24 and C-27, together with the ^1H-^1H COSY correlations of H-20–(Me-21)–H_2-22–H-23–H-24. The location of the acetyl group was assigned to be at C-7 by the HMBC correlation of H-7 with the acetyl carbonyl carbon (δ_C 170.0). The α configurations of the hydroxyl groups at C-3 and C-7 were determined by the small coupling constant values of H-3 and H-7 and the NOE correlations of H-3/Me-28 and Me-29 and of H-7/Me-30 (Fig. 1.6). The configurations of the cyclopropyl methylene group and C-17 side chain were shown to be the same as those of **1-3** by spectral analyses. From these evidences, the structure of **7** was characterized as shown (Figure 1.7).

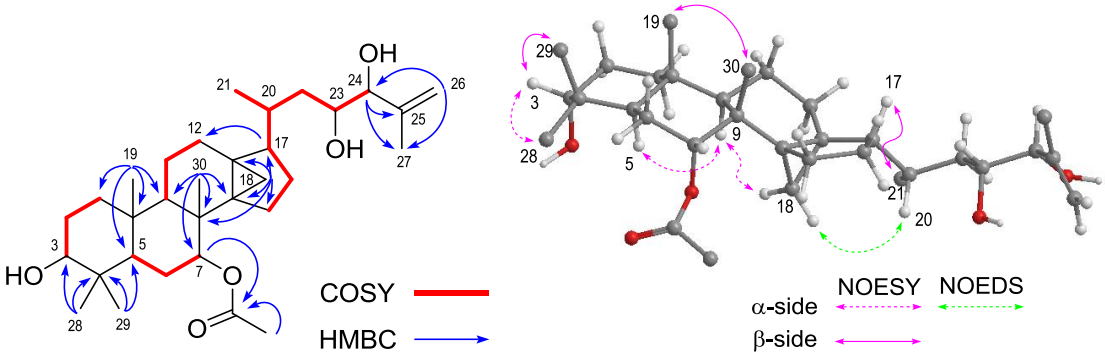

Figure 1.6. Key 2D correlations of **7**.

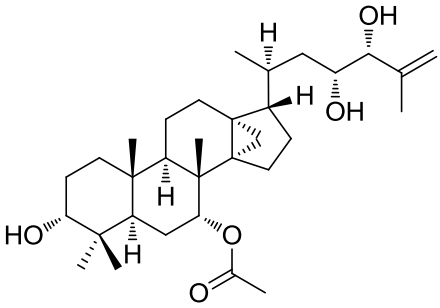

Figure 1.7. The structure of **7**.

1.4.4. Compound **11**

Compound **11** had the same molecular formula ($C_{32}H_{54}O_6$) as **1** on the basis of HRESIMS. The ^{1}H NMR spectrum of **11** was correlated with that of **1**. However, the cyclopropyl methylene signals characteristic of 14,18-cycloapotirucallne-type triterpenoids were absent, but instead signals due to a tri-substituted olefin [δ_H 5.29 (s)] and an additional tertiary methyl group (δ_H 1.07) were observed. The ^{13}C NMR spectrum with a DEPT experiment exhibited the existence of 32 carbons including eight methyls, seven sp^3 methylenes, four sp^3 methines, four oxygen-bearing sp^3 methines, a trisubstituted olefin [δ_C 118.0 (d) and 160.4 (s)], four sp^3 quaternary carbons, an oxygen-bearing sp^3 quaternary carbon and an acetyl group. From these spectral data, **11** was presumed to be an apotirucallane-type triterpenoid. The ^{1}H-^{1}H COSY correlations of H_2-1–H_2-2–H-3, H-5–H_2-6–H-7, H-9–H_2-11–H_2-12, H-15 [δ_H 5.29 (s)]–H_2-16–H-17–H-20–(Me-21)–H_2-22–H-23–H-24, coupled with the HMBC correlations of Me-28 and Me-29 with C-3, Me-18 [δ_H 1.07 (s)] with C-12, C-13, C-14 (δ_C 160.4) and C-17, Me-26 and Me-27 with C-24 and C-25 and of Me-30 with C-7 and C-14, provided a 3,7,23,24,25-pentahydroxy-apotirucallane. The acetyl group was concluded to be connected at C-7 from the HMBC cross peak of H-7 with the acetyl carbonyl resonance (δ_C 169.2). The configurations of the hydroxyl groups at C-3 and C-7 and the relationship between H-23 and H-24 were determined from the *J*-values of their ^{1}H

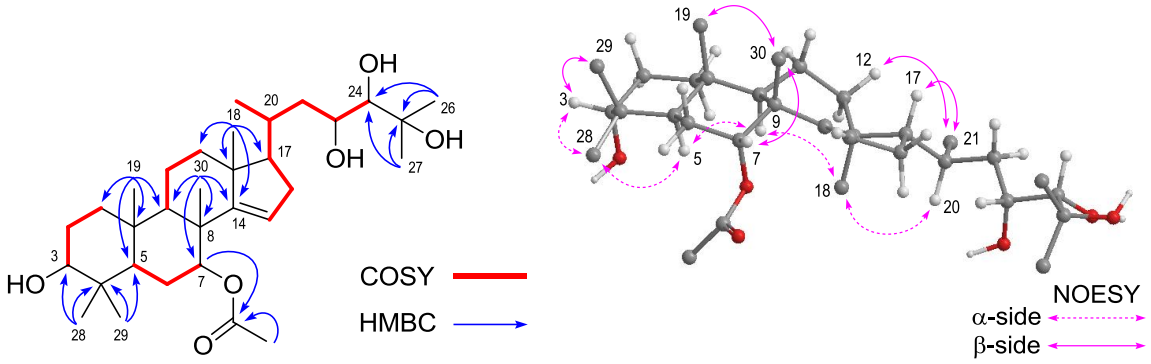

Figure 1.8. Key 2D NMR correlations of **11**.

NMR signals and NOESY correlations, which were the same as those seen in **1**. Furthermore, the configurations of H-17, Me-18, and C-20 were determined as β, α and *S**, respectively, from the NOE correlations of Me-18/H-9, Me-18/H-20 and of Me-21/H-12β and H-17 (Fig.1.8). Based on these findings, the structure of **11** was elucidated as shown in Figure 1.9.

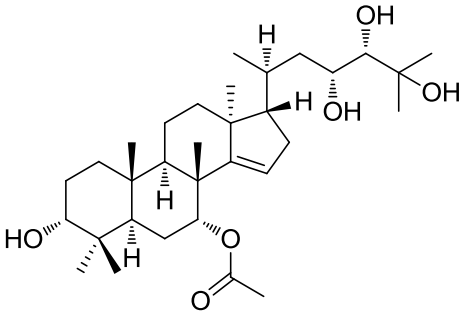

Figure 1.9. The structure of **11**.

1.4.5. Compound **12**

Compound **12** also possessed the molecular formula of $C_{32}H_{54}O_6$ on the basis of HRESIMS. The ^{1}H NMR spectrum showed the presence of seven tertiary methyl groups (δ_H 0.93, 0.97, 1.12, 1.16, 1.23, 1.40 and 1.48), two methoxyl groups (δ_H 3.27 and 3.43), five oxygenated methine groups [δ_H 3.64 (br s), 3.71 (d, J = 2.5 Hz), 4.12 (br s), 4.51 (dq, J = 2.5, 10.5 Hz) and 4.92 (d, J = 4.0 Hz)] and a trisubstituted olefin group [δ_H 5.45 (br d, J = 1.9 Hz)]. The ^{13}C NMR spectrum displayed 32 carbon signals including four sp^3 quaternary carbons (δ_C 37.5, 38.0, 44.4 and 47.0), an oxygen-bearing sp^3 quaternary carbon (δ_C 76.4), two olefinic carbons (δ_C 118.7 and 162.2), and an acetal carbon (δ_C 109.5). These spectral data suggested that **12** was also an apotirucallane-type triterpenoid, but the structure of the substituent at C-17 was different from that of **11**. By contrast, the acetal carbon was assigned to C-21 from the ^{1}H-^{1}H-COSY correlations of H-20–(H-21)–H$_2$-22–H-23–H-24, coupled with the fact that H-21 resonated with the acetal carbon signal in the HSQC spectrum. Furthermore, the HMBC cross peaks of H-21 with C-23 and a methoxyl signal (δ_H 3.43) with C-21 indicated the presence of a tetrahydrofuran structure with the methoxyl group at C-21. The HMBC correlations of Me-26 and Me-27 with C-24 and C-25, as well as the methoxyl signal at δ_H 3.27 with C-25 indicated that the methoxyl group was attached at C-25 (Fig. 1.10). The configurations of the hydroxyl groups at C-3 and C-7 were determined as α in each case, from the small coupling constant values of H-3 and H-7 and the NOESY correlations of H-3 with Me-28 and Me-29, and of H-7 with Me-30, while the α configuration of Me-18 was assigned from the NOESY correlation of Me-18 with H-9. The configurations of H-20, H-21, and H-23 were assigned as α, β, and α, respectively,

from the NOE correlations of H-20 with Me-18, H-22α and H-23 and of H-21 with H-17 and H-22β. The small coupling constant value of H-24 ($J_{23,24}$ = 2.5 Hz) and the NOE correlations of H-24 with H_2-22 and H-23, Me-26 with H-24 and of Me-27 with H-23 and H-24 indicated the configuration of H-24 to be β (Fig. 1.10). On the basis of these examinations, the structure of **12** was assigned as shown (Fig. 1.11).

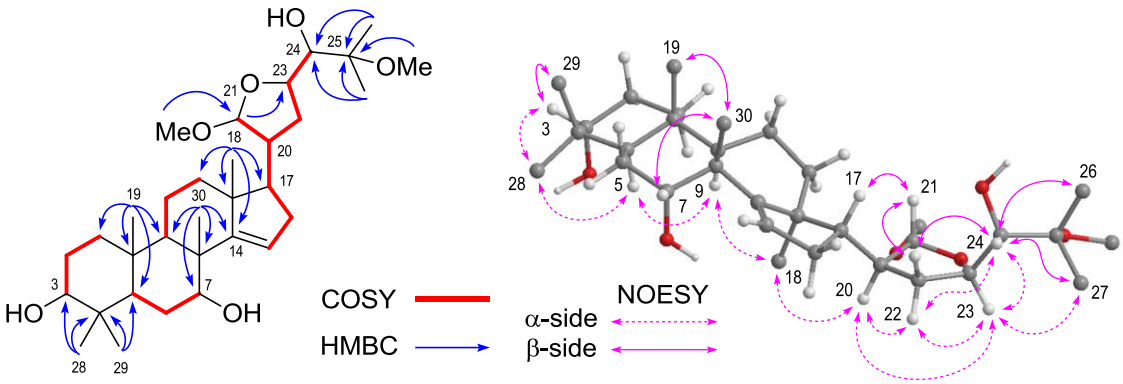

Figure 1.10. Key 2D NMR correlations of **12**.

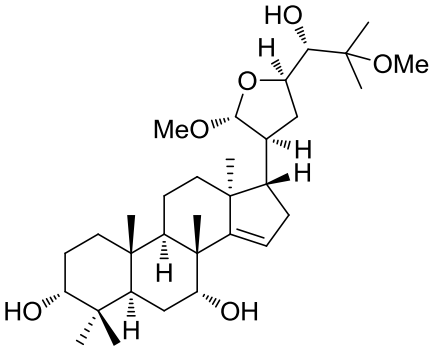

Figure 1.11. The structure of **12**.

1.4.6. Compound **15**

The molecular formula of **15** was established as $C_{32}H_{54}O_6$ by the HRESIMS. The ^{1}H NMR spectrum revealed the presence of seven tertiary methyl groups (δ_H 0.77, 0.80, 0.91, 1.11, 1.16, 1.63 and 1.65), a secondary methyl group [δ_H 1.16 (d, J = 6.4 Hz)], an acetyl group (δ_H 2.14), four oxygenated methines [δ_H 3.64 (br s), 3.69 (s), 4.59 (dd, J = 5.9, 7.3 Hz) and 5.37 (m)] and an olefinic group [δ_H 5.43 (t, J = 2.5 Hz)]. The ^{13}C NMR spectrum showed 32 carbon signals due to four sp^3 quaternary carbons, an oxygen-bearing sp^3 quaternary carbon, a trisubstituted olefin, four sp^3 methines, four oxygen-bearing sp^3 methines, seven sp^3 methylenes, eight methyls and an acetyl group. These spectral data suggested that **15** was a triterpenoid structurally related to **1-3**, **7** and **11**. The presence of a

tirucal-9(11)-en structure was indicated by the HMBC correlations of Me-18 with C-12, C-13, C-14 and C-17, Me-19 with C-9 and of Me-30 with C-8, C-13, C-14 and C-15, coupled with the ^{1}H-^{1}H COSY correlations of H-11–H_2-12. The ^{1}H-^{1}H COSY correlations of H_2-1–H_2-2–H-3, H-5–H_2-6–H-7–H-8, H-20–Me-21, H_2-22–H-23, coupled with the HMBC correlations of Me-28 and Me-29 with C-3 and C-5, Me-21 with C-17 and C-22, H-24 with C-22 and of Me-26 and Me-27 with C-24 and C-25, indicated the presence of oxygen functions at C-3, C-7, C-23, C-24 and C-25. The location of the acetyl group was elucidated to be at C-7 from the HMBC correlation of H-7 with acetyl carbonyl carbon (δ_C 170.2). The configurations of the hydroxyl groups at C-3 and C-7 and of the C-17 side chain were shown to be the same as the other compounds by NMR spectral analyses (Fig. 1.12). From these observations, the structure of **15** was determined as shown (Fig. 1.13).

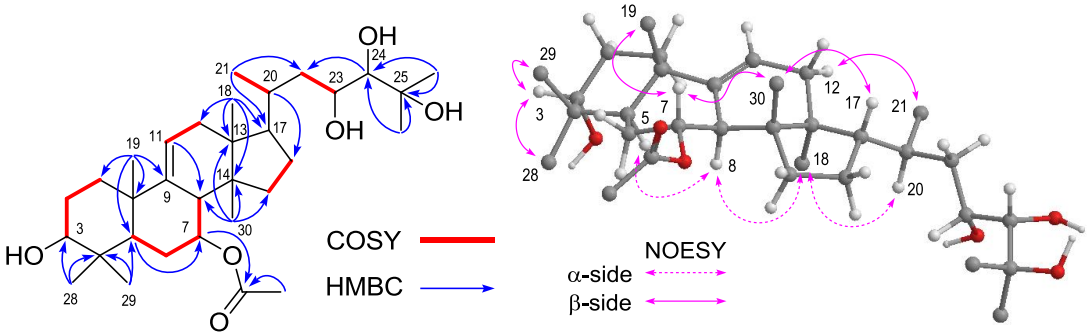

Figure 1.12. Key 2D NMR correlations of **15**.

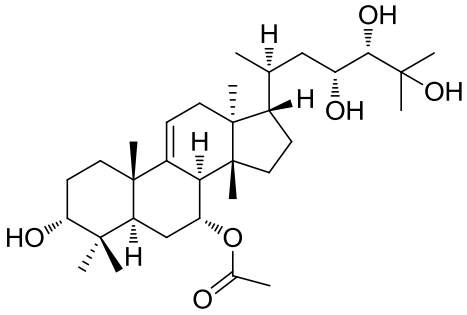

Figure 1.13. The structure of **15**.

Table 1.1. ^{1}H NMR data for **1-3**, **7**, **11**, **12** and **15** in pyridine-d_5+D_2O.

Position	**1**	**2**	**3**	**7**	**11**	**12**	**15**
3	3.62 (br s)	4.86 (br s)	3.63 (br s)	3.61 (br s)	3.63 (br s)	3.64 (br s)	3.64 (br s)
5	2.28 (d, 10.0)	2.33 (d, 12.5)	2.53 (d, 12.4)	2.29 (d, 12.5)	2.29 (m)	2.68 (dd, 2.1, 12.9)	2.44 (m)
7	5.20 (br s)	3.87 (br s)	4.12 (br s)	5.21 (br s)	5.36 (br s)	4.12 (br s)	5.37 (m)
11	1.25 (m)	1.25 (m)	1.21 (m)	1.28 (m)	1.69 (m)	1.70 (m)	5.43 (t, 2.5)
					1.46 (m)	1.48 (m)	
15	1.75 (m)	1.78 (m)	2.13 (m)	1.78 (m)	5.29 (s)	5.45 (br d, 1.9)	1.67 (m)
	1.43 (m)	1.48 (m)	1.78 (m)	1.48 (m)			1.43 (br t, 10.4)
18	0.70 (d, 5.2)	0.81 (d, 5.0)	0.82 (d, 5.8)	0.77 (d, 5.3)	1.07 (s)	1.16 (s)	0.77 (s)
	0.48 (d, 5.2)	0.54 (d, 5.0)	0.58 (d, 5.8)	0.53 (d, 5.3)			
19	0.90 (s)	0.85 (s)	1.13 (d, 6.4)	0.91 (s)	0.91 (s)	0.97 (s)	1.11 (s)
21	1.13 (d, 6.4)	1.11 (d, 6.5)	1.42 (s)	1.20 (d, 6.5)	1.16 (d, 6.4)	4.92 (d, 4.0)	1.16 (d, 6.4)
23	4.57 (br t, 6.8)	4.54 (br t, 7.0)	4.37 (br t, 6.8)	4.14 (dt, 5.0, 8.0)	4.60 (br t, 6.8)	4.51 (dq, 2.5, 10.5)	4.59 (dd, 5.9, 7.3)
24	3.67 (s)	3.61 (s)	3.59 (s)	4.31 (d, 5.5)	3.70 (s)	3.71 (d, 2.5)	3.69 (s)
26	1.64 (s)	1.61 (s)	0.93 (s)	5.32 (br s)	1.64 (s)	1.40 (s)	1.63 (s)
				5.07 (br s)			
27	1.68 (s)	1.64 (s)	1.43 (s)	2.00 (s)	1.66 (s)	1.48 (s)	1.65 (s)
28	1.12 (s)	0.95 (s)	1.32 (s)	1.12 (s)	1.12 (s)	1.23 (s)	1.16 (s)
29	0.85 (s)	0.84 (s)	0.90 (s)	0.85 (s)	0.86 (s)	0.93 (s)	0.91 (s)
30	1.07 (s)	1.00 (s)	1.06 (s)	1.08 (s)	1.12 (s)	1.12 (s)	0.80 (s)
Ac	2.02 (s)	1.91 (s)	–	2.01 (s)	2.02 (s)	–	2.14 (s)
21-OMe	–	–	–	–	–	3.27 (s)	–
25-OMe	–	–	3.23 (s)	–	–	3.43 (s)	–
Glucosyl							
1	–	–	4.85 (d, 7.6)	–	–	–	–
2	–	–	3.97 (m)	–	–	–	–
3	–	–	4.24 (t, 9.2)	–	–	–	–
4	–	–	4.12 (t, 9.2)	–	–	–	–
5	–	–	3.96 (m)	–	–	–	–
6	–	–	4.55 (dd, 2.4, 11.2)	–	–	–	–
			4.31 (dd, 5.6, 11.2)				

δ ppm (mult., *J* in Hz), 400 MHz.

Table 1.2. ^{13}C NMR data for **1**-**3**, **7**, **11**, **12** and **15** in pyridine-d_5+D_2O.

Position	**1**[a]	**2**[b]	**3**[a]	**7**[b]	**11**[a]	**12**[b]	**15**[b]
1	33.5	34.0	34.0	33.5	33.0	33.3	34.1
2	26.3	23.0	26.5	25.9	25.8	26.1	26.4
3	74.6	78.0	75.8	74.7	74.6	74.9	74.3
4	37.0	36.4	38.0	37.1	37.0	37.5	37.5
5	41.0	41.4	40.3	41.2	41.9	40.6	38.5
6	23.3	25.2	21.0	23.4	23.3	25.0	28.3
7	76.3	73.7	78.2	76.4	75.8	72.5	69.8
8	34.8	35.1	35.6	38.2	41.4	44.4	45.0
9	45.4	44.4	45.2	45.6	43.5	42.0	147.5
10	37.1	37.4	37.9	37.3	37.3	38.0	37.7
11	16.7	16.7	17.5	16.7	16.6	16.6	119.5
12	27.5	27.4	28.2	27.7	34.8	33.3	37.4
13	27.3	27.0	27.3	27.6	46.7	47.0	44.4
14	38.0	39.2	39.5	35.0	160.4	162.2	46.0
15	25.7	26.1	26.5	26.4	118.0	118.7	35.3
16	24.7	25.2	25.6	25.0	35.3	34.9	28.5
17	52.6	52.8	53.5	52.3	61.6	58.0	51.0
18	15.9	15.4	17.6	16.1	18.8	19.2	14.5
19	15.7	15.6	16.6	15.8	15.3	15.6	24.6
20	32.4	32.7	33.2	33.5	31.5	46.3	33.8
21	19.3	19.5	19.8	20.2	19.6	109.5	19.0
22	38.9	39.4	40.3	37.4	42.2	35.2	41.9
23	69.0	69.3	68.4	72.0	68.9	68.9	69.0
24	76.5	76.9	76.8	78.9	76.4	76.4	76.3
25	73.4	73.5	78.8	147.2	73.4	76.4	73.3
26	26.5	26.9	22.7	112.1	27.3	22.8	26.5
27	27.4	27.6	21.0	18.7	26.6	20.3	27.2
28	28.6	27.7	29.1	28.6	27.4	29.0	27.9
29	21.9	21.9	23.0	22.0	21.9	22.5	21.8
30	19.4	19.9	20.5	19.5	28.6	28.0	16.5
Ac	21.1 170.1	21.0 170.5	–	21.1 170.0	20.8 169.2	–	21.4 170.2
21-OMe	–	–	–	–	–	55.0	–
25-OMe	–	–	49.4	–	–	49.0	–
Glucosyl							
1	–	–	100.1	–	–	–	–
2	–	–	75.5	–	–	–	–
3	–	–	78.5	–	–	–	–
4	–	–	72.5	–	–	–	–
5	–	–	78.1	–	–	–	–
6	–	–	63.5	–	–	–	–

δ ppm. [a] Measured at 100 MHz. [b] Measured at 125 MHz.

1.4.7. Compound **20**

Compound **20** was obtained as a white amorphous powder. The molecular formula of **20** was elucidated as $C_{29}H_{50}O_4$ by HRESIMS. The ^{1}H NMR spectrum showed the presence of two *tert*-methyl groups (δ_H 0.74 and 1.45), two *sec*-methyl groups [δ_H 0.91 (d, J = 6.8 Hz) and 1.02 (d, J = 6.8 Hz)], an ethyl group [δ_H 0.97 (3H, t, J = 7.4 Hz); 1.40 and 1.57 (each 1H, m)], an oxygenated methylene [δ_H 4.15 (d, J = 10.2 Hz) and 4.41 (dd, J = 4.3, 10.2 Hz), three oxygenated methines [δ_H 3.87 (dt, J = 3.7, 11.5 Hz), 4.13 (br d, J = 10.0 Hz) and 4.56 (d, J = 3.7 Hz)], and a trisubstituted olefin [δ_H 5.70 (dd, J = 2.0, 5.0 Hz)]. The ^{13}C NMR spectrum displayed 29 carbon resonances due to two olefinic carbons [δ_C 126.5 (d) and 144.7 (s)], three oxygen-bearing methine carbons (δ_C 72.3, 73.0, and 78.1), an oxygen-bearing methylene carbon (δ_C 63.0), two sp^3 quaternary carbons (δ_C 36.7 and 42.7), seven sp^3 methine carbons (δ_C 29.4, 32.4, 41.8, 49.1, 49.8, 50.8, and 56.8), nine sp^3 methylene carbons (δ_C 21.0, 24.0, 24.5, 26.4, 28.0, 31.8, 32.4, 38.2, and 39.5), and five methyl carbons (δ_C 12.1, 12.3, 18.1, 20.7, and 21.3). The spectroscopic data suggested that **20** is a C_{29} steroidal compound. The locations of the hydroxyl groups were determined to be at C-3, C-4, C-21, and C-22 based on the ^{1}H-^{1}H COSY correlations of H_2-1–H_2-2–H-3–H-4 and of H-17–H-20–(H_2-21)–H-22–H_2-23–H-24–H_2-28–H_3-29, coupled with the HMBC correlations of Me-19 with C-1 and C-5 and of Me-18 with C-17. The presence of a trisubstituted olefin between C-5 and C-6 was elucidated from the HMBC cross peak of H-6 with C-4. Furthermore, the stigmastane-type skeleton was indicated from the ^{1}H-^{1}H COSY correlations of H-6–H_2-7, H-9–H_2-11–H_2-12, and of H_2-15–H_2-16, along with the HMBC correlations of Me-19 with C-9 and C-10, H-6 with C-8, H-15 with C-14, H-17 with C-16, Me-18 with C-12/C-13/C-14, and of Me-26 and 27 with C-24 and C-25. The β orientation of the C-17 side chain was also assigned from the NOESY correlations of H-17 with H-14, H-14 with H-12α, H-12α with H-9, and of H-9 with H-1α. The orientations of the hydroxyl groups at C-3 and C-4 were determined to be β from the NOESY correlations of H-3 with H-1α/H-4, and of H-4 with H-6, as well as the small coupling constant of H-4 ($J_{3,4}$ = 3.7

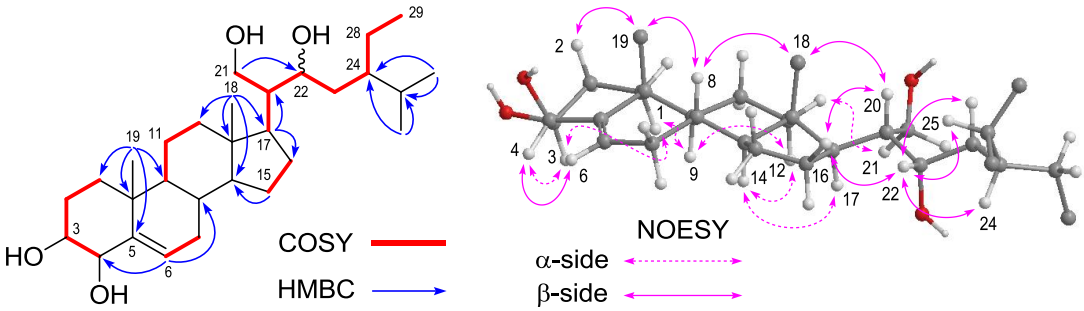

Figure 1.14. Key 2D NMR correlations of **20**.

Hz). The *R** configuration of C-20 was elucidated from the NOESY correlations of H-20 with Me-18 and H-16β and of H_2-21 with H-12β (Fig. 1.14). The configurations of C-22 and C-24 still remain to be determined. On the basis of these findings, the structure of **20** was elucidated as shown in Fig. 1.15.

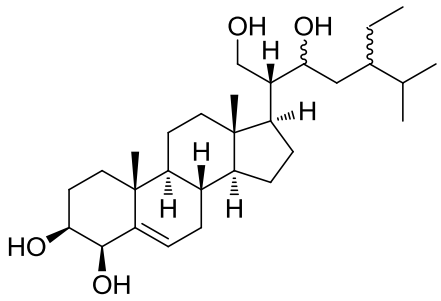

Figure 1.15. The strucuture of **20**.

1.4.8. Compound **22**

A pseudo-molecular ion peak at *m/z* 355.2260 (calcd for 355.2249 $[M+Na]^+$) was observed in the positive-ion HRESIMS of **22**, indicating the molecular formula $C_{21}H_{32}O_3$. The ^1H NMR spectrum revealed the presence of two *tert*-methyl groups (δ_H 0.58 and 1.08), an ethyl group [δ_H 1.04 (3H, t, *J* = 7.5 Hz), 1.24, and 1.70 (each 1H, m)], two oxygenated methines [δ_H 3.85 (ddd, *J* = 5.5, 9.0, 11.0 Hz) and 4.16 (ddd, *J* = 4.2, 9.0, 11.0 Hz)], and a trisubstituted olefin [δ_H 5.41 (d, *J* = 5.3 Hz)]. The ^{13}C NMR spectrum and a DEPT experiment indicated the presence of 21 carbons, including a carbonyl carbon (δ_C 218.2), two sp^3 quaternary carbons (δ_C 38.5 and 41.7), four sp^3 methines (δ_C 30.5, 50.3, 50.5, and 64.8), and seven sp^3 methylenes (δ_C 17.9, 20.8, 32.0, 37.8, 38.4, 40.7, and 46.3). The spectroscopic data suggested that **22** is a pregnane derivative. The assignments of the hydroxyl groups at C-2 and C-3 were based on the ^1H-^1H COSY correlations of H_2-1–H-2–H-3–H_2-4, together with the HMBC correlations of Me-19 with C-1 and C-5. The location of the trisubstituted olefin was concluded to be at C-5(6) from the HMBC cross peak of H-6 with C-4. In addition, the carbonyl group was determined to be at C-16 based on the ^1H-^1H COSY correlations of H-8–H-14–H_2-15, coupled with the HMBC correlations of H_2-15 with C-16, H-17 with C-16, and of Me-18 with C-17. Furthermore, the ^1H-^1H COSY correlations of H-6–H_2-7–H-8–H-9–H_2-11–H_2-12, along with the HMBC correlations of Me-19 with C-9/C-10, Me-18 with C-12/C-13/C-14, and of Me-21 with C-17, suggested that the planar structure of **22** is 2,3-dihydroxy-16-oxo-pregn-5(6)-ene (Fig. 1.16). The orientations of the hydroxyl groups were assigned as 2α and 3β, based on the coupling

patterns of H-2 [δ_H 4.16 (ddd, J = 4.2, 9.0, 11.0 Hz)] and H-3 [δ_H 3.85 (ddd, J = 5.5, 9.0, 11.0 Hz)], as well as the NOESY cross peaks of H-2 with Me-19 and H-3 with H-1α. The β configuration of the ethyl group was determined from the NOESY correlation of Me-18 with H_2-20. From these observations, the structure of **22** was fully determined as shown in Figure 1.17.

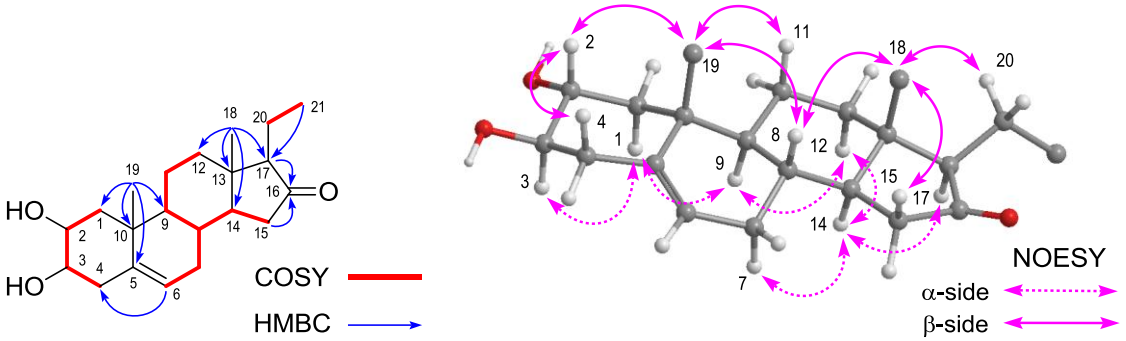

Figure 1.16. Key 2D NMR correlations of **22**.

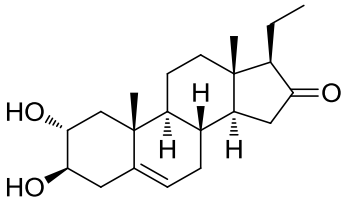

Figure 1.17. The structure of **22**.

1.4.9. Compound **24**

On the basis of HRESIMS, compounds **22** and **24** have the same molecular formula ($C_{21}H_{32}O_3$). The ^{1}H and ^{13}C NMR spectra of **24** were similar to those of **22**, indicating that **24** is also a pregnane-type steroid. However, signals for a vinylic methyl [δ_H 1.70 (d, J = 7.8 Hz); δ_C 13.0] were observed rather than signals for the terminal methyl of the ethyl group in **22**. The ^{1}H-^{1}H COSY and HMBC spectra of **24** were also similar to those found in **22**, except for the ^{1}H-^{1}H COSY correlation of H-20 [δ_H 6.60 (q, J = 7.8 Hz)] with Me-21 [δ_H 1.70 (d, J = 7.8 Hz)], as well as the HMBC correlations of Me-18 (δ_H 0.87) with C-17 (δ_C 148.5) and of H-20 with C-16 (δ_C 205.2) observed for **24**. These data indicated that a trisubstituted olefin was present at C-17(20). The orientations of the hydroxyl groups at C-2 and C-3 in **24** were determined to be α and β, respectively, from the J-values of H-2 and H-3, as well as the analysis of the NOESY spectrum, and were the same as those found in **22**. The α orientation of H-5 was elucidated from the NOESY cross peaks of H-3 with H-5 and of H-5 with H-9 (Fig. 1.18). The geometry of the double bond was assigned by comparison of the proton chemical shifts of H-20 and Me-21 with those of the structurally

related *E*/*Z* isomers of 2β,3β-dihydroxy-5α-pregn-17(20)-(*E*/*Z*)-en-16-one [19], which are the C-2 epimer of **24**. The signals due to H-20 and Me-21 in the *E*-isomer [H-20: δ_H 6.49; Me-21: δ_H 1.84 (in $CDCl_3$)] appeared at lower field as compared with those in the *Z*-isomer [H-20: δ_H 5.69; Me-21: δ_H 2.07 (in $CDCl_3$)]. The ^1H NMR signals due to H-20 and Me-21 in **24** appeared at δ_H 6.50 and 1.85 (in $CDCl_3$), respectively, which were good agreement with those of *E*-isomer [H-20: δ_H 6.49; Me-21: δ_H 1.84 (in $CDCl_3$)] [19], indicating the geometry of C-17(20) double bond to be *E*. From the evidence described above, the structure of **24** was determined as shown in Figure 1.19.

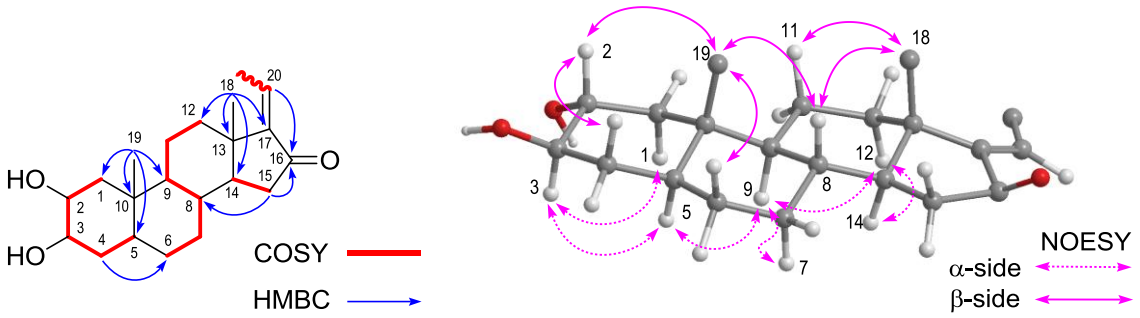

Figure 1.18. Key 2D NMR correlations of **24**.

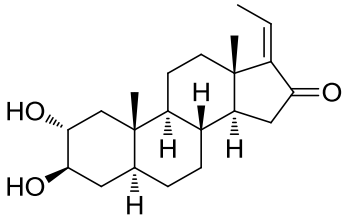

Figure 1.19. The structure of **24**.

Table 1.3. ^{1}H and ^{13}C NMR data for compounds **22** and **24** in pyridine-d_5+D_2O.

	22		**24**	
Position	$^{1}H^{a}$	$^{13}C^{b}$	$^{1}H^{a}$	$^{13}C^{b}$
1	2.39 (dd, 4.2, 12.5)	46.3	2.25 (dd, 4.5, 12.5)	46.1
	1.43 (m)		1.26 (m)	
2	4.16 (ddd, 4.2, 9.0, 11.0)	72.5	4.05 (ddd, 4.5, 9.0, 11.0)	73.0
3	3.85 (ddd, 5.5, 9.0, 11.0)	76.3	3.85 (ddd, 5.0, 9.0, 11.0)	76.6
4	2.72 (m)	40.7	1.86 (dd, 2.0, 5.0, 13.0)	37.1
	2.68 (dd, 5.5, 13.5)		1.68 (m)	
5	–	141.3	1.20 (m)	45.1
6	5.41 (d, 5.3)	120.3	1.25 (m)	28.1
			1.20 (m)	
7	1.83 (ddd, 2.5, 5.3, 17.0)	32.0	1.46 (m)	32.1
	1.57 (m)		0.83 (m)	
8	1.49 (m)	30.5	1.37 (m)	33.6
9	1.16 (m)	50.3	0.75 (m)	54.3
10	–	38.5	–	54.3
11	1.59 (m)	20.8	1.62 (qt, 3.0, 4.0, 13.0)	21.3
	1.43 (m)		1.30 (m)	
12	1.75 (m)	37.8	2.10 (br dt, 3.3, 12.5)	36.3
	1.23 (m)		1.43 (m)	
13	–	41.7	–	43.5
14	1.31 (m)	50.5	1.24 (m)	50.0
15	2.19 (dd, 7.8, 18.3)	38.4	2.19 (dd, 6.8, 17.1)	38.0
	1.74 (m)		1.97 (dd, 14.3, 17.1)	
16	–	218.2	–	205.2
17	1.62 (m)	64.8	–	148.5
18	0.58 (s)	13.2	0.87 (s)	17.6
19	1.08 (s)	20.6	0.86 (s)	13.6
20	1.70 (m)	17.9	6.60 (q, 7.8)	128.1
	1.24 (m)			
21	1.04 (t, 7.5)	13.6	1.70 (d, 7.8)	13.0

[a] δ_H ppm (mult., J in Hz), 500 MHz. [b] δ_C ppm, 125 MHz.

1.5. Cytotoxicity Assay

Compounds **1-3**, **11**, **13-15**, **17**, **20** and **22-24** were evaluated for their cytotoxicity against three human cancer cell lines including KB (human epidermoid carcinoma of the nasopharynx), MCF7 (breast carcinoma) as well as a multi-drug resistant (MDR) cell line KB-C2 (colchicine resistant KB). The cytotoxicity against KB-C2 cells in the presence of 2.5 μM colchicine was also evaluated. Since colchicine had no effect on the growth of KB-C2 cells at this concentration level, enhancement of the cytotoxicity in the presence of colchicine is suggestive of a possibility of MDR revering effect. The IC_{50} values are shown in Table 1.3. Compound **11** showed moderate cytotoxicity against MCF7 cells with an IC_{50} value of 7.1 μg/mL. The other compounds also showed weak cytotoxicity against tested cancer cell line with IC_{50} values ranging from 11.6 to 58.1 μg/mL. Although the cytotoxic activities for the evaluated compounds against the sensitive (KB) and resistant (KB-C2) cell lines were similar, compounds **1**, **2**, **11** and **20** demonstrated significantly enhanced cytotoxicity against KB-C2 cells in the presence of 2.5 μM colchicine with IC_{50} values of 1.20, 1.30, 0.78 and 1.64 μg/mL, respectively. From this result, these compounds might show some MDR-reversing effect.

Table 1.3. Cytotoxicity (IC_{50}[a] in μg/mL) of compounds **1-3**, **11**, **13-15**, **17**, **20** and **22-24** against three human cancer cell lines.

	KB	KB-C2	KB-C2 (+ 2.5 μM col.)	MCF7
1	13.6 ± 0.29	17.0 ± 0.28	**1.20 ± 0.05**	19.4 ± 0.69
2	52.3 ± 0.29	39.5 ± 2.65	**1.30 ± 0.03**	31.5 ± 1.41
3	29.3 ± 0.25	35.6 ± 0.85	36.2 ± 1.9	18.2 ± 0.23
11	12.7 ± 0.97	16.4 ± 0.26	**0.78 ± 0.01**	7.1 ± 0.83
13	21.8 ± 0.50	28.7 ± 0.32	10.1 ± 0.33	25.3 ± 0.75
14	17.4 ± 0.99	30.8 ± 2.55	11.0 ± 0.49	16.2 ± 1.15
15	14.9 ± 1.25	35.6 ± 0.85	> 100	22.1 ± 0.58
17	42.2 ± 2.87	40.3 ± 1.76	7.0 ± 0.41	17.3 ± 1.75
20	11.6 ± 0.47	19.6 ± 0.83	**1.64 ± 0.04**	NT[b]
22	31.4 ± 1.02	33.9 ± 0.93	11.4 ± 1.32	> 100
23	15.4 ± 0.63	30.6 ± 1.42	30.4 ± 2.64	26.1 ± 0.23
24	40.9 ± 0.19	37.9 ± 1.83	18.2 ± 0.56	58.1 ± 3.01
daunorubicin	0.44 ± 0.05	7.87 ± 0.24	11.6 ± 1.4	0.22 ± 0.02

[a] Data are mean ± SE from three or four experiments. [b] NT: not tested. col.: colchicine.

1.6. Conclusion

Chemical study on the 90% MeOH-soluble fraction of the leaves of *D. cumingianum* led to the isolation of ten new compounds, including six triterpenoids, one triterpenoid glucoside, one stigmastane and two pregnanes, together with fifteen known compounds. The structures of the isolated compounds were elucidated by extensive spectroscopic analyses.

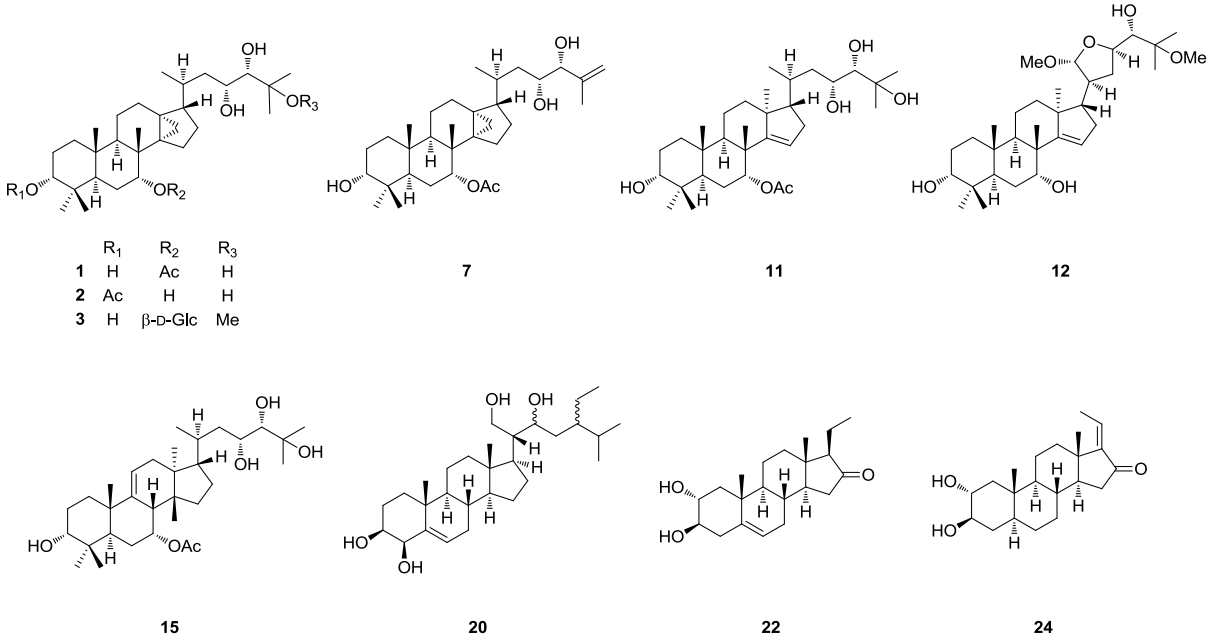

Figure 1.20. New compounds from the 90% MeOH-soluble fraction of *D. cumingianum*.

Cytotoxic activities of twelve compounds (**1-3**, **11**, **13-15**, **17**, **20** and **22-24**) against three human cancer cell lines were evaluated. All the tested compounds, except for **22**, displayed moderate or weak cytotoxicity against three cancer cell lines. Except for compounds **3** and **23**, tested compounds had a tendency to increase cytotoxicity against KB-C2 cells in the presence of 2.5 μM colchicine. Among these compounds, **1**, **2**, **11** and **20** showed significant enhanced cytotoxicity in the presence of colchicine, indicating that they might have some MDR-reversal effect.

Chapter 2
Study on the constituents of *Azadirachta indica* A. Juss

2.1. Introduction

Azadirachta indica A. Juss (Meliaceae), well known as the "Neem tree" or "Indian lilac", is widely distributed in the tropical zones of Africa, South Asia, and India. *A. indica* has been used as a traditional medicine for more than 2000 years in India, because of its valuable biological activities (anti-inflammatory, anti-ulcer, anti-malarial, anti-bacterial, and anti-oxidant activities, among others) [20-22]. Thus, many research groups have been carrying out chemical investigations of *A. indica* since the early 20th century [23-28]. Their investigations revealed that *A. indica* is a rich source of structurally unique bioactive compounds such as azadirachtin, a highly oxygenated limonoid with a rearranged C-*seco* structure and strong anti-feedant activity [29, 30]. The fruits of *A. indica* were utilized for treatment of piles, intestinal worms, urinary disorder, epistaxis, phlegm, eye problem, diabetes mellitus, wounds and leprosy in Ayurveda system [20]. Although the chemical constituents of leaves, seeds and oil have been well investigated, there are only few papers on those of fruits [31-37]. As part of our search for structurally interesting bioactive compounds from medicinal plants, we have investigated the MeOH extract of the fruits of *A. indica*, resulting in the isolation of four new triterpenoids, along with three nine compounds.

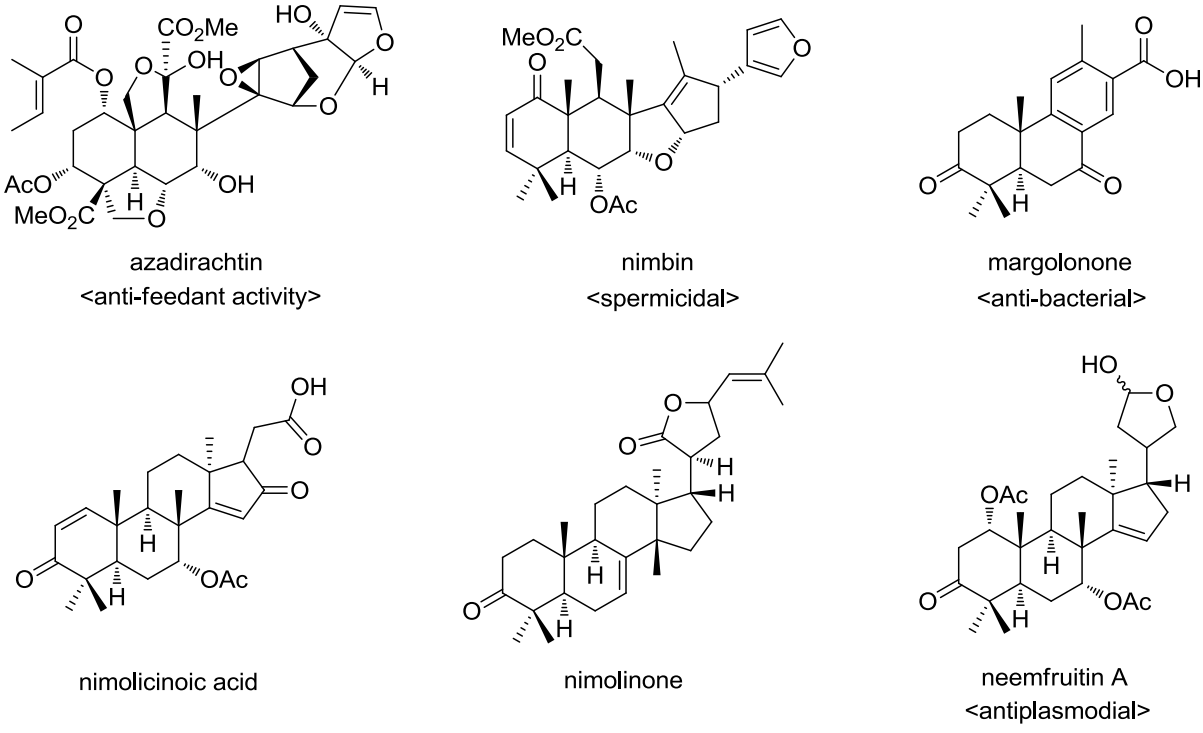

Figure 2.1. Previously isolated compounds from *A. indica*.

2.2. Extraction and isolation

The dried fruits of *A. indica* (2.4 kg) were powdered and extracted with MeOH for 1 day at room temperature nine times. After concentration, the MeOH extract (235 g) was successively partitioned with *n*-hexane, EtOAc and H_2O. The *n*-hexane-soluble fraction and EtOAc-soluble fraction were separated by repeated column chromatography (Scheme 2) to give twelve compounds, including four new triterpenoids (**26-29**).

Scheme 2

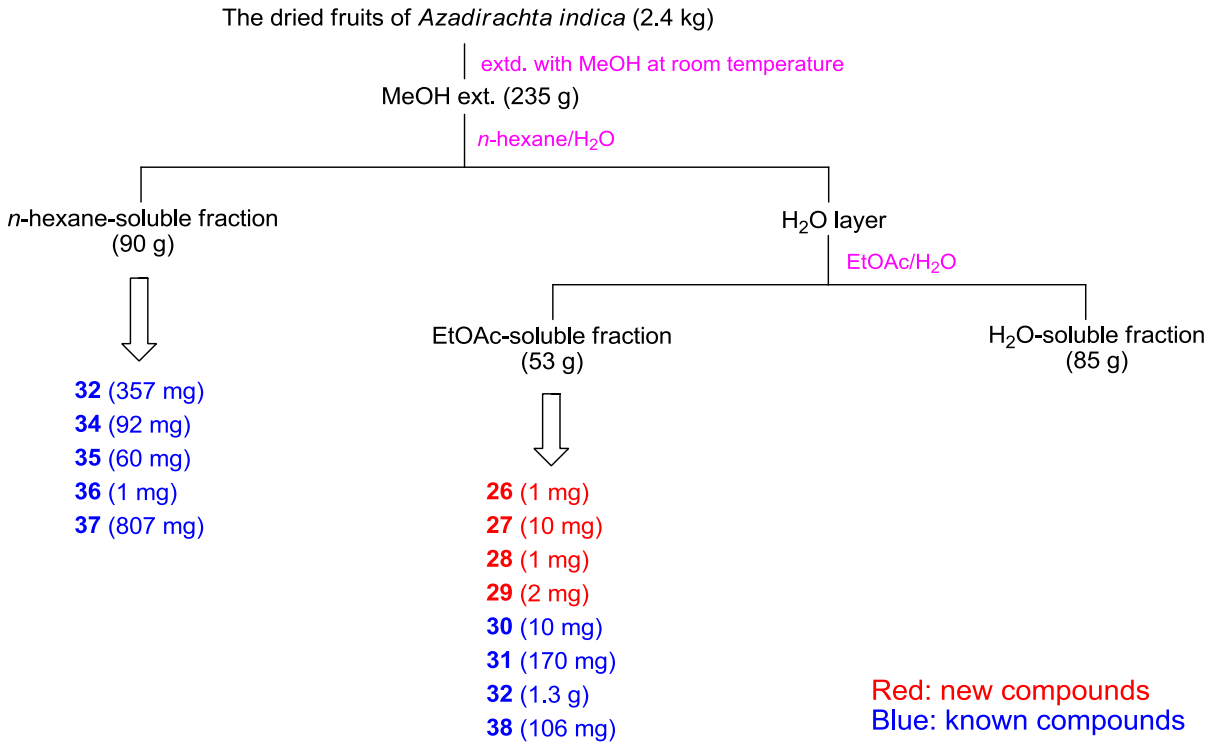

2.3. Identification of known compounds

The structure of **31** was assigned as meliantriol [38] by the spectroscopic examination, and was confirmed by reduction of melianodiol (**32**) by $NaBH_4$, which gave a major product identical to **31**. Since the ^{1}H and ^{13}C NMR data for meliantriol have not been reported previously, the spectroscopic data are shown in Table 2.2 and the experimental section.

Compounds **30**, **32** and **34-38** were identified as meliasenin S (**30**) [39], melianodiol (**32**) [40], 21α-methylmelianodiol (**34**) [41], 21β-methylmelianodiol (**35**) [41], 21β,25-dimethylmelianodiol (**36**) [42], melianone (**37**) [43] and vanillic acid (**38**) [44], respectively, by comparing their spectral data with those described in the literature.

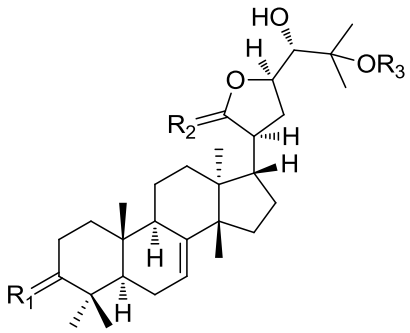

	R_1	R_2	R_3
30	α-H, β-OH	α-OMe, β-H	H
31	α-H, β-OH	α-OH, β-H	H
32	O	α-OH, β-H	H
34	O	α-OMe, β-H	OH
35	O	α-H, β-OMe	OH
36	O	α-H, β-OMe	OMe

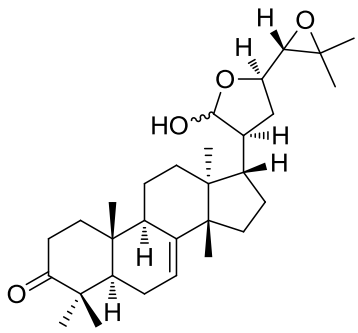

37

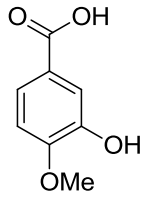

38

Figure 2.2. The structures of known compounds from *A. indica*.

2.4. Structure elucidation

2.4.1. Compound **26**

Compound **26** was obtained as a white amorphous powder. A pseudo-molecular ion peak at *m/z* 539.3372 (calcd for 539.3349 $[M+Na]^+$) in the positive-ion HRESIMS of **26** indicated the molecular formula of $C_{31}H_{48}O_6$. The ^1H NMR spectrum of **26** showed the presence of one methoxy group, seven *tert*-methyls, and four oxygenated methines. The ^{13}C NMR and DEPT spectra displayed 31 carbon signals, including eight sp^3 methylenes, two sp^3 methines, three oxygen-bearing sp^3 methines, four sp^3 quaternary carbons, two oxygen-bearing sp^3 quaternary carbons, two sp^2 quaternary carbons, one acetal carbon, and one carbonyl carbon. These data were similar to those of 21α-methylmelianodiol (**34**), a tirucallane-type triterpenoid isolated from *Poncirus trifoliate* [41], except for signals ascribable to A, B-rings. In contrast, the ^1H-^1H COSY and HMBC correlations shown in Fig. 2.3 indicated that the structures of the C, D-rings and side chain were identical to those of 21α-methylmelianodiol. The locations of a tetrasubstituted olefin, a carbonyl carbon (δ_C 215.4), and a methyl group (δ_H 1.20) were elucidated at C-5(10), C-3, and C-9, respectively, from the HMBC correlations of Me-28 and Me-29 with C-3 and C-5 (δ_C 127.8), H_2-2 with C-10 (δ_C 135.5), H_2-6 with C-5 and C-10, and of the methyl proton (δ_H 1.20) with C-8, C-9, C-10, and C-11. The presence of an epoxy group between C-7 and C-8 was assigned from the chemical shifts of C-7 (δ_C 51.9) and C-8 (δ_C 66.8) as well as from the ^1H-^1H COSY correlation of H_2-6–H-7, coupled with the HMBC correlations of Me-30 and H_2-6 with C-8. The β configurations of H-7 and Me-19 were determined by the NOESY correlations of

Me-30 with H-7 and the NOE enhancement of Me-19 on irradiation of Me-30 in the NOE difference experiment, respectively. The configurations of C-20, C-21, and C-23 were elucidated as *S**, *R**, and *R**, respectively, from the NOESY correlations of Me-18 with H-20, of H-20 with H-23, and of H-21 with H-12α and H-17 (Fig. 2.3). Thus, the structure of **26** was characterized as shown in Fig. 2.4.

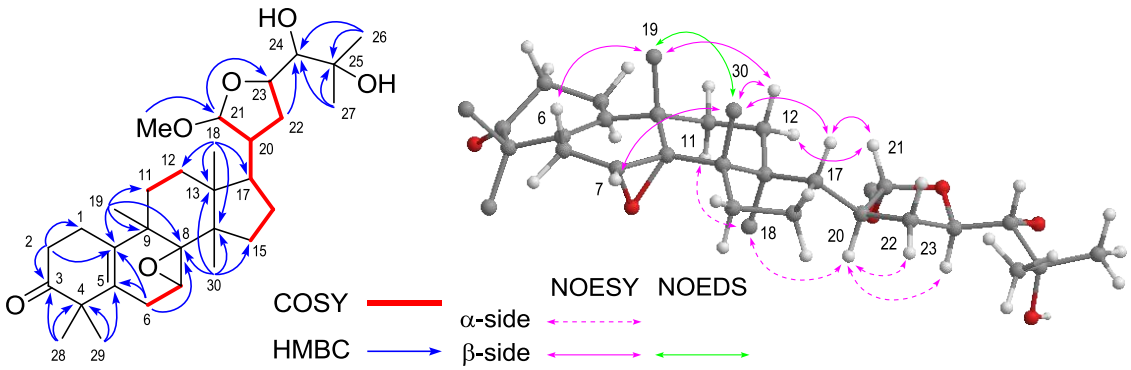

Figure 2.3. Key 2D NMR correlations of **26**.

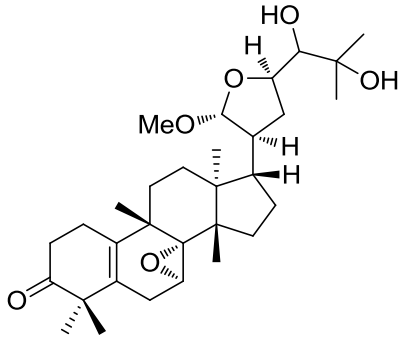

Figure 2.4. The structure of **26**.

2.4.2. Compound **27**

The molecular formula of **27** was established as $C_{30}H_{48}O_5$ by the HRESIMS. The ^{1}H and ^{13}C NMR spectra were closely correlated with those of meliasenin S (**30**) [39], except for the absence of acetal and methoxy signals and the observation of one carbonyl carbon resonance, together with the coupling pattern of H-3. The downfield shift of H-23 as compared with that of **30** suggested that **27** possessed an ester carbonyl group at C-21. This was further confirmed by the ^{1}H-^{1}H COSY correlations of H-17–H-20–H_2-22–H-23, along with the HMBC cross peak of H_2-22 with the ester carbonyl carbon. The α configuration of the hydroxyl group at C-3 was assigned by the small coupling constant value of H-3 (δ_H 3.46, br s). The NOESY correlations of H-20 with H-23 indicated they were co-facial (Fig. 2.5), but relative configurations of the side chain couldn't be elucidated from the NOESY data. To determine the absolute configuration of **27**, its chemical conversion was performed. Oxidation of 24,25-acetonide of **27** (**27a**) by pyridinium chlorochromate (PCC) furnished a

3-oxo-24,25-acetonide derivative (**27b**), which was found to be identical to 21-oxo-melianodiol 24,25-acetonide, prepared by Fetizon oxidation [45, 46] of melianodiol (**32**), followed by the introduction of an acetonide (Fig. 2.7). Therefore, the absolute configuration of **27** was identical to that of **32**. From the spectral and chemical examinations described above, the structure of **27** was characterized as shown in Figure 2.6.

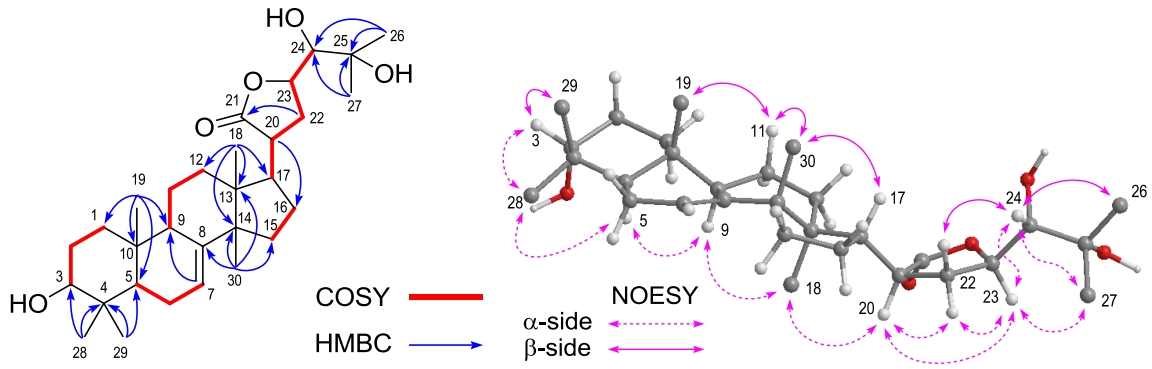

Figure 2.5. Key 2D NMR correlations of **27**.

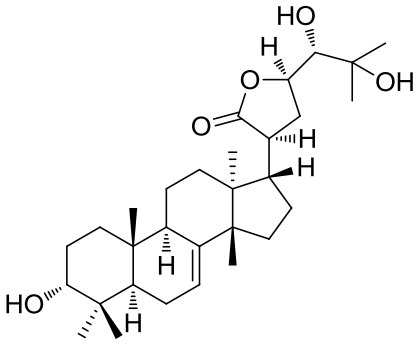

Figure 2.6. The structure of **27**.

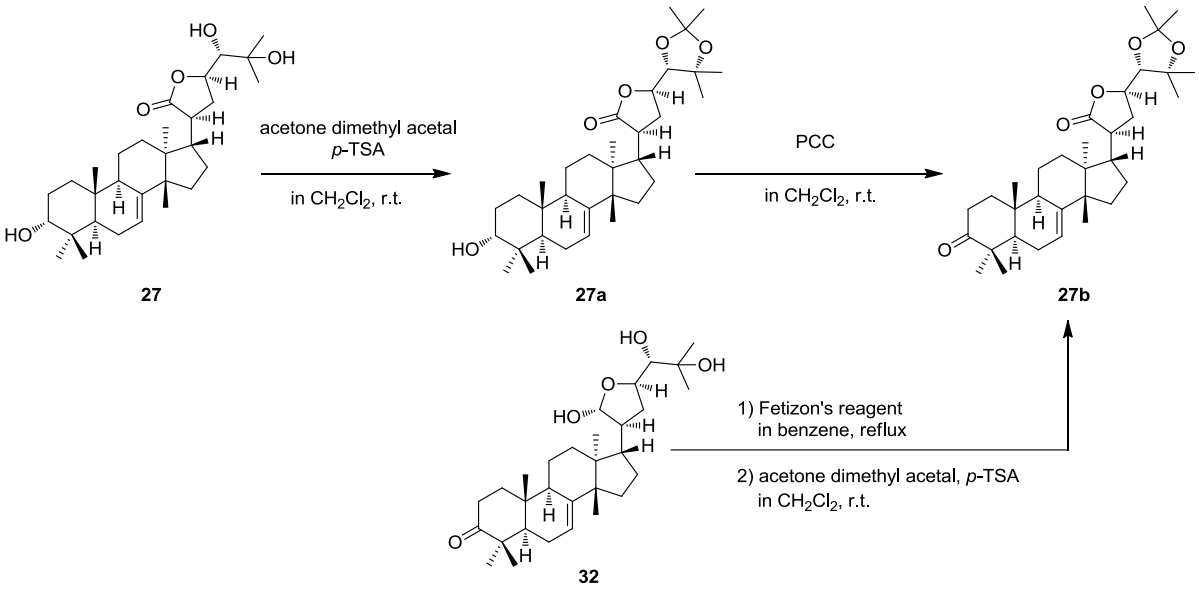

Figure 2.7. Chemical conversions of **27** and **32** into **27b**.

2.4.3. Compound **28**

The molecular formula of **28** was assigned as $C_{31}H_{50}O_5$ from the HRESIMS. The ^1H and ^{13}C NMR spectra were quite similar to those of **30**, but differed in the observation of signals due to one trisubstituted olefin and the absence of one methine and one methylene seen in **30**. The location of the additional trisubstituted olefin was assigned to be C-9(11) from the HMBC correlations of H-5 and Me-19 with sp^2 quaternary carbon (δ_C 145.9) and of Me-18 with C-12, along with the ^1H-^1H COSY correlations of H-11–H_2-12. The β configuration of H-3 was determined from the coupling constant value of H-3 [δ_H 3.48 (dd, J = 5.6, 10.0 Hz)]. The configurations of C-17 side chain were concluded to be the same as those of **30** by the analyses of the ^1H NMR and NOESY spectra (Fig. 2.8). From these data, the structure of **28** was characterized as shown in Fig. 2.9.

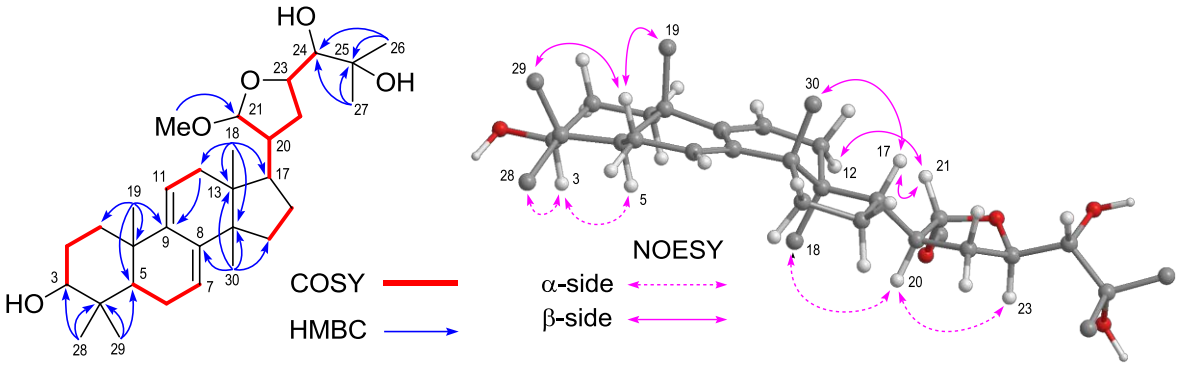

Figure 2.8. Key 2D NMR correlations of **28**.

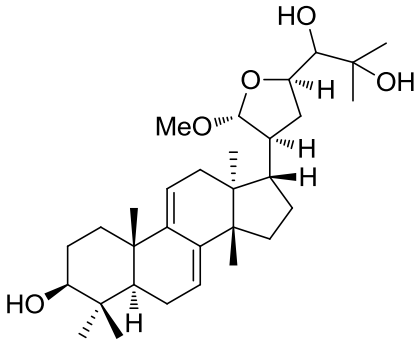

Figure 2.9. The structure of **28**.

2.4.4. Compound **29**

Compound **29** was obtained as a white amorphous powder. The molecular formula of **29**, $C_{30}H_{44}O_5$, established by HRESIMS (*m/z* 507.3078 $[M+Na]^+$, calcd for 507.3086), indicated nine degrees of unsaturation. The ^1H and ^{13}C NMR spectra revealed the presence of seven *tert*-methyls, six sp^3 methylenes, four sp^3 methines, two oxygen-bearing sp^3 methines, four sp^3 quaternary carbons, one oxygen-bearing sp^3 quaternary carbon, one disubstituted olefin, one trisubstituted olefin, and two carbonyl groups. These data implied that **29** was a

euphane- or tirucallane-type triterpenoid. The locations of disubstituted olefin and trisubstituted olefin were determined to be C-23(24) and C-7(8), respectively, from the ^{1}H-^{1}H COSY correlations of H-5–H_2-6–H-7, and of H_2-22–H-23–H-24, coupled with the HMBC cross peaks of Me-30 with C-8 (δ_C 143.1), and of Me-26 and Me-27 with C-24 (δ_C 140.6). The ^{1}H-^{1}H COSY correlations of H-9–H_2-11–H-12 (δ_H 3.92), and of H_2-15–H-16 (δ_H 4.25)–H-17, along with the HMBC correlations of Me-18 with C-12 and C-17, Me-30 with C-15, and of Me-26 and Me-27 with C-25 (δ_C 70.5), indicated that three hydroxyl groups were located at C-12, C-16, and C-25. The positions of the carbonyl groups at C-3 and C-21 were assigned from the HMBC correlations of H-2, Me-28, and Me-29 with C-3 (δ_C 216.2), and of H-20 with C-21 (δ_C 179.6). In addition, the connectivity between C-16 and C-21 through an ester linkage was concluded from the chemical shifts of H-16 and C-21 as well as from the unsaturation degree of **29**. The α configurations of H-12, H-16, and H-20 were determined from the coupling constant value of H-12 (J = 5.5, 9.7 Hz) and the NOESY correlations of H-12 with Me-18, and of H-16 with Me-18 and H-20, while the β configuration of H-17 was elucidated from the NOESY correlations of H-17 with Me-30 (Fig. 2.10). The geometry of disubstituted olefin between C-23 and C-24 was assigned as *E* from the *J*-values of H-23 and H-24 (J = 15.6 Hz). On the basis of these observations, compound **29** was a euphane-type triterpenoid as shown in Figure 2.11.

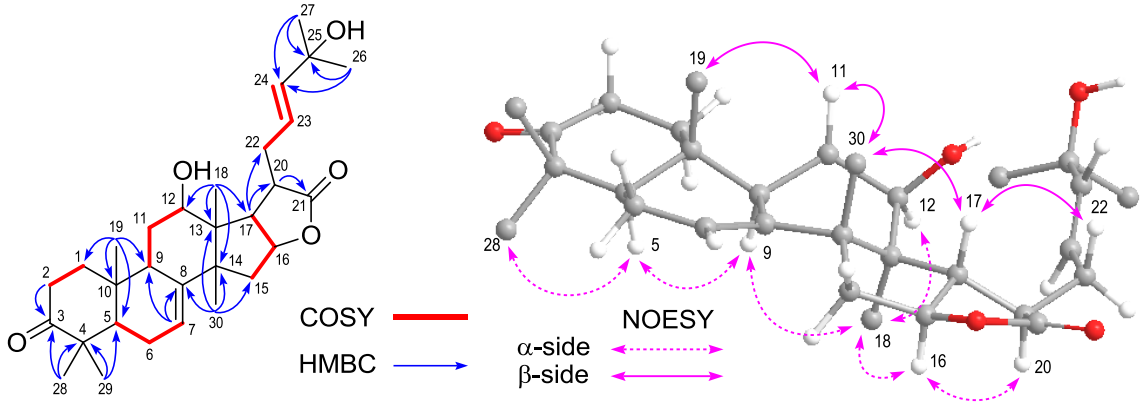

Figure 2.10. Key 2D NMR correlations of **29**.

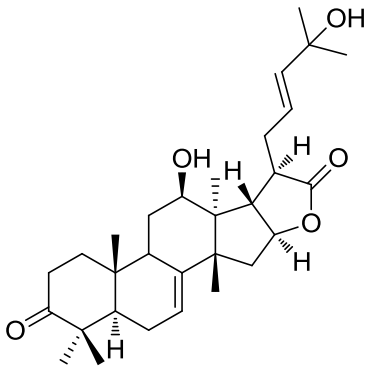

Figure 2.11. The structure of **29**.

Table 2.1. ^{1}H NMR data for **26-29**.

Position	**26**[a]	**27**[a]	**28**[b]	**29**[a]
1	2.38 (m)	1.49 (m)	1.85 (m)	2.01 (ddd, 2.9, 5.2, 14.2)
	2.33 (m)	1.38 (dt, 3.4, 13.4)	1.59 (m)	1.57 (ddd, 3.7, 14.2, 14.2)
2	2.62 (m)	1.93 (m)	1.96 (m)	2.79 (ddd, 5.2, 14.2, 14.2)
	2.39 (m)	1.61 (m)		2.27 (m)
3	—	3.46 (br s)	3.48 (dd, 5.6, 10.0)	—
5	—	1.78 (m)	1.44 (dd, 4.9, 11.6)	1.73 (t, 8.8)
6	2.60 (m)	2.05 (br d, 17.5)	2.27 (dt, 4.9, 18.0)	2.16 (m)
	2.33 (m)	1.94 (m)	2.16 (m)	
7	2.98 (d, 2.9)	5.26 (dd 2.6, 5.8)	5.43 (br s)	5.40 (d, 2.7)
11	2.00 (ddd, 5.0, 13.8, 13.8)	1.62 (m)	5.29 (br s)	2.00 (ddd, 5.5, 13.8, 13.8)
	1.48 (m)	1.52 (m)		1.48 (m)
12	2.07 (m)	1.77 (m)	2.17 (m)	3.92 (dd, 5.5, 9.7)
	1.50 (m)	1.68 (m)	2.11 (m)	
15	1.63 (ddd, 8.6, 10.8, 12.2)	1.55 (m)	1.74 (m)	2.29 (m)
	0.95 (m)		1.35 (m)	1.77 (dd, 7.4, 13.2)
16	1.87 (m)	1.82 (m)	1.89 (m)	4.25 (ddd, 7.4, 10.6, 11.9)
	1.37 (m)	1.49 (m)	1.33 (m)	
17	1.72 (m)	2.36 (m)	1.89 (m)	2.49 (dd, 11.9, 11.9)
18	0.97 (s)	0.84 (s)	0.88 (s)	0.86 (s)
19	1.20 (s)	0.78 (s)	1.03 (s)	1.05 (s)
20	2.23 (ddd, 3.1, 10.4, 17.8)	2.69 (ddd, 5.7, 8.8, 11.8)	2.33 (m)	2.58 (ddd, 3.2, 9.2, 11.9)
21	4.73 (d, 3.1)	—	4.86 (d, 3.8)	—
22	1.94 (m)	2.38 (m)	2.09 (m)	2.86 (br d, 15.2)
	1.77 (m)	2.20 (dd, 6.2, 8.8, 12.5)	1.99 (m)	2.31 (m)
23	4.23 (dd, 3.5, 10.7)	4.59 (ddd, 1.3, 6.2, 8.7)	4.67 (ddd, 2.7, 4.7, 10.8)	5.74 (ddd, 4.9, 7.8, 15.6)
24	3.26 (br s)	3.29 (d, 1.3)	3.75 (d, 2.7)	5.84 (d, 15.6)
26	1.27 (s)	1.30 (s)	1.67 (s)	1.35 (s)
27	1.30 (s)	1.34 (s)	1.61 (s)	1.35 (s)
28	1.19 (s)	0.93 (s)	1.18 (s)	1.07 (s)
29	1.08 (s)	0.92 (s)	1.15 (s)	1.14 (s)
30	1.14 (s)	1.03 (s)	0.88 (s)	1.39 (s)
OMe	3.34 (s)	—	3.42 (s)	—

δ ppm (mult, *J*, in Hz), 500 MHz. [a] in $CDCl_3$. [b] in pyridine-d_5

Table 2.2. ^{13}C NMR data for **26**-**29** and **31**.

Position	**26**[a]	**27**[a]	**28**[b]	**29**[a]	**31**[a]
1	24.3	31.2	36.3	38.4	37.2
2	36.6	25.4	28.6	34.7	27.7
3	215.4	76.3	78.1	216.2	79.3
4	46.9	37.4	39.6	47.9	39.0
5	127.8	44.6	48.9	52.5	50.8
6	26.0	23.9	24.3	24.4	24.0
7	51.9	118.3	119.6	119.2	118.2
8	66.8	145.5	141.4	143.1	145.5
9	40.8	48.5	145.9	47.9	48.8
10	135.4	34.9	36.7	35.3	35.0
11	30.3	17.4	115.1	29.0	17.5
12	28.7	31.2	36.7	71.6	31.6
13	45.9	43.7	44.5	44.8	43.6
14	48.5	50.5	49.5	54.8	50.8
15	28.6	33.9	31.4	36.3	34.2
16	26.1	23.8	27.3	82.6	27.3
17	48.0	47.2	48.9	52.9	50.8
18	17.6	23.5	17.4	19.9	23.2
19	25.0	13.0	21.1	12.4	13.1
20	46.6	40.3	48.4	45.6	46.5
21	109.8	178.2	109.6	179.6	97.0
22	34.3	29.6	36.4	31.9	34.2
23	76.8	77.3	77.2	124.8	78.7
24	75.5	76.3	78.7	140.6	75.1
25	73.1	72.5	72.6	70.5	73.4
26	26.4	26.6	28.3	29.6	26.7
27	26.5	26.6	26.0	30.0	26.7
28	24.1	27.8	28.3	24.3	27.6
29	24.0	21.8	16.1	21.5	14.7
30	24.5	27.4	23.3	33.6	27.3
OMe	55.5	—	55.2	—	—

δ ppm, 125 MHz. [a] in $CDCl_3$. [b] in pyridine-d_5.

2.5. Cytotoxicity assay

Cytotoxicity against two cancer cell lines (KB and MCF7) and against an MDR cancer cell line (KB-C2) was evaluated for compounds **27**, **30-32**, and meliasenin T (**33**) [39] prepared by methylation of **31**. Compounds **27** and **31-33** showed moderate cytotoxicity against all the tested cell lines, with IC_{50} values ranging from 9.04 to 25.7 μg/mL, while compound **30** was not cytotoxic against any of the tested cancer cell lines. However, **30** showed cytotoxicity against KB-C2 cells in the presence of 2.5 μM colchicine with an IC_{50} value of 6.48 μg/mL, suggesting that **30** might have an MDR-reversal effect. Considering that compound **33**, the C-21 epimer of **30**, showed moderate cytotoxicity against three cancer cell lines, the stereochemistry of C-21 might play an important role in cytotoxic effect.

Table 2.3. Cytotoxicity (IC_{50}[a] in μg/mL) of compounds **27, 30-33** against three human cancer cell lines.

	KB	KB-C2	KB-C2 (+2.5 μM col.)	MCF7
27	15.0 ± 1.35	16.1 ± 0.91	7.29 ± 0.28	19.0 ± 0.30
30	> 100	> 100	6.48 ± 0.89	> 100
31	25.7 ± 0.46	15.9 ± 0.51	9.51 ± 0.51	13.5 ± 0.30
32	15.4 ± 1.39	15.1 ± 0.44	4.60 ± 0.37	9.04 ±0.44
33	17.1 ± 0.87	15.6 ± 0.08	6.67 ± 0.46	16.0 ± 0.29
daunorubicin	0.67 ± 0.02	19.7 ± 1.06	20.9 ± 1.80	0.27 ± 0.01

[a] Data are mean ± SE from three or four experiments.
col. : colchicine

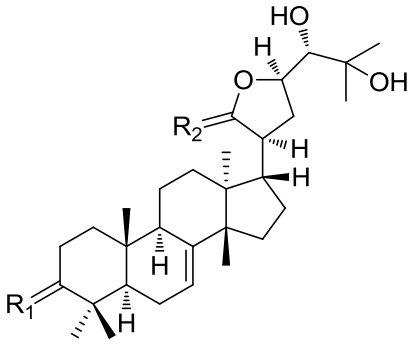

	R_1	R_2
27	α-OH, β-H	O
30	α-H, β-OH	α-OMe, β-H
31	α-H, β-OH	α-H, β-OH
32	O	α-OH, β-H
33	α-H, β-OH	α-H, β-OMe

Figure 2.12. Compounds applied to cytotoxicity assay.

2.6. Conclusion

Four new triterpenoids, including one 19(10→9β)*abeo*-tirucallane derivative, two tirucallanes and one euphane, together with eight known compounds were isolated from the MeOH extract of the fruits of *A*. *indica*. The structures of new compounds were elucidated by spectroscopic analyses. The absolute configuration of **2** was determined by chemical conversion of **2** into 21-oxo-melianodiol 24,25-acetonide (**27b**).

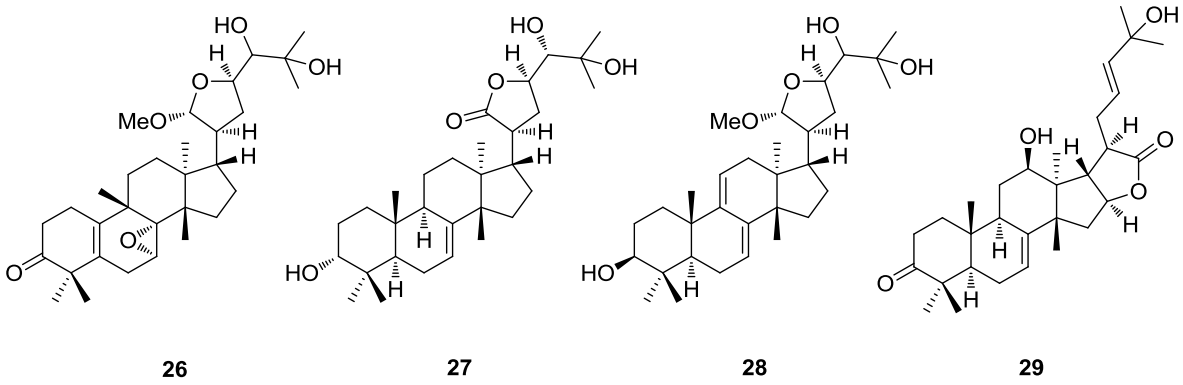

Figure 2.13. New triterpenoids from the MeOH extract of *A*. *indica*.

Cytotoxic activities of five compounds (**27**, **30**-**33**) against three human cancer cell lines (KB, KB-C2 and MCF7) were assessed. Compounds **27**, **31**-**33** were exhibited moderate cytotoxicity against tested cancer cell lines. Although compound **30** was not cytotoxic against any of the tested cancer cell lines, **30** showed cytotoxicity against KB-C2 cells in presence of 2.5 μM colchicine, indicating that **30** might have an MDR-reversal effect.

Chapter 3
Study on the constituents of *Scutellaria coleifolia* Levl.

3.1. Introduction

Scutellaria plants, belonging to the Lamiaceae family, include about 350 species, and are widely distributed in template zone and tropical zone of Europe, North America and East Asia. They have been used as traditional medicines in many countries [47]. For example, roots of *S*. *baicalensis* have been used as pharmacopoeial medicine for removing fever and resolution in Japan and China [48, 49], while aerial parts of *S*. *galericulata* have been used as sedative and an antispasmodic in United States [50]. Flavonoids, flavonoid glycosides and *neo*-clerodane-type diterpenoids were shown to be major constituents of the *Scutellaria* plants by previous studies. Biological activities including anti-cancer, anti-inflammatory and anti-feedant activity of the isolated compounds were also reported [47, 51]. *Scutellaria coleifolia* Levl. is distributed in high altitude regions of Yunnan and Sichuan Provinces. There are no reports of chemical investigation on this plant. As part of our investigation for searching new drug seeds from unexplored plant resources, we have studied the constituents of the aerial parts of *S*. *coleifolia* to give thirty-one new terpenoids, along with six known compounds.

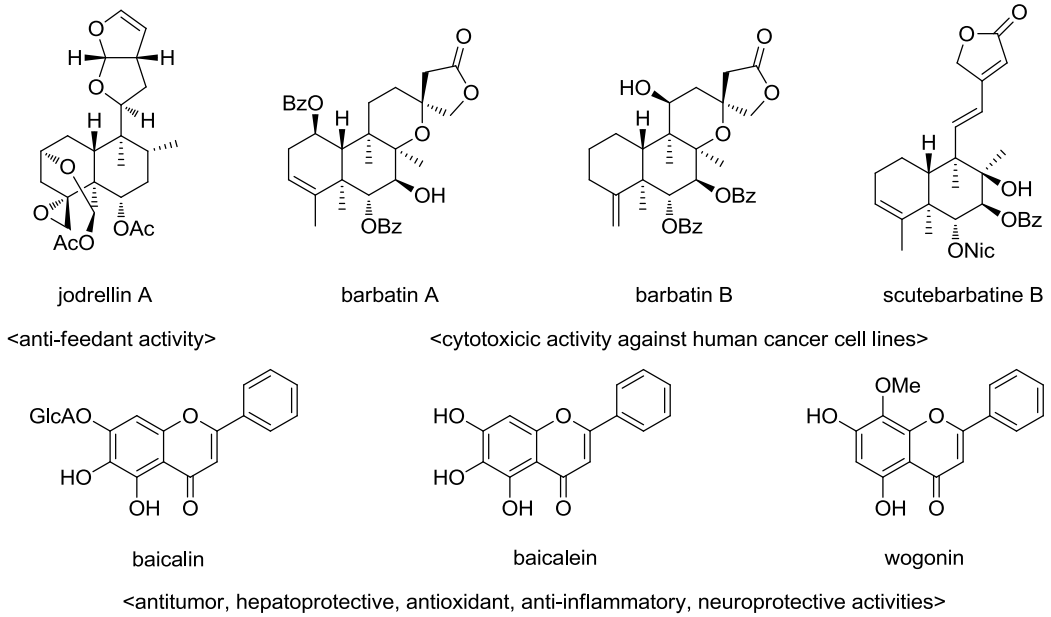

Figure 3.1. Biological active compounds isolated from *Scutellaria* plants.

3.2. Extraction and isolation

The dried aerial parts of *S. coleifolia*, collected in Sichuan Province in August 2011, were extracted with 70% aqueous acetone (3×15 L) at room temperature. The extract was partitioned between EtOAc and H_2O three times. The EtOAc-soluble fraction (130 g) was repeatedly subjected to column chromatography as shown in scheme 3, giving thirty-one new terpenoids, along with six known compounds.

Scheme 3

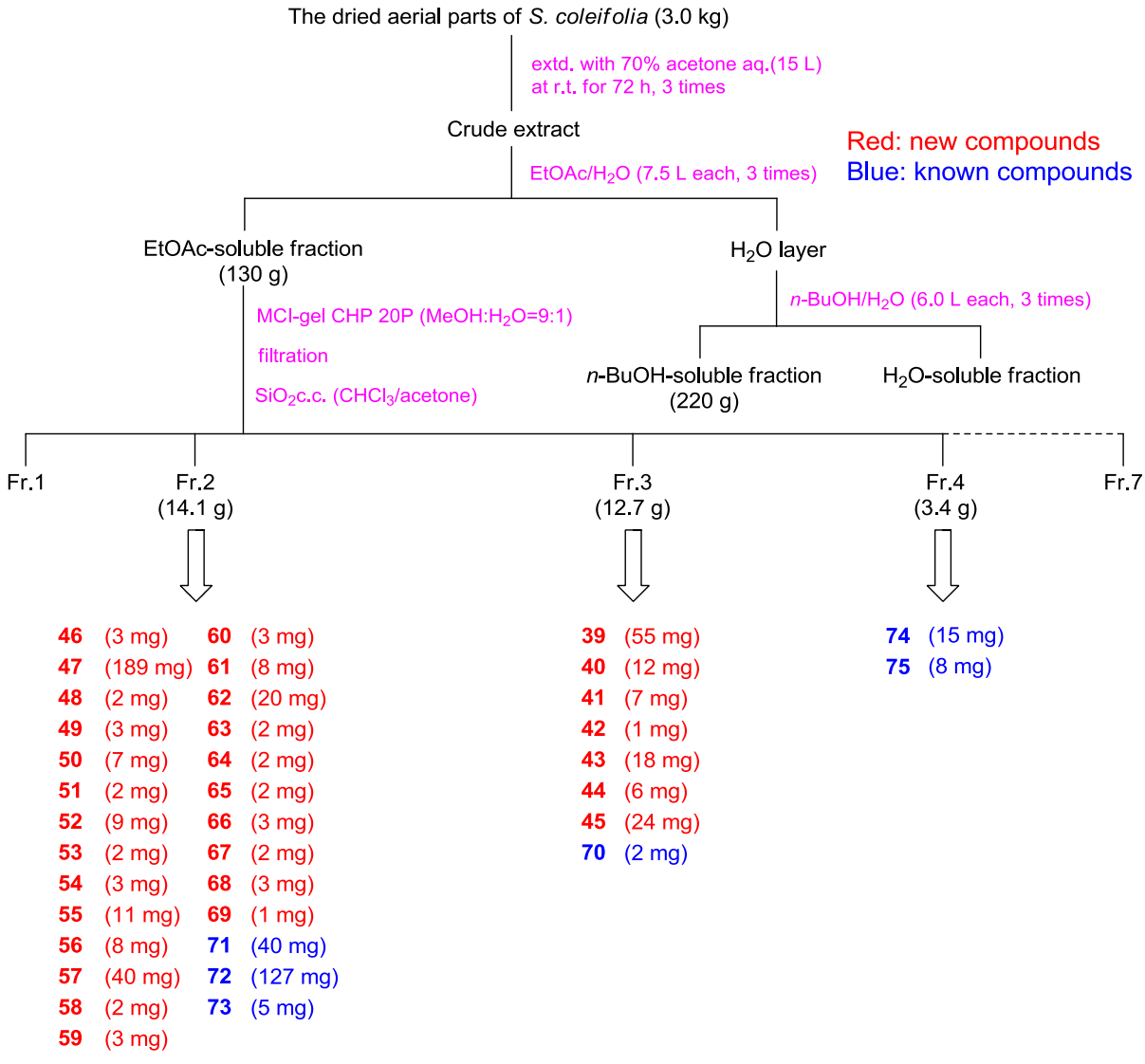

3.3. Identification of known compounds

Compounds **70-75** were identified as irroratin A (**70**) [52], teucvin (**71**) [53], palmitic acid (**72**) [54], 12-epi-teucvin (**73**) [53], clovan-2β,9α-diol (**74**) [55] and dimethylmartynoside (**75**) [56], respectively, by comparisons of their spectroscopic data with those described in the literature.

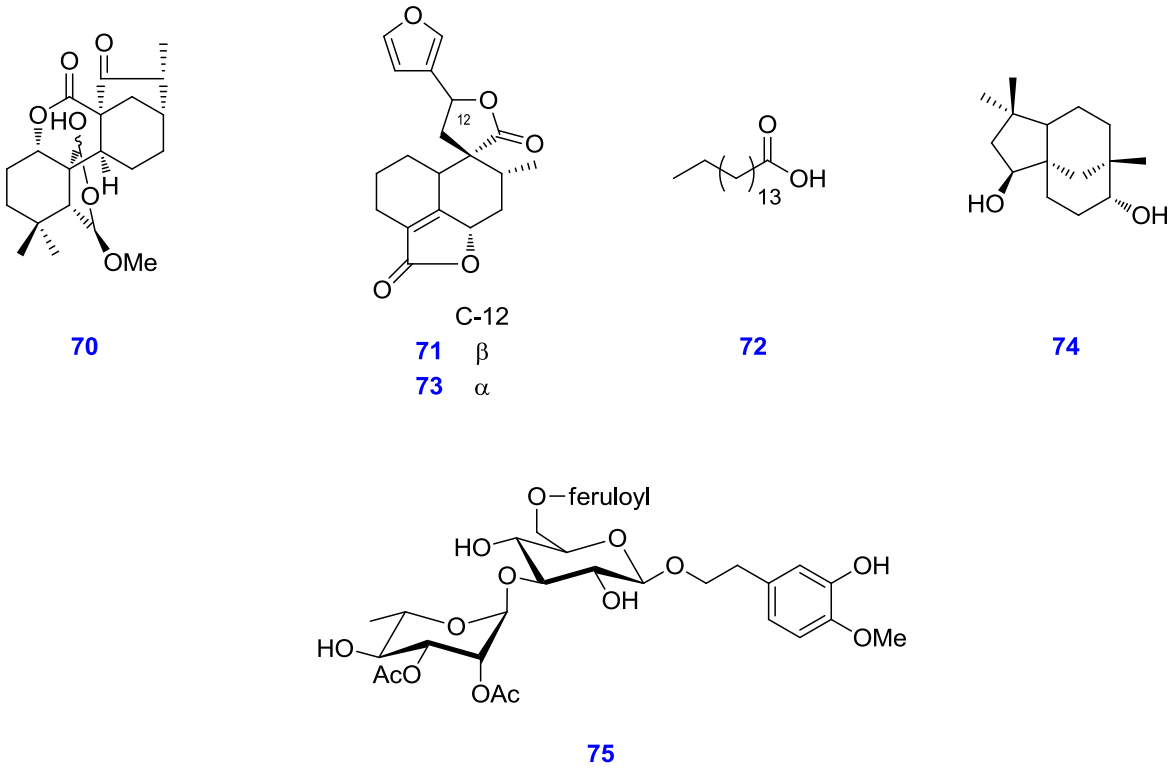

70 **71** β **73** α **72** **74** **75**

Figure 3.2. The structures of known compounds from *S. coleifolia*.

3.4. Structure elucidation

3.4.1. Compound **39**

Compound **39** was obtained as colorless oil. The molecular formula of **39** was determined as $C_{25}H_{38}O_4$ by HRESIMS (*m/z* 425.2657 $[M+Na]^+$ calcd for 425.2667). The ^1H NMR spectrum showed signals due to five *tert*-methyls [δ_H 1.59 (s), 1.60 (s), 1.81 (s), 1.88 (s), 2.01 (s)], one hydroxymethyl [δ_H 4.43 (d, *J* = 12.1 Hz), 4.50 (d, *J* = 12.1 Hz)], two oxygenated methine [δ_H 4.34 (br t, *J* = 5.5 Hz), 4.96 (t, *J* = 5.0 Hz)] and five olefinic protons [δ_H 5.16 (m), 5.18 (m), 5.18 (m), 5.62 (m), 5.91 (br s)]. The ^{13}C NMR spectrum with a DEPT experiment displayed 25 carbon resonances including six sp^3 methylene carbons (δ_C 26.5, 26.6, 30.4, 34.6, 39.7, 39.8), five trisubstituted olefins [δ_C 117.2 (d), 169.2 (s), 117.0 (d), 139.5 (s), 124.3 (d), 135.1 (s), 124.9 (d), 138.7 (s), 124.2 (d), 137.8 (s)] and one carbonyl carbon (δ_C 173.1). The existence of a β-methyl-α,β-unsaturated-γ-lactone moiety was deduced from the HMBC correlations of Me-25 [δ_H 1.88 (s)] with C-2 (δ_C 117.2), C-3 (δ_C 169.2) and C-4 (δ_C 84.3), H-2 [δ_H 5.91 (br s)] with C-1 (δ_C 173.1), and of H-4 [δ_H 4.96 (t, *J* = 5.0 Hz)] with C-1. In contrast, the ^1H-^1H COSY correlations of H_2-5 [δ_H 2.29 (m), 2.63 (m)]–H-6 [δ_H 5.16 (m)], H_2-8 [δ_H 2.01 (m)]–H_2-9 [δ_H 2.10 (m)]–H-10 [δ_H 5.18 (m)], H_2-12 [δ_H 2.07 (m)]–H_2-13 [δ_H 2.21 (m)]–H-14 [δ_H 5.62 (m)], and of H-16 [δ_H 4.34 (br t, *J* = 5.5 Hz)]–H_2-17 [δ_H 2.57 (m)]–H-18 [δ_H 5.18 (m)], coupled with the HMBC cross peaks of Me-21 [δ_H 2.01, (s)] with C-18 (δ_C 124.2), C-19 (δ_C 137.8) and C-20 (δ_C 61.0), Me-23 [δ_H 1.59 (s)] with C-10 (δ_C 124.3), C-11 (δ_C 135.1) and C-12 (δ_C 39.7), and of Me-24 [δ_H 1.60 (s)] with C-6 (δ_C 117.0), C-7 (δ_C 139.5) and C-8 (δ_C 39.8), revealed the presence of a 12,16-dihydroxy-geranylgeranyl moiety. Furthermore, the ^1H-^1H COSY correlations of H-4 with H_2-5, as well as the HMBC cross peak of H-6 with C-4 indicated that the dihydroxy geranylgeranyl moiety was connected to C-4 of the β-methyl-α,β-unsaturated-γ-lactone moiety, and thus the planer structure of **39** was elucidated (Fig. 3.3). The geometries of double bonds were elucidated as 6*E*, 10*E*, 14*E* and 18*Z* from the ROESY correlations of H_2-5 with Me-24, H_2-9 with Me-23, H_2-13 with Me-22, H_2-17 with H_2-20, and of H-18 with Me-21 (Fig. 3.3).

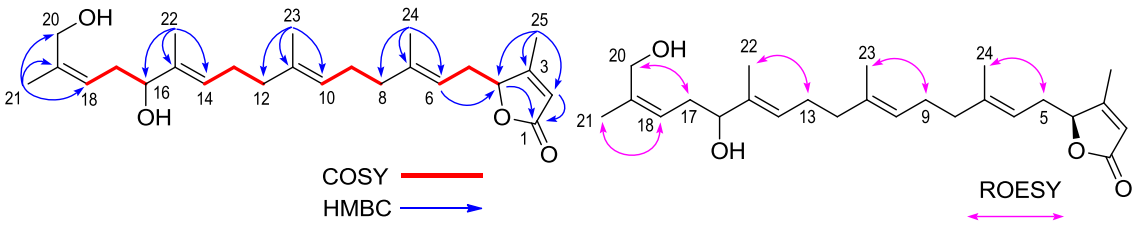

Figure 3.3. Key 2D NMR correlations of **39**.

To determine the absolute configuration, 20-pivaloate of **39** (**39a**) was treated with (*R*)- or (*S*)-α-methoxy-2-naphthylacetic acid (2-NMA) [57], giving two diastereomers mixture (major:minor = 5:3). Therefore, **39** was considered to be a partial racemic mixture. This was also confirmed by the fact that treatment of **39a** with (*R*)-(-)-α-methoxyphenylacetic acid (MPA) also yielded a racemic mixture in the same ratio. The absolute configuration of C-16 of the major isomer was determined as *R* from the Δδ value (δ_R-δ_S) of the isolated proton signals (Fig. 3.4) [57]. Furthermore, the 4*S* configuration of the major enantiomer was assigned by comparison of the CD spectrum of **39** with those of manoalide derivatives. Thus, the CD spectrum of **39** showed positive Cotton effect at 209 nm (Δε: +10.2) while manoalide derivatives with 4*R* configuration structurally related to **39** were reported to show negative Cotton effect at 212 nm [58, 59]. From these observations, the structure for major isomer of **39** was assigned as shown in Fig. 3.5.

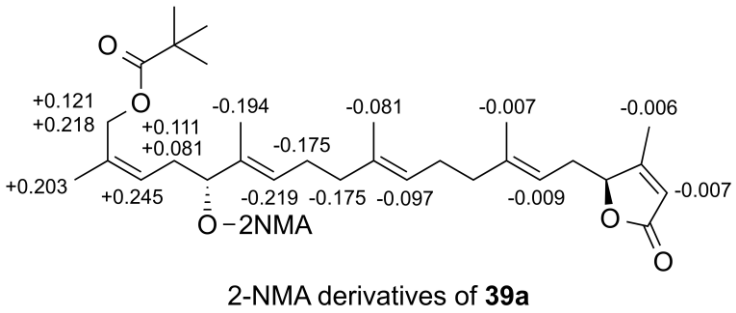

Figure 3.4. Δδ values (δ_R–δ_S) for 2-NMA ester of **39a**.

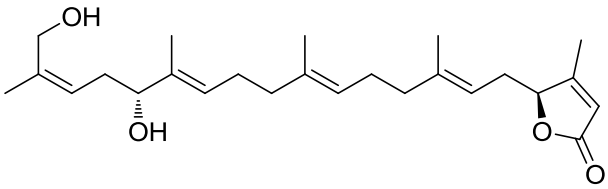

Figure 3.5. The structure of major isomer of **39**.

3.4.2. Compound **40**

Compound **40** was shown to have the same molecular formula ($C_{25}H_{38}O_4$) as that of **39**. The ^{1}H and ^{13}C NMR were quite similar to those of **39** except for the observation of signals due to an additional hydroxymethyl [δ_H 4.49 (s)] instead of one *tert*-methyl and one oxymethine seen in **39**, indicating **40** also to be a sesterterpenoid with a β-methyl-α,β-unsaturated-γ-lactone moiety. The ^{1}H-^{1}H COSY cross peaks of H_2-17 [δ_H 2.48 (m)]–H-18 [δ_H 5.44 (br s)], coupled with the HMBC correlations of Me-21 [δ_H 2.00 (s)] with C-18 (δ_C 126.9), C-19 (δ_C 136.6) and C-20 (δ_C 61.0), H_2-17 with C-16 (δ_C 36.1) and of H_2-22 [δ_H 4.49 (s)] with C-14 (δ_C 126.9), C-15 (δ_C 140.2) and C-16 indicated the positions of the

hydroxymethyls to be C-20 and C-22 (Fig. 3.6). The relative configurations of double bond were determined as 6*E*, 10*E*, 14*Z* and 18*Z* from the same ROESY correlations as seen in **39**. The CD spectrum of **40** showed the positive Cotton effect at 209 nm, indicating the *S* configuration of C-4. However, considering its Δε value (Δε: +9.0) similar to that (Δε: +10.2) of **39** as well as its small optical rotation value {$[\alpha]_D^{17}$ +7.4 (*c* 0.50, $CHCl_3$)}, coupled with biogenetical relationship between **39** and **40**, **40** was also a partially racemic mixture, although the 4*S* isomer was predominant. Thus, the structure of the major isomer of **40** was concluded as shown (Fig. 3.7).

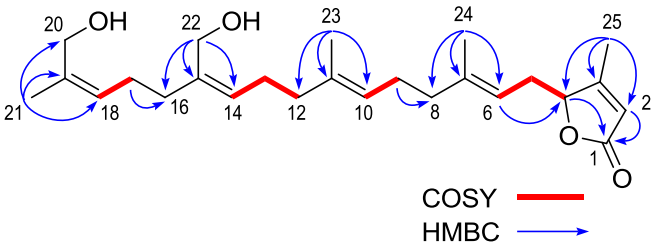

Figure 3.6. Key 2D NMR correlations of **40**.

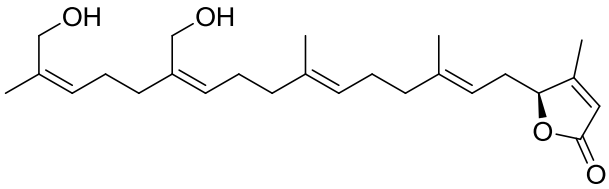

Figure 3.7. The structure of major isomer of **40**.

Table 3.1. ^{1}H and ^{13}C NMR data of **39** and **40** in pyridine-d_5.

Position	**39**		**40**	
	^{1}H[a]	^{13}C[b]	^{1}H[a]	^{13}C[b]
1	–	173.1	–	173.1
2	5.91 (br s)	117.2	5.91 (br s)	117.4
3	–	169.2	–	169.1
4	4.96 (t, 5.0)	84.3	4.95 (t, 5.0)	84.4
5	2.63 (m)	30.4	2.62 (m)	30.6
	2.29 (m)		2.26 (m)	
6	5.16 (m)	117.0	5.15 (m)	117.2
7	–	139.5	–	139.6
8	2.01 (m)	39.8	2.00 (m)	40.0
9	2.10 (m)	26.6	2.09 (m)	26.6
10	5.18 (m)	124.3	5.17 (m)	124.6
11	–	135.1	–	135.5
12	2.07 (m)	39.7	2.07 (m)	40.8
13	2.21 (m)	26.5	2.30 (m)	26.8
14	5.62 (m)	124.9	5.39 (t, 7.1)	126.9
15	–	138.7	–	140.2
16	4.34 (br t, 5.5)	76.9	2.48 (m)	36.1
17	2.71 (m)	34.6	2.48 (m)	27.1
	2.57 (m)			
18	5.18 (m)	124.2	5.44 (br s)	126.9
19	–	137.8	–	136.6
20	4.50 (d, 12.1)	61.0	4.46 (s)	61.0
	4.43 (d, 12.1)			
21	2.01 (s)	22.2	2.00 (s)	21.8
22	1.81 (s)	11.9	4.49 (s)	59.7
23	1.59 (s)	16.0	1.56 (s)	16.1
24	1.60 (s)	16.3	1.60 (s)	16.4
25	1.88 (s)	13.5	1.87 (s)	13.6

[a] δ ppm (mult., *J* in Hz), 500 MHz. [b] δ ppm, 125 MHz.

3.4.3. Compounds **41** and **42**

A pseudo-molecular ion peak at *m/z* 513.2464 (calcd for 513.2464 $[M+Na]^+$) in the positive HRESIMS of **41** indicated the molecular formula of $C_{27}H_{38}O_8$. The ^{1}H NMR spectrum showed the presence of three tertiary methyls, one secondary methyl, one acetyl group, three oxymethylenes, one oxymethine, and two olefinic protons. The ^{13}C NMR and DEPT spectra of **41** represented 27 carbon resonances including six sp^3 methylenes, one sp^3 methine, two sp^3 quaternary carbons, three oxygen-bearing sp^3 quaternary carbons, two sp^2 quaternary carbons and three carbonyl carbons. These data were well correlated with those of acylated 18-epoxy-8β-hydroxy-*neo*-clerod-13-en-15,16-γ-lactones, isolated from the *Scutellaria* plants [47]. The existence of the 18-epoxy-8β-hydroxy-*neo*-clerod-13-en-15,16-γ-lactone structure was further confirmed from ^{1}H-^{1}H COSY and HMBC correlations shown in Figure 3.8. The locations of the hydroxyl groups at C-6 and C-19 were determined from the ^{1}H-^{1}H COSY correlations of H-6 [δ_H 5.88 (dd, J = 4.8, 11.9 Hz)]–H_2-7, coupled with the HMBC correlations of H_2-19 with C-4 (δ_C 65.3), C-5 (δ_C 46.0), C-6 (δ_C 70.0) and C-10 (δ_C

44.2), Me-17 with C-7 (δ_C 40.6), C-8 (δ_C 76.1), and of Me-20 with C-8, C-9 (δ_C 42.2) and C-10. The presence of a tigloyl group was indicated by the ^1H-^1H COSY cross peak (H-3'/H_3-4'), the HMBC correlations (Me-5'/C-1', C-2' and C-3'), and the ROESY correlation (H_3-4'/H_3-5'), and its location at C-6 was elucidated from the HMBC correlation of H-6 with C-1' (δ_C 167.1). The acetyl group at C-19 was concluded from the HMBC correlation of H_2-19 with acetyl carbonyl carbon (δ_C 171.2). The relative configuration of **41** was elucidated by ROESY experiment (Fig. 3.9). The β configurations of H-6 and the C-18 oxymethylene were assigned from the ROESY correlations of H-10 [δ_H 2.49 (dd, J = 1.7, 11.0 Hz)] with H-6 and H-18a (δ_H 3.33). The orientations of Me-17, the C-19 hydroxymethyl and Me-20 were concluded to be α from the ROESY correlations of Me-20 with H_2-19 and Me-17. From these observations, the structure of **41** was assigned as shown (Fig. 3.10).

Compound **42** gave in the HRESIMS a pseudo-molecular ion peak at *m/z* 515.2635 $[M+Na]^+$ (calcd for 515.2620, $C_{27}H_{40}O_8Na$), which was 2 mass units more than that of **41**.

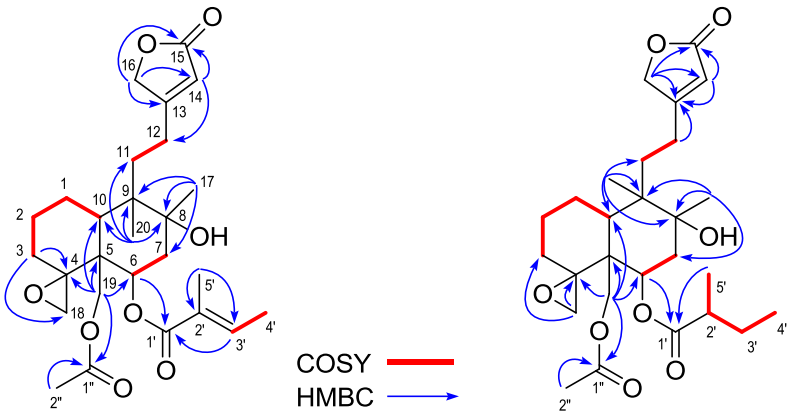

Figure 3.8. Key 2D NMR correlations of **41** and **42**.

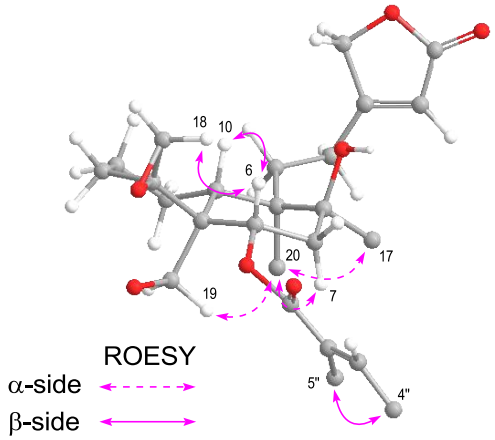

Figure 3.9. Key ROESY correlations of **41**.

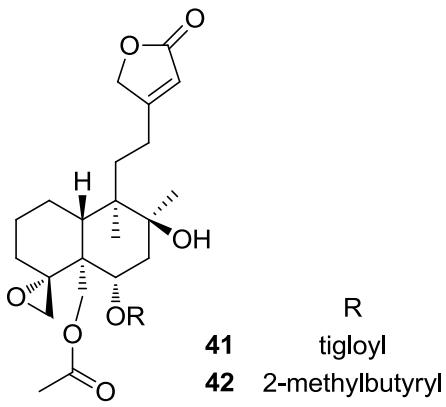

Figure 3.10. The structures of **41** and **42**.

The ^{1}H and ^{13}C NMR spectra were closely similar to those of **41** except for observation of the signals due to a 2-methylbutyryl group instead of the tigloyl group. Detailed analyses of 2D NMR revealed that **42** had the 2-methylbutyryl group at C-6 and the other structure including relative configuration was same as those of **41** (Fig. 3.10).

Table 3.2. ^{1}H and ^{13}C NMR data of **41** and **42** in pyridine-d_5.

	41		**42**	
Position	$^{1}H^{a}$	$^{13}C^{b}$	$^{1}H^{a}$	$^{13}C^{b}$
1	1.67 (m)	22.0	1.65 (m)	22.0
	1.50 (m)		1.49 (m)	
2	1.85 (m)	25.4	1.86 (m)	25.4
	1.50 (m)		1.50 (m)	
3	2.20 (m)	33.3	2.22 (m)	33.3
	1.06 (br d, 13.2)		1.07 (br d, 13.1)	
4	—	65.3	—	65.2
5	—	46.0	—	45.9
6	5.88 (dd, 4.8, 11.9)	70.0	5.79 (dd, 4.7, 11.9)	70.0
7	2.12 (dd, 11.9, 13.2)	40.6	2.12 (dd, 11.9, 13.5)	40.6
	1.84 (m)		1.77 (dd, 4.7, 13.5)	
8	—	76.1	—	76.1
9	—	42.2	—	42.3
10	2.49 (dd, 1.7, 11.0)	44.2	2.47 (br d, 12.6)	44.3
11	1.95 (m)	34.7	1.94 (m)	34.8
	1.53 (m)		1.53 (m)	
12	3.28 (br dt, 3.7, 16.4)	25.7	3.28 (m)	25.7
	2.34 (ddd, 3.7, 13.0, 16.4)		2.33 (ddd, 3.4, 13.4, 16.9)	
13	—	173.3	—	173.1
14	6.37 (s)	114.2	5.99 (s)	114.3
15	—	174.6	—	173.1
16	4.75 (d, 17.2)	73.6	4.74 (d, 17.1)	73.5
	4.70 (d, 17.2)		4.69 (d, 17.1)	
17	1.33 (s)	25.7	1.32 (s)	25.6
18	3.33 (dd, 1.7, 3.6)	48.6	3.31 (br dd, 1.9, 4.1)	48.6
	2.23 (m)		2.23 (m)	
19	5.00 (d, 12.1)	62.7	5.06 (m)	62.5
	4.84 (d, 12.1)		4.70 (m)	
20	0.83 (s)	21.1	0.81 (s)	20.9
1'	—	167.1	—	175.2
2'	—	129.7	2.40 (q, 6.9)	41.4
3'	7.04 (m)	136.8	1.90 (m)	26.7
			1.50 (m)	
4'	1.64 (br d, 7.2)	14.2	0.95 (t, 7.4)	11.9
5'	1.90 (br s)	12.4	1.21 (d, 6.9)	16.8
1"	—	171.2	—	170.9
2"	2.19 (s)	21.3	2.21 (s)	20.9

[a] δ ppm (mult., *J* in Hz), 500 MHz. [b] δ ppm, 125 MHz.

3.4.4. Compounds **43-45**

Compound **43** gave a peudo-molecular ion peak at *m/z* 559.2896 (calcd for 559.2883 $[M+Na]^+$) in the positive-ion HRESIMS, indicating the molecular formula of $C_{29}H_{44}O_9$. The ^1H NMR spectrum revealed the presence of three tertiary methyls, two secondary methyls, two oxymethylenes, two oxymethines and a tigloyl group. The ^{13}C NMR spectrum as well as a DEPT experiment displayed 29 carbon signals due to seven methyls, six sp^3 methylenes, two oxygen-bearing sp^3 methylenes, two sp^3 methines, two oxygen-bearing sp^3 methines, two quaternary sp^3 carbons, three oxygen-bearing sp^3 carbons, one sp^2 methine carbon, one sp^2 quaternary carbon and three carbonyl carbons. These data were similar to those of hastifolin E (Fig. 3.13) isolated from *Scutellaria hasilifolia* [60], indicating that **43** was also an *neo*-clerodane type diterpenoid with a 13-*spiro*-15,16-γ-lactone structure. The location of the tigloxy group was assigned to be C-6 from the HMBC correlations of Me-19 with C-5 (δ_C 46.8), C-6 (δ_C 71.7), and of H-6 [δ_H 6.19 (d, J = 10.3 Hz)] with C-1' (δ_C 167.3). The presence of an isobutyroxy group at C-7 was determined from the ^1H-^1H COSY correlations of H-6–H-7 [δ_H 5.66 (d, J = 10.3 Hz)], and of H-2"–(Me-3")–Me-4" as well as the HMBC correlations of H-7, Me-3 and Me-4 with C-1" (δ_C 177.0). The configurations of H-6, H-7 and the C-18 hydroxymethyl were concluded to be β, α, β, respectively, from the ROESY correlations of H-10 with H-6 and H-18b (δ_H 4.44), H-7 with Me-17, Me-19 and Me-20, respectively. The *S** configuration of C-13 was elucidated from the ROESY correlations of H_2-16 with Me-17 (Fig. 3.12). On the basis of these data, the structure of **43** was characterized as shown in Figure 3.13.

Compounds **44** and **45** had the same molecular formula of $C_{30}H_{44}O_9$. The ^1H and ^{13}C NMR spectra of **44** and **45** showed the presence of the same functional groups, indicating that both compounds had the identical planar structure. Furthermore, the ^1H and ^{13}C NMR spectra of both compounds were correlated with those of **43** except for showing the presence of two tigloyl groups, implying the isobutyryl group seen in **43** was replaced by the tigloyl group in **44** and **45**. This was further confirmed by analyses of ^1H-^1H COSY and HMBC spectra (Fig. 3.11). The relative configurations of **44** and **45** were elucidated by analyses of ROESY spectra. Compounds **44** and **45** showed similar ROESY correlations to each other, which resembled with those found in **43**. However, Me-17 showed the ROESY correlation with H-14a (δ_H 2.92) in **44**, while the ROESY correlation of Me-17 with H_2-16 was observed in **45** as seen in **43**. Therefore, compounds **44** and **45** were concluded to be a pair of C-13 epimers, in which configurations of C-13 in **44** and **45** were assigned as 13*R** and 13*S**, respectively (Fig. 3.12). Thus, the structures of **44** and **45** were elucidated as shown in Fig. 3.13.

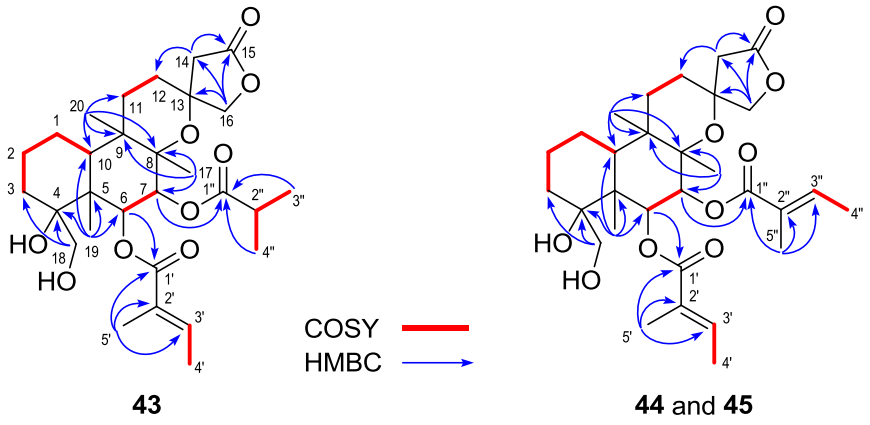

Figure 3.11. Key 2D NMR correlations of **43-45**.

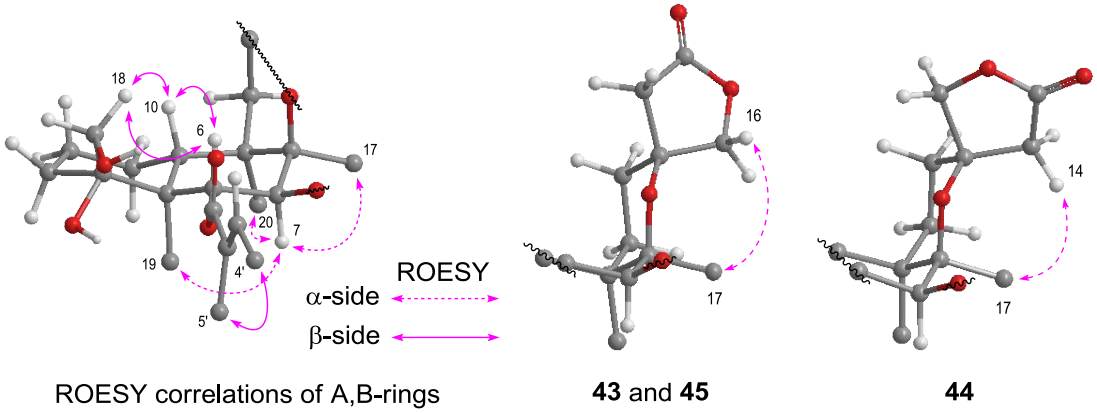

Figure 3.12. Key ROESY correlations of **43-45**.

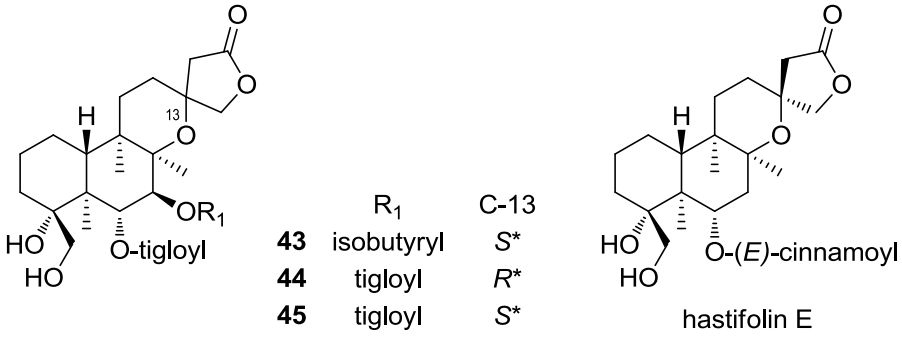

	R_1	C-13
43	isobutyryl	*S**
44	tigloyl	*R**
45	tigloyl	*S**

Figure 3.13. The structures of **43-45** and hastifolin E.

Table 3.3. ^{1}H and ^{13}C NMR data of **43-45** in pyridine-d_5.

	43		**44**		**45**	
Position	^{1}H[a]	^{13}C[b]	^{1}H[a]	^{13}C[b]	^{1}H[a]	^{13}C[b]
1	1.39 (m)	21.0	1.36 (m)	21.1	1.35 (m)	21.0
2	1.67 (m)	23.2	1.67 (m)	23.2	1.68 (m)	23.2
3	2.37 (br d, 5.9)	31.5	2.38 (br d, 6.1)	31.6	2.39 (br d, 6.0)	77.7
	1.67 (m)		1.67 (m)		1.66 (m)	
4	—	77.7	—	77.7	—	77.7
5	—	46.8	—	46.7	—	46.7
6	6.19 (d, 10.3)	71.7	6.24 (d, 10.2)	71.9	6.23 (d, 10.2)	71.9
7	5.66 (d, 10.3)	74.3	5.73 (d, 10.2)	75.1	5.72 (d, 10.2)	74.9
8	—	81.2	—	81.5	—	81.3
9	—	38.3	—	38.3	—	38.4
10	2.45 (dd, 3.4, 11.4)	37.3	2.49 (dd, 3.9, 11.1)	37.5	2.48 (dd, 3.6, 11.6)	37.4
11	1.55 (m)	27.9	1.59 (m)	27.9	1.55 (m)	27.9
12	1.71 (m)	28.6	1.81 (m)	28.7	1.72 (m)	28.5
			1.54 (m)			
13	—	76.5	—	76.2	—	76.5
14	2.88 (d, 17.0)	44.3	2.92 (d, 16.8)	42.8	2.97 (d, 17.0)	44.3
	2.51 (d, 17.0)		2.79 (d, 16.8)		2.55 (d, 17.0)	
15	—	174.0	—	175.3	—	174.0
16	4.34 (d, 8.6)	77.1	4.24 (d, 8.8)	79.7	4.30 (d, 8.6)	76.9
	4.27 (d, 8.6)		4.08 (d, 8.8)		4.19 (d, 8.6)	
17	1.23 (s)	19.7	1.33 (s)	20.1	1.25 (s)	19.9
18	4.76 (d, 10.5)	62.8	4.77 (d, 10.6)	63.2	4.77 (d, 10.6)	62.9
	4.44 (d, 10.5)		4.48 (d, 10.6)		4.47 (d, 10.6)	
19	1.58 (s)	12.7	1.60 (s)	12.6	1.60 (s)	12.7
20	0.86 (s)	20.7	0.89 (s)	20.9	0.88 (s)	20.7
1'	—	167.3	—	167.4	—	167.4
2'	—	130.1	—	130.0	—	130.0
3'	6.98 (m)	136.5	6.91 (m)	136.1	6.91 (m)	136.1
4'	1.56 (br d, 7.2)	14.1	1.49 (br d, 7.0)	14.1	1.50 (br d, 7.1)	14.1
5'	1.89 (br s)	12.3	1.82 (br s)	12.2	1.82 (br s)	12.2
1"	—	177.0	—	168.2	—	168.2
2"	2.60 (sept, 7.0)	34.5	—	128.9	—	128.8
3"	1.15 (d, 7.0)	19.3	7.06 (m)	138.0	7.08 (m)	138.0
4"	1.12 (d, 7.0)	19.0	1.49 (br d, 7.1)	14.0	1.52 (br d. 7.1)	14.0
5"		—	1.85 (br s)	12.2	1.87 (br s)	12.2

[a]δ ppm (mult., *J* in Hz), 500 MHz. [b]δ ppm, 125 MHz.

3.4.5. Compounds **46** and **47**

The molecular formulae of **46** and **47** were determined as $C_{30}H_{42}O_8$ on the basis of the HRESIMS. The ^{1}H and ^{13}C NMR spectra of **46** and **47** were closely correlated with those of **44** and **45**, respectively, indicating that they are also a pair of C-13 epimers. However, the signals attributed to C-4 and C-18 were appeared in higher field in the ^{13}C NMR spectra of **46** and **47** as compared with **44** and **45**, whose chemical shifts rather resembled with those of **41** and **42**. Therefore, the presence of an epoxy group between C-4 and C-18 was suggested, which was in good agreement with their degree of unsaturation. The ^{1}H-^{1}H COSY and the HMBC correlations of **46** and **47** were consistent with this structure (Fig.

3.14). The configurations of the C-18 oxymethylene were elucidated as β from the ROESY correlations of H-6 with H-18a and H-10. The relative configurations of A, B-rings were elucidated to be the same as those seen in **44** and **45**. The 13*R** configuration of **46** was assigned from the ROESY cross peak between H-14a (δ_H 2.94) and Me-17, while the ROESY correlation of H_2-16 with Me-17 in **47** indicated the configuration at C-13 to be *S**. Thus, the structures of **46** and **47** were characterized as shown in Figure 3.13.

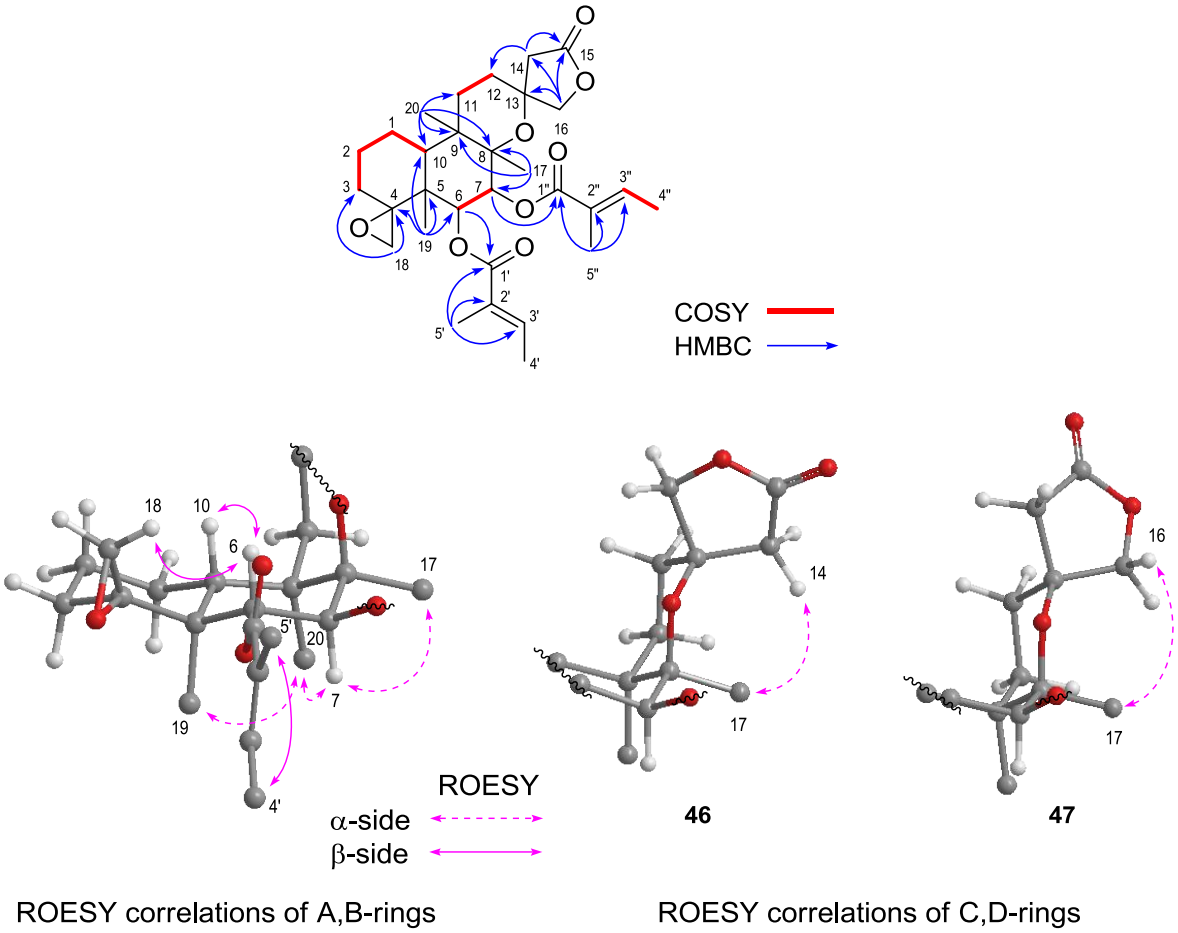

Figure 3.14. Key 2D NMR correlations of **46** and **47**.

3.4.6. Compounds **48-50**

Compounds **48** and **49** were found to possess the same molecular formula of $C_{27}H_{38}O_8$ by the HRESIMS experiments. The ^1H and ^{13}C NMR spectra of **48** and **49** were correlated with those of **46** and **47**, respectively, suggesting that **48** and **49** are a pair of C-13 epimers as well. However, the signals due to one of tigloyl groups were absent, but instead the signals ascribable to an acetyl group were observed in each case. The location of the acetyl group was assigned to be at C-7 from the HMBC correlation of H-7 with C-1" (Fig. 3.15). The relative configuration of **48** was determined to be the same as that of **46**, while **49** had the

same relative configuration as **47** by the analyses of ROESY spectra. From these observations, the structures of **48** and **49** were assigned as shown in Figure 3.16.

The molecular formula of **50** was established as $C_{29}H_{42}O_8$ from the HRESIMS. The ^{1}H and ^{13}C NMR spectra were similar to those of **49** except for the appearance of signals due to an isobutyryl group instead of the acetyl group. The position of the isobutyryl group was determined to be at C-7 from the HMBC correlations of H-7 [δ_H 5.54 (d, J = 10.2 Hz)] with C-1" (δ_C 176.9). The relative configuration of **50** was concluded to be the same as those of **47** and **49** by the analysis of ROESY spectrum. Therefore, the structure of **50** was characterized as shown (Fig. 3.16).

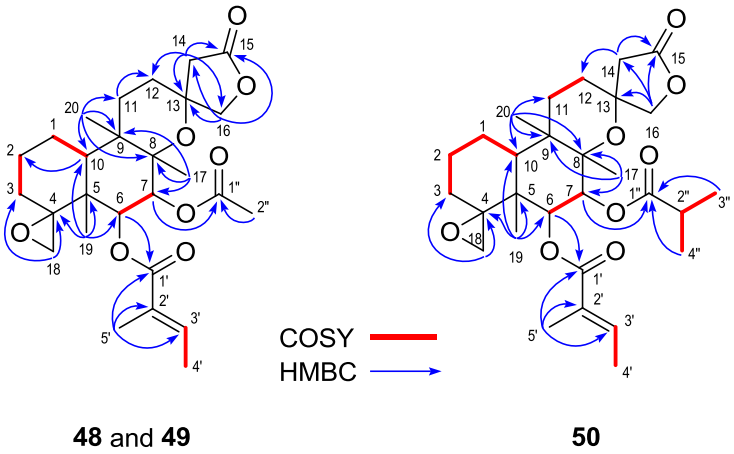

Figure 3.15. Key 2D NMR correlations of **48**-**50**.

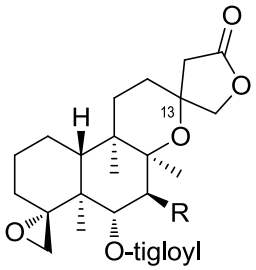

	R	C-13
46	O-tigloyl	*R**
47	O-tigloyl	*S**
48	O-Ac	*R**
49	O-Ac	*S**
50	O-isobutyryl	*S**

Figure 3.16. The structures of **46**-**50**.

Table 3.4. ^{1}H NMR data of **46-50** in pyridine-d_5.

Position	**46**	**47**	**48**	**49**	**50**
1	1.37 (m)	1.38 (m)	1.36 (m)	1.36 (m)	1.38 (m)
2	1.76 (m)	1.78 (m)	1.74 (m)	1.76 (m)	1.77 (m)
	1.36 (m)	1.37 (m)	1.34 (m)	1.36 (m)	1.37 (m)
3	2.07 (m)	2.07 (br t, 12.6)	2.05 (br t, 13.2)	2.06 (br t, 12.7)	2.06 (br t, 12.7)
	0.93 (br d, 12.2)	0.93 (br d, 12.6)	0.92 (m)	0.92 (br d, 12.7)	0.92 (br d, 12.7)
6	5.69 (d, 10.3)	5.69 (d, 10.3)	5.64 (d, 10.3)	5.64 (d, 10.2)	5.64 (d, 10.2)
7	5.61 (d, 10.3)	5.61 (d, 10.3)	5.53 (d, 10.3)	5.52 (d, 10.2)	5.54 (d, 10.2)
10	2.21 (dd, 3.2, 11.0)	2.22 (br d, 11.2)	2.18 (dd, 2.7, 11.0)	2.19 (br d, 11.2)	2.19 (br d, 10.7)
11	1.58 (m)	1.56 (m)	1.57 (m)	1.55 (m)	1.56 (m)
12	1.81 (m)	1.74 (m)	1.80 (m)	1.69 (m)	1.72 (m)
	1.55 (m)	1.60 (m)	1.55 (m)	1.58 (m)	1.61 (m)
14	2.94 (d, 16.8)	3.05 (d, 17.0)	2.98 (d, 16.8)	2.94 (d, 17.1)	2.96 (d, 17.2)
	2.81 (d, 16.8)	2.62 (d, 17.0)	2.85 (d, 16.8)	2.58 (d, 17.1)	2.59 (d, 17.2)
16	4.30 (d, 8.9)	4.31 (d, 8.6)	4.21 (d, 8.8)	4.34 (d, 8.6)	4.36 (d, 8.7)
	4.17 (d, 8.9)	4.21 (d, 8.6)	4.14 (d, 8.8)	4.25 (d, 8.6)	4.28 (d, 8.7)
17	1.31 (s)	1.24 (s)	1.29 (s)	1.21 (s)	1.14 (s)
18	3.65 (dd, 2.3, 4.1)	3.64 (dd, 2.2, 4.3)	3.61 (dd, 2.3, 4.2)	3.60 (dd, 2.3, 4.1)	3.61 (dd, 2.2, 4.2)
	2.38 (d, 4.1)	2.38 (d, 4.3)	2.38 (d, 4.2)	2.38 (d, 4.1)	2.38 (d, 4.2)
19	1.45 (s)	1.44 (s)	1.43 (s)	1.42 (s)	1.44 (s)
20	0.83 (s)	0.83 (s)	0.81 (s)	0.80 (s)	0.82 (s)
3'	6.88 (m)	6.89 (m)	6.97 (m)	6.97 (m)	6.96 (m)
4'	1.50 (br d, 7.1)	1.50 (br d, 7.2)	1.55 (dd, 0.9, 7.1)	1.55 (dd, 0.8, 7.0)	1.57 (br d, 7.0)
5'	1.81 (br s)	1.81 (br s)	1.87 (br s)	1.87 (br s)	1.87 (br s)
2"	—	—	1.96 (s)	2.00 (s)	2.59 (m)
3"	7.04 (m)	7.06 (m)			1.13 (d, 7.0)
4"	1.50 (br d, 7.1)	1.52 (br d, 7.1)			1.10 (d, 7.0)
5"	1.83 (br s)	1.85 (br s)			

δ ppm (mult., *J* in Hz), 500 MHz.

Table 3.5. ^{13}C NMR data of **46-50** in pyridine-d_5.

Position	**46**	**47**	**48**	**49**	**50**
1	20.9	20.9	20.8	20.7	20.8
2	25.1	25.1	25.0	25.0	25.1
3	32.1	32.1	32.0	32.0	32.0
4	66.9	66.8	66.8	66.8	66.9
5	43.0	43.1	42.9	42.9	43.0
6	71.3	71.4	71.1	71.2	71.1
7	74.6	74.5	74.5	74.4	73.8
8	81.4	81.2	81.1	80.9	81.0
9	38.3	38.4	38.2	38.3	38.3
10	41.5	41.6	41.3	41.3	41.4
11	27.6	27.6	27.4	27.4	27.5
12	28.5	28.3	28.8	28.5	28.4
13	76.3	76.7	76.2	76.6	76.7
14	42.6	44.3	42.5	43.9	44.1
15	175.4	174.0	175.3	174.0	174.0
16	79.6	76.9	79.3	76.8	76.9
17	20.3	20.0	20.0	19.7	19.8
18	52.0	52.0	52.0	51.9	52.0
19	15.4	15.4	15.3	15.6	15.5
20	20.5	20.4	20.4	20.3	20.3
1'	166.9	166.8	166.7	166.7	166.7
2'	129.5	129.5	129.3	129.3	129.4
3'	136.7	136.5	137.0	137.0	137.1
4'	14.1	14.0	14.1	14.1	14.1
5'	12.2	12.2	12.3	12.3	12.3
1"	168.0	168.0	170.9	170.9	176.9
2"	128.6	128.6	20.6	20.6	34.4
3"	138.3	136.5	—	—	19.2
4"	14.2	14.0	—	—	18.9
5"	12.3	12.2	—	—	—

δ ppm, 125 MHz.

3.4.7. Compounds **51**-**55**

The molecular formulae of **51** and **52** were assigned as $C_{30}H_{40}O_9$ by the HRESIMS. The ^{1}H and ^{13}C NMR data of **51** were similar to those of **46** except for the observation of a signal ascribable to an aldehyde group instead of one of *tert*-methyl signals. The aldehyde group at C-5 was assigned by the HMBC correlation of the aldehyde proton signal (δ_H 10.6, s) with C-4 (δ_C 64.1), C-5 (δ_C 57.2), C-6 (δ_C 70.1) and C-10 (δ_C 43.5) (Fig. 3.17). The relative configurations were determined as the same as those of **46** by the NOESY and ROESY experiments, in which the α configuration of the aldehyde group was elucidated from the NOESY correlations of H-7 with H-19, Me-17 and Me-20. Compound **52** was assigned as the C-13 epimer of **51** by comparison of the ^{1}H and ^{13}C NMR spectra of **52** with those of **51**, coupled with the analyses of 2D NMR spectra (Figures 3.17 and 3.18). Therefore, the structures of **51** and **52** were concluded as shown in Figure 3.19.

The same molecular formula of $C_{27}H_{36}O_9$ for **53** and **54** was determined on the basis of the HRESIMS. The C-13 epimeric relationship of **53** and **54** was suggested by analysis of

the ^{1}H and ^{13}C NMR spectra; the ^{1}H and ^{13}C NMR spectra of **53** and **54** were quite similar to those of **51** and **52**, respectively, except for the appearance of an acetyl signal instead of the signals due to one of tigloyl groups. The presence of the acetyl group at C-7 was assigned from the HMBC correlation of H-7 with C-1". The analyses of the ^{1}H-^{1}H COSY and HMBC spectra of **53** and **54** confirmed that they had the same planner structure (Fig. 3.17). The relative configurations of **53** and **54** were elucidated to be the same as **51** and **52**, respectively, by the analyses of ROESY spectra (Fig. 3.18). Thus, the structures of **53** and **54** were determined as shown (Fig. 3.19).

A pseudo-molecular ion peak at *m/z* 555.2565 (calcd for 555.2570 $[M+Na]^{+}$), observed in positive HRESIMS of **55**, indicated the molecular formula of $C_{29}H_{40}O_9$. The ^{1}H and ^{13}C NMR spectra of **55** were correlated with those of **54**, but the signals ascribable to an isobutyryl group were observed instead of the signals due to the acetyl group seen in **54**.

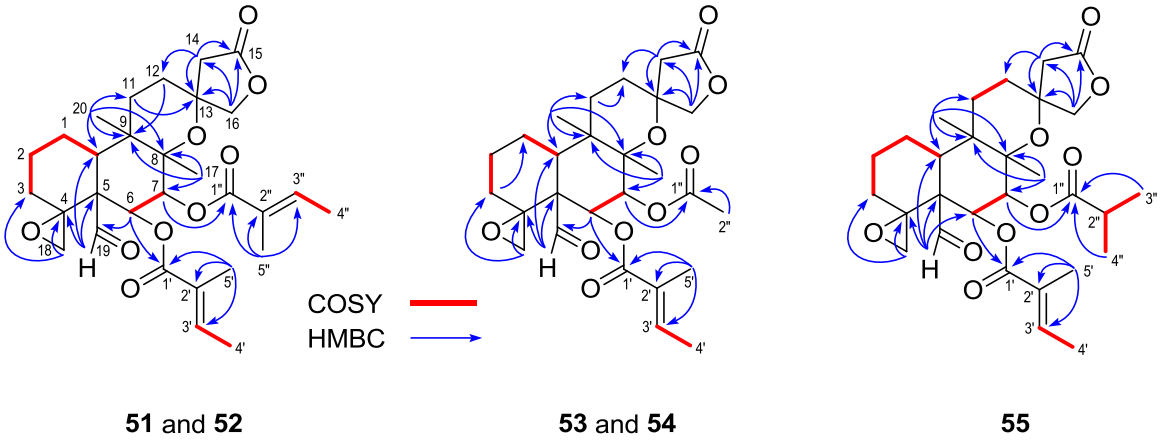

Figure 3.17. Key 2D NMR correlations of **51**-**55**.

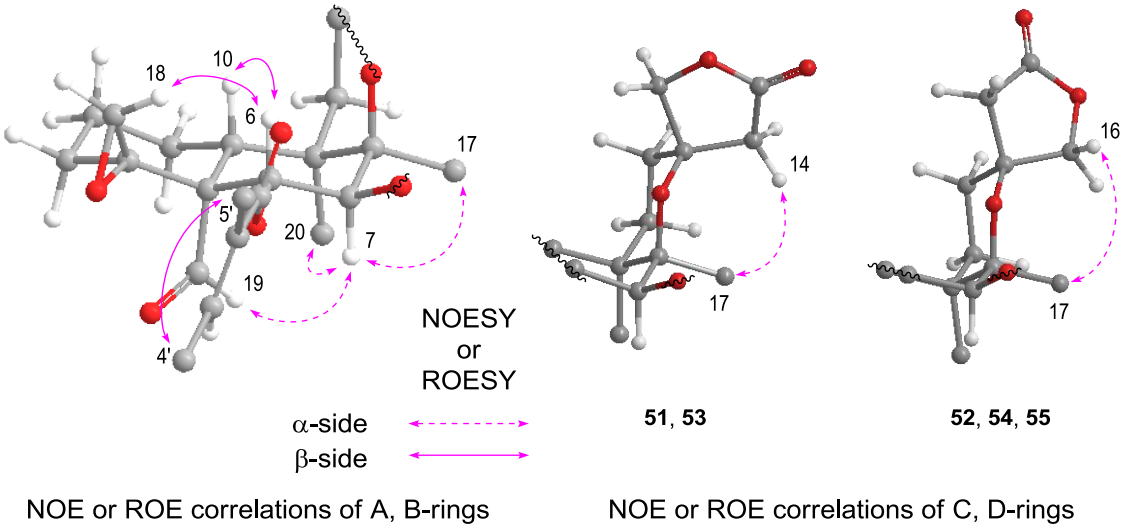

Figure 3.18. Key NOE or ROE correlations of **51**-**55**.

The presence of the isobutyryl group at C-7 was elucidated from the HMBC correlations of H-7 [δ_H 5.79 (d, J = 10.5 Hz)] with C-1" (δ_C 176.7). The ROESY data showed that the relative configurations of **55** were identical with **54**. From these data, the structure of **55** was characterized as shown in Figure 3.19.

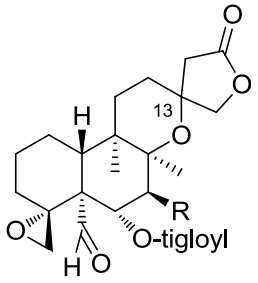

	R	C-13
51	O-tigloyl	*R**
52	O-tigloyl	*S**
53	O-Ac	*R**
54	O-Ac	*S**
55	O-isobutyryl	*S**

Figure 3.19. The structures of **51**-**55**.

Table 3.6. ^{1}H NMR data of **51-55** in pyridine-d_5.

Position	**51**	**52**	**53**	**54**	**55**
1	1.58 (m)	1.56 (m)	1.51 (m)	1.50 (m)	1.55 (m)
	1.46 (m)	1.48 (m)	1.43 (m)	1.43 (m)	1.47 (m)
2	1.83 (m)	1.84 (m)	1.81 (m)	1.83 (m)	1.83 (m)
	1.44 (m)	1.48 (m)	1.45 (m)	1.44 (m)	1.46 (m)
3	2.54 (br t, 13.0)	2.54 (br t, 13.7)	2.52 (ddd, 2.2, 4.5, 13.3)	2.53 (ddd, 2.2, 4.4, 13.2)	2.53 (m)
	1.13 (br d, 13.0)	1.14 (br d, 13.7)	1.13 (br d, 13.3)	1.14 (br d, 13.2)	1.14 (m)
6	5.94 (d, 10.5)	5.94 (d, 10.5)	5.88 (d, 10.5)	5.88 (d, 10.5)	5.89 (d, 10.5)
7	5.85 (d, 10.5)	5.85 (d, 10.5)	5.77 (d, 10.5)	5.77 (d, 10.5)	5.79 (d, 10.5)
10	2.41 (m)	2.42 (m)	2.39 (m)	2.39 (d, 12.9)	2.39 (m)
11	1.66 (m)	1.64 (m)	1.64 (m)	1.66 (m)	1.67 (m)
				1.60 (m)	1.60 (m)
12	1.83 (m)	1.75 (m)	1.80 (m)	1.66 (m)	1.70 (m)
	1.62 (m)	1.67 (m)	1.61 (m)		
14	2.99 (d, 16.8)	3.08 (d, 17.0)	3.01 (d, 16.9)	2.97 (d, 17.1)	2.99 (d, 17.0)
	2.87 (d, 16.8)	2.66 (d, 17.0)	2.89 (d, 16.9)	2.61 (d, 17.1)	2.62 (d, 17.0)
16	4.32 (d, 8.8)	4.36 (d, 8.7)	4.23 (d, 8.9)	4.38 (d, 8.6)	4.40 (d, 8.7)
	4.19 (d, 8.8)	4.25 (d, 8.7)	4.16 (d, 8.9)	4.28 (d, 8.6)	4.32 (d, 8.7)
17	1.37 (s)	1.28 (s)	1.34 (s)	1.26 (s)	1.26 (s)
18	3.53 (br s)	3.52 (br s)	3.49 (dd, 2.3, 4.1)	3.48 (dd, 2.3, 4.2)	3.49 (dd, 2.2, 3.9)
	2.40 (d, 3.8)	2.41 (d, 4.1)	2.40 (d, 4.1)	2.41 (d, 4.2)	2.41 (d, 3.9)
19	10.62 (s)	10.61 (s)	10.59 (s)	10.59 (s)	10.59 (s)
20	0.96 (s)	0.96 (s)	0.95 (s)	0.94 (s)	0.95 (s)
3'	6.83 (m)	6.84 (m)	6.92 (m)	6.92 (m)	6.90 (m)
4'	1.44 (br d, 6.9)	1.44 (br d, 7.0)	1.49 (br dd, 1.0, 7.0)	1.50 (br d, 7.1)	1.50 (br d, 7.1)
5'	1.75 (br s)	1.75 (br s)	1.81 (br t, 1.3)	1.81 (br t, 1.3)	1.81 (s)
2"	—	—	1.97 (s)	2.02 (s)	2.56 (sept, 7.0)
3"	7.03 (m)	7.06 (m)			1.12 (d, 7.0)
4"	1.50 (br d, 7.0)	1.53 (br d, 7.1)			1.09 (d, 7.0)
5"	1.82 (br s)	1.83 (br s)			

δ ppm (mult., *J* in Hz), 500 MHz.

Table 3.7. ^{13}C NMR data of **51-55** in pyridine-d_5.

Position	**51**	**52**	**53**	**54**	**55**
1	22.0	22.0	21.9	21.9	22.0
2	25.3	25.3	25.4	25.3	25.3
3	33.1	33.1	33.0	33.0	33.1
4	64.1	64.1	64.0	64.0	64.1
5	57.2	57.2	57.2	57.2	57.4
6	70.1	70.2	70.0	70.0	69.9
7	74.1	73.9	74.1	73.9	73.3
8	81.2	81.0	81.0	80.7	80.9
9	38.4	38.4	38.3	38.5	38.3
10	43.5	43.5	43.4	43.4	43.5
11	27.2	27.2	27.1	27.1	27.2
12	28.6	28.4	28.9	28.6	28.5
13	76.5	76.9	76.4	76.8	76.9
14	42.5	44.1	42.4	43.9	44.0
15	175.2	174.0	175.1	173.8	173.9
16	79.4	76.7	79.4	76.6	76.8
17	20.3	20.0	20.0	19.7	19.8
18	49.8	49.8	49.8	49.8	49.8
19	204.4	204.4	204.2	204.2	204.3
20	21.3	21.1	21.2	21.0	21.1
1'	166.5	166.5	166.4	166.4	166.4
2'	128.7	128.7	128.7	128.7	128.8
3'	138.0	137.9	138.2	138.2	138.4
4'	14.1	14.1	14.1	14.1	14.2
5'	12.1	12.1	12.1	12.1	12.2
1"	167.7	167.7	170.7	170.7	176.7
2"	128.3	128.3	20.5	20.5	34.4
3"	138.7	138.7	—	—	19.2
4"	14.2	14.2	—	—	18.9
5"	12.1	12.2	—	—	—

δ ppm, 125 MHz.

3.4.8. Compounds **56-61**

The molecular formulae of **56** and **57** were established as $C_{30}H_{42}O_9$ by the HRESIMS. The ^{1}H and ^{13}C NMR spectra of **56** and **57** were similar to those of **46** and **47**, respectively, except for the appearance of a hydroxymethyl signal instead of one of *tert*-methyl signals. The presence of the hydroxymethyl at C-5 was assigned by the HMBC correlations of H_2-19 with C-4, C-5, C-6 and C-10 in each case (Fig. 3.20). The relative configurations at C-13 of **56** and **57** were assigned as *R** and *S**, respectively, from the ROESY correlations shown in Figure 3.21. From these data, the structures of **56** and **57** were elucidated as shown (Fig. 3.22).

Compounds **58** and **59** were found to possess the same molecular formula ($C_{27}H_{38}O_9$) from the HRESIMS. The presence of an acetyl group at C-7 in **58** and **59** instead of the tigloyl group seen in **56** and **57** was suggested by comparisons of the ^{1}H and ^{13}C NMR data of **58** and **59** with those of **56** and **57**. This was further confirmed by analyses of the ^{1}H-^{1}H COSY and HMBC spectra (Fig. 3.20). The assignment of the relative configurations of **58** and **59** to be the same as those seen in **56** and **57**, respectively, were revealed by the ROESY experiments (Fig. 3.21). From these observations, the structures of **58** and **59** were characterized as shown in Figure 3.22.

The molecular formulae of **60** and **61** were established as $C_{29}H_{42}O_9$ by HRESIMS. The ^{1}H and ^{13}C NMR spectra of **60** and **61** were closely related with those of **56** and **57**, respectively, but differed in the observation of the signals due to an isobutyryl group instead

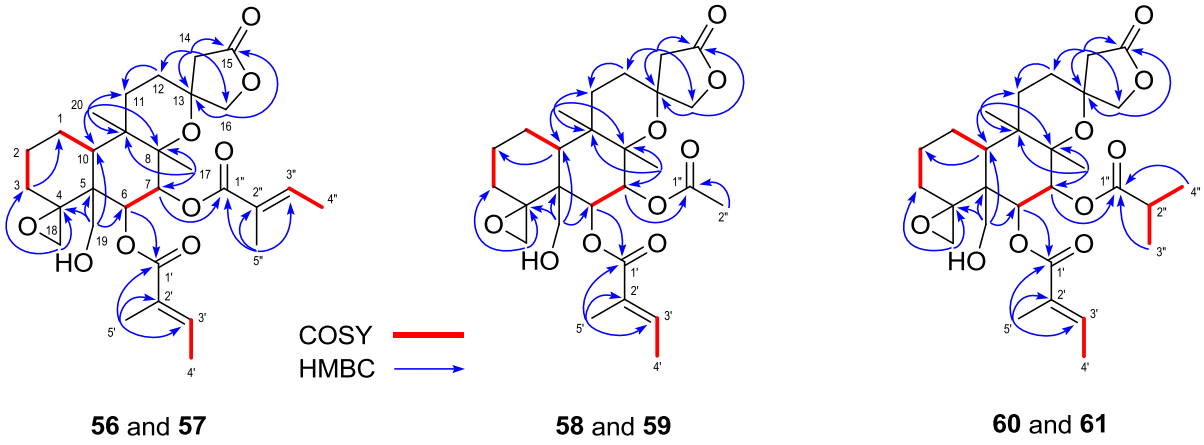

Figure 3.20. Key 2D NMR correlations of **56-61**.

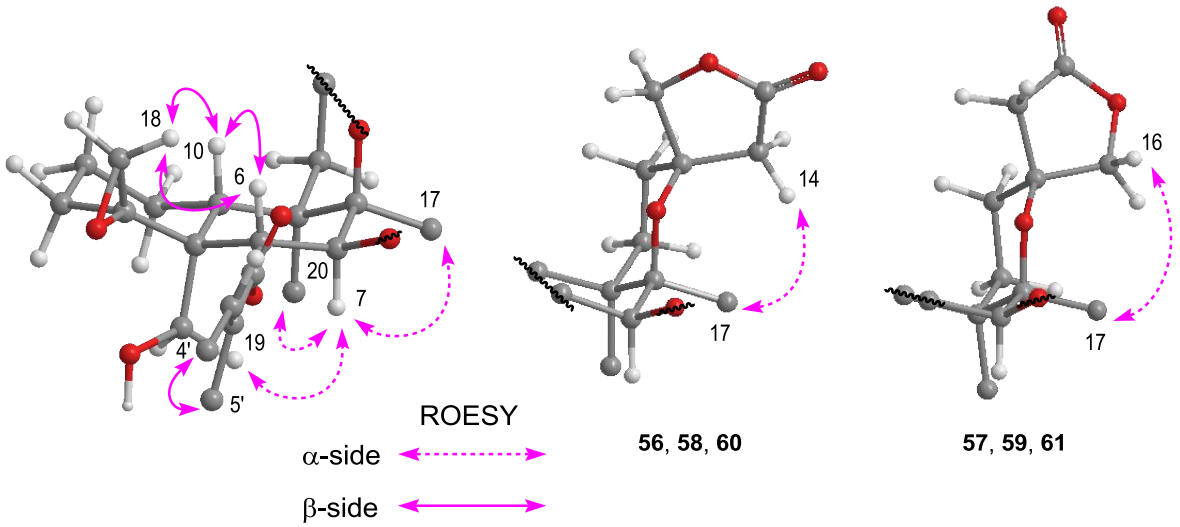

Figure 3.21. Key ROESY correlations of **56-61**.

of one of signals due to the tigloyl groups. The location of the isobutyryl group at C-7 was elucidated by the analyses of the ^{1}H-^{1}H COSY and HMBC spectra (Fig. 3.20). The relative configurations of C-13 in **60** and **61** were determined to be *R** and *S**, respectively, from the ROESY correlations (Fig. 3.21). Thus, the structures of **60** and **61** were elucidated as shown in Fig. 3.22.

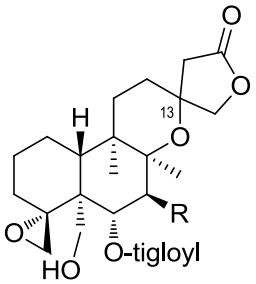

	R	C-13
56	O-tigloyl	*R**
57	O-tigloyl	*S**
58	O-Ac	*R**
59	O-Ac	*S**
60	O-isobutyryl	*R**
61	O-isobutyryl	*S**

Figure 3.22. The structures of **56**-**61**.

Table 3.8. ^{1}H NMR data of **56-61** in pyridine-d_5.

Position	**56**	**57**	**58**	**59**	**60**	**61**
1	1.64 (m)	1.65 (m)	1.65 (m)	1.62 (m)	1.67 (m)	1.63 (m)
	1.44 (m)	1.43 (m)	1.44 (m)	1.41 (m)	1.46 (m)	1.42 (m)
2	1.84 (m)	1.85 (m)	1.84 (m)	1.84 (m)	1.86 (m)	1.84 (m)
	1.45 (m)	1.46 (m)	1.44 (m)	1.45 (m)	1.47 (m)	1.45 (m)
3	2.49 (br t, 12.7)	2.49 (br t, 13.1)	2.47 (br t, 13.6)	2.47 (br t, 13.1)	2.50 (br t, 13.1)	2.46 (br t, 13.1)
	1.06 (br d, 12.7)	1.07 (br d, 13.1)	1.06 (br d, 13.6)	1.07 (br d, 13.1)	1.07 (m)	1.06 (m)
6	5.79 (d, 10.2)	5.79 (d, 10.2)	5.75 (d, 10.3)	5.75 (d, 10.3)	5.76 (d, 10.3)	5.75 (d, 10.2)
7	6.02 (d, 10.2)	6.02 (d, 10.2)	5.99 (d, 10.3)	5.98 (d, 10.3)	5.99 (d, 10.3)	5.97 (d, 10.2)
10	2.36 (m)	2.36 (m)	2.34 (dd, 2.4, 12.5)	2.34 (d, 12.2)	2.35 (m)	2.33 (m)
11	1.61 (m)	1.58 (m)	1.61 (m)	1.62 (m)	1.63 (m)	1.63 (m)
				1.57 (m)		1.57 (m)
12	1.80 (m)	1.73 (m)	1.80 (dd, 6.0, 12.6)	1.69 (m)	1.80 (dd, 6.1, 12.3)	1.71 (m)
	1.58 (m)	1.61 (m)	1.57 (m)	1.61 (m)	1.60 (m)	1.63 (m)
14	2.95 (d, 16.8)	3.07 (d, 17.0)	2.99 (d, 16.9)	2.97 (d, 17.1)	3.03 (d, 16.8)	2.98 (d, 17.0)
	2.83 (d, 16.8)	2.65 (d, 17.0)	2.85 (d, 16.9)	2.46 (d, 17.1)	2.87 (d, 16.8)	2.62 (d, 17.0)
16	4.32 (d, 8.8)	4.32 (d, 8.7)	4.24 (d, 8.8)	4.36 (d, 8.6)	4.28 (d, 8.8)	4.37 (d, 8.7)
	4.20 (d, 8.8)	4.23 (d, 8.7)	4.17 (d, 8.8)	4.26 (d, 8.6)	4.18 (d, 8.8)	4.30 (d, 8.7)
17	1.34 (s)	1.26 (s)	1.33 (s)	1.24 (s)	1.34 (s)	1.24 (s)
18	3.55 (br dd, 1.8, 4.0)	3.55 (br dd, 2.0, 4.0)	3.53 (dd, 2.2, 4.3)	3.51 (dd, 2.2, 4.2)	3.54 (dd, 2.3, 4.1)	3.51 (dd, 1.9, 4.3)
	2.34 (d, 4.0)	2.35 (d, 4.0)	2.34 (d, 4.3)	2.35 (d, 4.2)	2.35 (d, 4.1)	2.34 (d, 4.3)
19	4.66 (d, 11.5)	4.65 (d, 11.6)	4.64 (dd, 1.3, 11.7)	4.63 (d, 11.7)	4.66 (dd, 2.5, 11.6)	4.64 (br d, 11.7)
	4.42 (dd, 8.0, 11.5)	4.42 (dd, 7.9, 11.6)	4.42 (dd, 7.5, 11.7)	4.41 (br d, 11.7)	4.43 (dd, 7.8, 11.6)	4.40 (m)
20	0.96 (s)	0.96 (s)	0.96 (s)	0.96 (s)	0.98 (s)	0.95 (s)
3'	6.89 (m)	6.89 (m)	6.97 (m)	6.98 (m)	6.98 (m)	6.96 (m)
4'	1.39 (dd, 1.0, 7.0)	1.39 (br d, 7.1)	1.43 (dd, 1.0, 7.1)	1.44 (dd, 0.9, 7.1)	1.47 (dd, 0.9, 7.1)	1.45 (br d, 7.0)
5'	1.77 (br s)	1.78 (br s)	1.84 (br t, 1.4)	1.85 (br t, 1.3)	1.86 (br t, 1.2)	1.84 (br s)
2"	—	—	1.97 (s)	2.01 (s)	2.56 (sept, 7.0)	2.58 (sept, 6.9)
3"	7.04 (m)	7.06 (m)			1.14 (d, 7.0)	1.14 (d, 6.9)
4"	1.51 (br d, 7.0)	1.53 (dd, 1.2, 7.2)			1.10 (d, 7.0)	1.10 (d, 6.9)
5"	1.83 (br s)	1.85 (br s)				

δ ppm (mult., *J* in Hz), 500 MHz.

Table 3.9. ^{13}C NMR data of **56-61** in pyridine-d_5.

Position	**56**	**57**	**58**	**59**	**60**	**61**
1	20.9	20.9	20.9	20.8	20.9	20.8
2	25.3	25.4	25.3	25.3	25.4	25.3
3	32.8	32.8	32.8	32.8	32.9	32.6
4	66.2	66.3	66.2	66.2	66.3	66.2
5	47.2	47.2	47.2	47.2	47.3	47.2
6	71.7	71.8	71.6	71.7	71.5	71.5
7	74.8	74.7	74.9	74.7	74.3	74.1
8	81.4	81.2	81.3	81.0	81.4	81.1
9	38.0	38.1	38.0	38.0	38.0	38.0
10	42.1	42.1	42.1	42.1	42.1	42.0
11	27.4	27.5	27.4	27.4	27.4	27.4
12	28.3	28.4	29.0	28.7	28.9	28.5
13	76.2	76.8	76.2	76.6	76.3	76.9
14	42.6	44.2	42.6	44.0	42.7	44.0
15	175.3	174.1	175.3	174.0	175.3	174.0
16	79.5	76.7	79.5	76.8	79.6	76.6
17	20.2	20.1	20.0	19.8	20.2	19.8
18	49.4	49.4	49.5	49.5	49.5	49.4
19	62.0	62.0	61.9	61.9	62.0	61.9
20	20.0	20.0	20.0	19.9	20.0	19.8
1'	166.5	166.7	166.5	166.5	166.4	166.4
2'	129.1	129.1	129.1	129.1	129.2	129.1
3'	137.1	137.1	137.4	137.4	137.5	137.5
4'	13.9	14.0	14.0	14.0	14.0	14.0
5'	12.2	12.2	12.3	12.3	12.3	12.2
1"	167.9	168.0	170.9	170.9	176.9	176.8
2"	128.5	128.7	20.6	20.6	34.4	34.3
3"	138.2	138.3	—	—	19.3	19.2
4"	14.1	14.1	—	—	18.9	18.8
5"	12.1	12.2	—	—	—	—

δ ppm, 125 MHz.

3.4.9. Compound **62**

A pseudo-molecular ion peak at *m/z* 485.2148 (calcd for 485.2151 $[M+Na]^+$) in the positive-ion HRESIMS indicated the molecular formula of $C_{25}H_{34}O_8$. The ^{1}H and ^{13}C NMR spectra were quite similar to those of **46**. However, the signals ascribable to one of tigloyl groups, an oxymethine and one of tertiary methyls were absent, but instead the resonances due to one carboxyl group and an sp^3 methylene were observed. The positions of the methylene and carboxyl group were assigned at C-7 and C-19, respectively, from the ^{1}H-^{1}H COSY cross peak of H-6 [δ_H 5.65 (dd, J = 4.5, 11.9 Hz)]–H_2-7 [δ_H 2.71 (dd, J = 11.9, 12.8 Hz), 1.91 (m)], along with the HMBC correlations of H_2-18 with C-5 (δ_C 55.2), H-6 and H-10 with C-5 and carboxyl carbon (δ_C 175.6), and of Me-17 with C-7 (δ_C 39.4) (Fig. 3.23). The *trans*-fusion of A/B ring as well as the β orientations of H-6 and the C-18 oxymethylene were determined from the ROESY correlations of H-10 with H-6 and H-18a (δ_H 3.28), and of H-18a with H-6. The *R** configuration of C-13 was elucidated from the

ROESY correlations of H_2-14 with Me-17 (Fig. 3.23). On the basis of these observations, the structure of **62** was characterized as shown (Fig. 3.24).

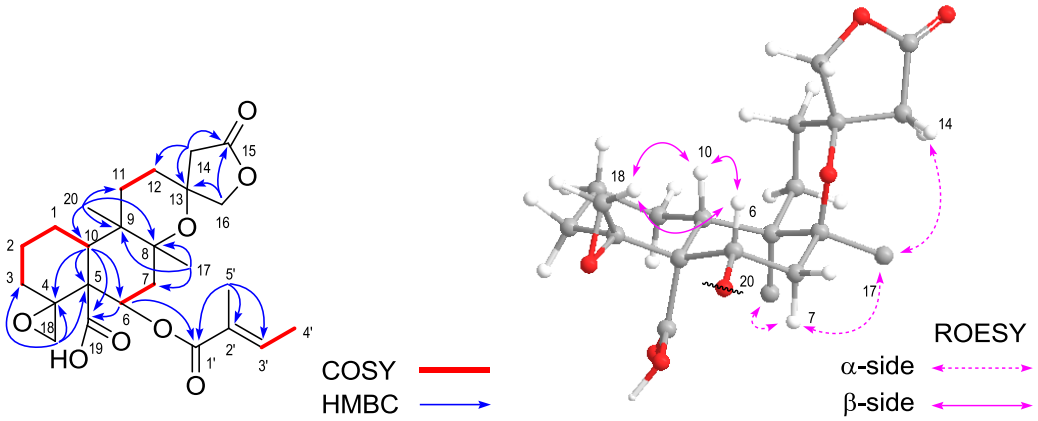

Figure 3.23. Key 2D NMR spectrum of **62**.

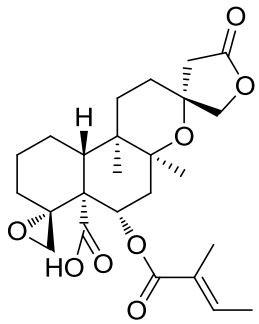

Figure 3.24. Key ROESY correlatins of **62**.

3.4.10. Compound **63**

The molecular formula of **63** was assigned as $C_{27}H_{38}O_8$ (*m/z* 513.2460, calcd for 513.2464 $[M+Na]^+$). Analyses of the ^1H and ^{13}C NMR spectra revealed that **63** possessed the same functional groups as **49**. But, the chemical shifts attributed to H-6 and H-7 were differed from those of **49**, implying that the locations of two acyl groups in **63** were interchanged with those seen in **49**. This was confirmed by the HMBC correlations of H-6 [δ_H 5.59 (d, *J* = 10.3 Hz)] with acetyl carbonyl carbon (δ_C 169.7), H-7 [δ_H 5.55 (d, *J* = 10.3 Hz)] with C-1" (δ_C 168.0), Me-17 with C-7 (δ_C 74.3), and of Me-19 with C-5 (δ_C 42.7) and C-6 (δ_C 71.6) (Fig. 3.25). The β configurations of H-6, and the C-18 oxymethylene were assigned from the NOESY correlations of H-6 with H-10 and H-18a (δ_H 3.55), while the NOESY correlations of H-7 with Me-17, Me-19, and Me-20 indicated that they were located on the α-face. The *S** configuration of C-13 was also assigned by the NOESY correlation of Me-17 with H_2-16. Therefore, the structure of **63** was elucidated as shown in Fig. 3.27.

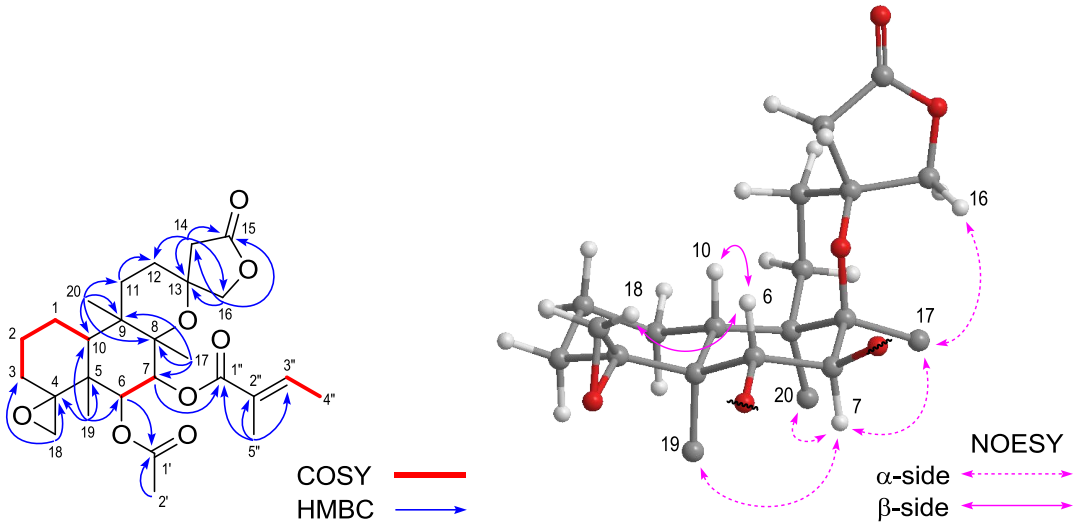

Figure 3.25. Key 2D NMR correlations of **63**.

3.3.11. Compound **64**

Compound **64** gave a pseudo-molecular ion peak at *m/z* 571.2872 (calcd for 571.2883 $[M+Na]^+$) in the positive ion HRESIMS, suggesting the molecular formula $C_{30}H_{44}O_9$. The ^1H and ^{13}C NMR spectra were correlated with those of **57** except for the absence of the signals for one of tigloyl groups, but instead the signals due to a 2-methylbutyryl group were observed. The location of the 2-methylbutyryl group was determined to be C-6 from the HMBC correlations of H_2-19 with C-5 (δ_C 47.1) and C-6 (δ_C 71.2), and of H-6 with C-1' (δ_C 174.9) (Fig. 3.26). The relative configuration of **64** was concluded to be the same as **57** by the analysis of ROESY spectrum (Fig. 3.26). Thus, the structure of **64** was determined as shown (Fig. 3.27).

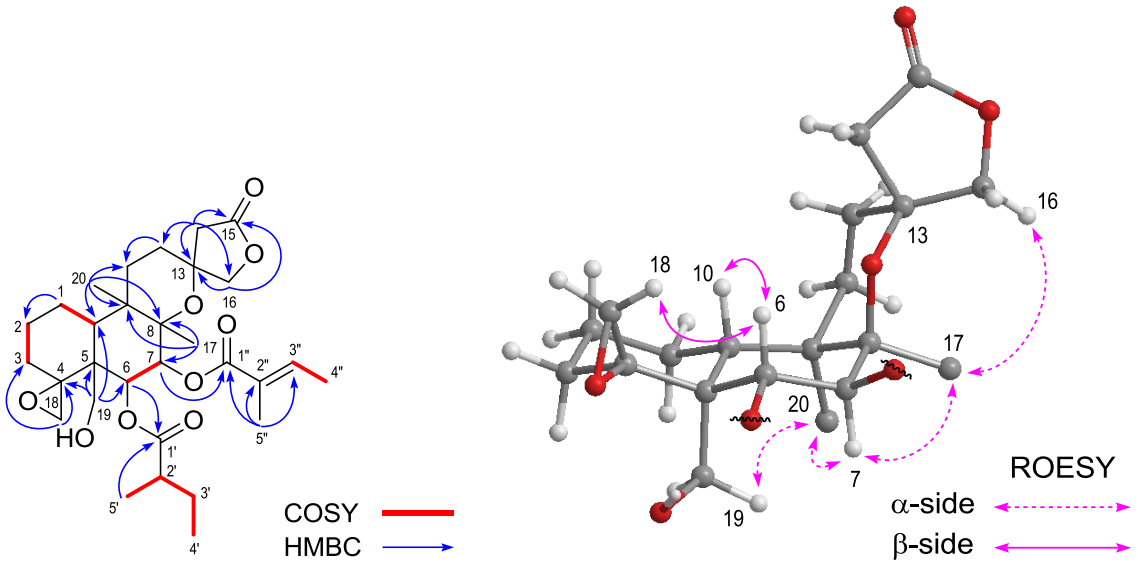

Figure 3.26. Key 2D correlations of **64**.

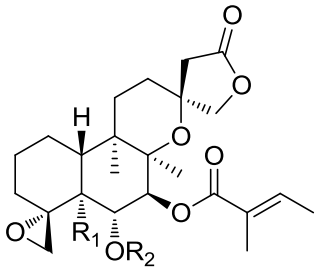

	R_1	R_2
63	CH_3	Ac
64	CH_2OH	2-methylbutyryl

Figure 3.27. The structures of **63** and **64**.

Table 3.10. ^{1}H and ^{13}C NMR data of **62-64** in pyridine-d_5.

	62		**63**		**64**	
Position	$^{1}H^{a}$	$^{13}C^{b}$	$^{1}H^{a}$	$^{13}C^{b}$	$^{1}H^{a}$	$^{13}C^{b}$
1	1.82 (m) 1.56 (m)	23.1	1.38 (m)	20.8	1.65 (m) 1.44 (m)	20.8
2	1.89 (m) 1.50 (m)	25.8	1.78 (m) 1.37 (m)	25.1	1.86 (m) 1.47 (m)	25.4
3	3.06 (br t, 13.4) 1.23 (m)	34.4	2.07 (br t, 12.5) 0.94 (br d, 12.5)	32.0	2.46 (br t, 13.1) 1.06 (m)	32.8
4	—	64.8	—	66.9	—	66.3
5	—	55.2	—	42.7	—	47.1
6	5.65 (dd, 4.5, 11.9)	69.4	5.59 (d, 10.3)	71.6	5.70 (d, 10.2)	71.2
7	2.71 (dd, 11.9, 12.8) 1.91 (m)	39.4	5.55 (d, 10.3)	74.3	6.01 (d, 10.2)	74.5
8	—	80.1	—	81.2	—	81.3
9	—	37.1	—	38.3	—	38.0
10	2.34 (d, 12.0)	44.3	2.19 (dd, 2.7, 11.4)	41.4	2.33 (m)	42.0
11	1.62 (m)	27.8	1.55 (m)	27.6	1.60 (m) 1.56 (m)	27.5
12	1.79 (m) 1.56 (m)	28.9	1.73 (m) 1.59 (m)	28.3	1.71 (dd, 5.5, 14.4) 1.61 (m)	28.3
13	—	76.4	—	76.7	—	76.6
14	2.89 (d, 16.6) 2.85 (d, 16.6)	42.4	3.03 (d, 17.0) 2.61 (d, 17.0)	42.3	3.04 (d, 16.9) 2.62 (d, 16.9)	44.2
15	—	175.6	—	174.0	—	174.1
16	4.26 (d, 8.7) 4.17 (d, 8.7)	79.9	4.31 (d, 8.7) 4.21 (d, 8.7)	76.8	4.30 (d, 8.7) 4.22 (d, 8.7)	76.9
17	1.19 (s)	24.6	1.23 (s)	20.0	1.24 (s)	20.1
18	3.28 (dd, 1.9, 4.3) 2.41 (d, 4.3)	50.8	3.55 (dd, 2.4, 4.1) 2.40 (d, 4.1)	51.9	3.43 (dd, 2.2, 4.1) 2.32 (d, 4.1)	49.4
19	—	174.4	1.39 (s)	15.4	4.59 (dd, 3.3, 11.9) 4.36 (dd, 7.9, 11.9)	61.8
20	1.19 (s)	20.8	0.81 (s)	20.3	0.96 (s)	19.8
1'	—	167.1	—	169.7	—	174.9
2'	—	129.5	1.94 (s)	21.0	2.26 (sext, 6.9)	41.2
3'	7.15 (m)	137.4		—	1.79 (m) 1.38 (m)	26.6
4'	1.48 (br d, 6.9)	14.1		—	0.85 (t, 7.5)	11.6
5'	1.90 (br s)	12.2		—	1.04 (d, 6.9)	16.3
1"		—	—	168.0	—	167.8
2"		—	—	128.6	—	128.6
3"		—	7.13 (m)	138.5	7.14 (m)	138.7
4"		—	1.58 (dd, 1.0, 7.1)	14.2	1.60 (dd, 0.8, 7.2)	14.2
5"		—	1.92 (br t, 1.3)	12.2	1.92 (br s)	12.3

[a] δ ppm (mult., *J* in Hz), 500 MHz. [b] δ ppm, 125 MHz.

3.4.12. Compounds **65-67**

The molecular formula of **65** was found to be $C_{29}H_{40}O_8$ by the HRESIMS. The ^1H and ^{13}C NMR spectra showed the presence of two tertiary methyls, six sp^3 methylenes, two oxymetylenes, one sp^3 methine, two oxymethines, one sp^3 quaternary carbon, two oxygen-bearing sp^3 quaternary carbons, one tetrasubstituted olefin, two tigloyl groups and one carbonyl carbon, indicating that **65** was an acylated *nor*-diterpenoid. These NMR data were similar to those of **46**, **51** and **56** except for the resonances arising from the A-ring moiety. The structure of the A-ring was elucidated as shown in Figure 3.28. The lack of the C-19 as well as the presence of a double bond at C-4(5) were elucidated from the ^1H-^1H COSY correlations of H-1–H_2-2–H_2-3, coupled with the HMBC correlations of H-3 and H-18 with C-4 (δ_C 137.5), H-6 with C-4, C-5 (δ_C 127.2), H-10 with C-5, and of Me-20 with C-10 (δ_C 36.7). The relative configuration of **65** was assigned as the same as **46**, **51** and **56** by the ROESY experiment (Fig. 3.29). From the evidence described above, compound **65** was characterized as 19-*nor*-*neo*-clerodane type diterpenoid shown in Figure 3.30.

Compound **66** had the same molecular formula ($C_{29}H_{40}O_8$) as **65**, and its ^1H and ^{13}C NMR spectra were closely similar to **65** except for the chemical shifts of C-14 (**65**: δ_C 42.7; **66**: δ_C 44.2) and C-16 (**65**: δ_C 79.5; **66**: δ_C 76.9), indicating that **66** is the C-13 epimer of **65**. This was further confirmed by detailed analyses of the ^1H-^1H COSY, HMBC and ROESY data (Figures 3.28 and 3.29). Thus, the structure of **66** was determined as shown (Fig. 3.30).

The positive-ion HRESIMS of **67** showed a pseudo-molecular ion peak at *m/z* 527.2631 (calcd for 527.2621 $[M+Na]^+$), suggesting the molecular formula $C_{28}H_{40}O_8$. The ^1H and ^{13}C NMR spectra were correlated with those of **66**. However, the signals due to an isobutyl group were observed instead of the signals attributed to one of the tigloyl groups seen in **66**. The location of the isobutyl group at C-7 was assigned from the ^1H-^1H COSY correlations of H-6 [δ_H 6.20 (d, J = 10.9 Hz)]–H-7 [δ_H 5.53 (d, J = 10.9 Hz)], as well as the HMBC cross peaks of Me-17 with C-7 (δ_C 76.4), C-9 (δ_C 41.0), and of H-7 with C-1" (δ_C 176.7) (Fig. 3.28). The stereochemistry of **67** was concluded to be identical with that of **66** on the basis of ROESY correlations shown in Fig. 3.29. Therefore, the structure of **67** was established as shown in Figure 3.30.

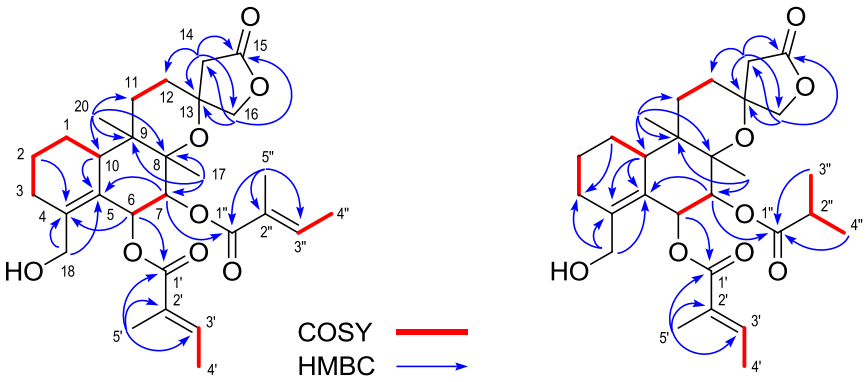

Figure 3.28. Key 2D NMR correlations of **65-67**.

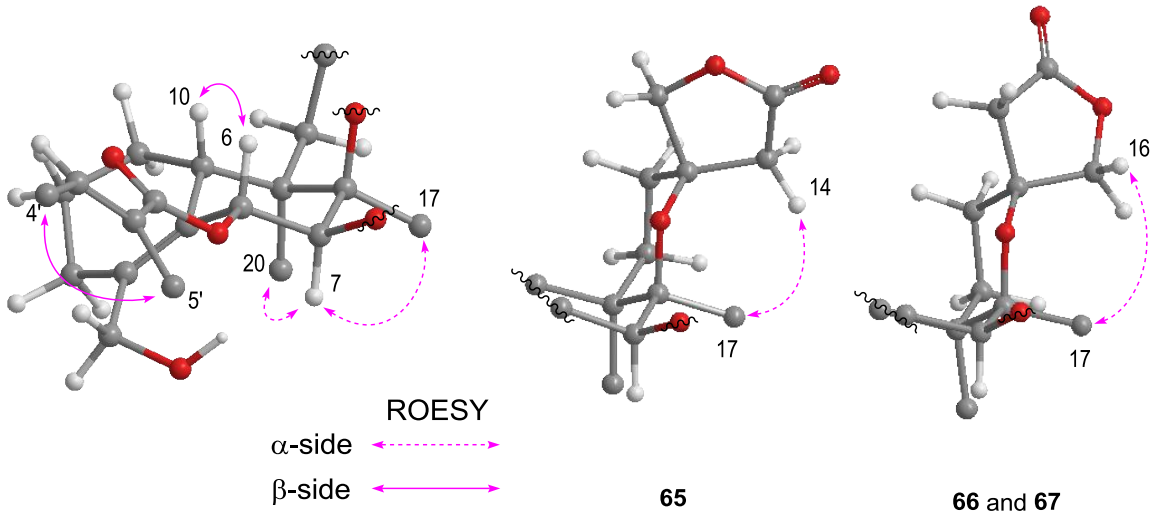

Figure 3.29. Key ROESY correlations of **65-67**.

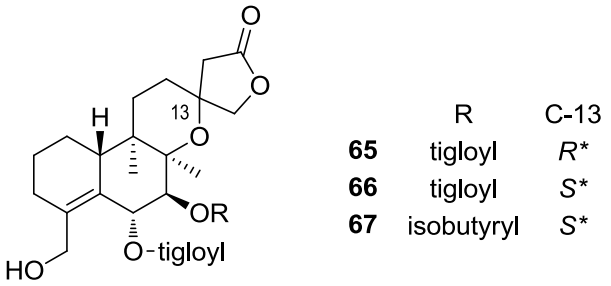

	R	C-13
65	tigloyl	*R**
66	tigloyl	*S**
67	isobutyryl	*S**

Figure 3.30. The structures of **65-67**.

Table 3.11. ^{1}H and ^{13}C NMR data of **65-67** in pyridine-d_5.

	65		**66**		**67**	
Position	$^{1}H^{a}$	$^{13}C^{b}$	$^{1}H^{a}$	$^{13}C^{b}$	$^{1}H^{a}$	$^{13}C^{b}$
1	1.52 (m)	23.3	1.52 (m)	23.4	1.53 (m)	23.4
	1.17 (m)		1.15 (m)		1.16 (m)	
2	1.66 (m)	22.6	1.65 (m)	22.6	1.65 (m)	22.6
	1.26 (m)		1.25 (m)		1.26 (m)	
3	2.52 (br d, 17.6)	29.7	2.52 (br d, 16.9)	29.4	2.51 (br d, 17.2)	29.5
	2.11 (m)		2.11 (m)		2.11 (m)	
4	—	137.5	—	137.5	—	137.6
5	—	127.2	—	127.5	—	127.3
6	6.23 (d, 11.0)	74.5	6.25 (d, 10.9)	74.5	6.20 (d, 10.9)	74.3
7	5.61 (d, 11.0)	77.2	5.60 (d. 10.9)	77.1	5.53 (d, 10.9)	76.4
8	—	80.9	—	80.8	—	80.7
9	—	41.0	—	41.0	—	41.0
10	3.10 (br t, 8.3)	36.7	3.11 (br t, 8.2)	36.7	3.10 (br t, 8.4)	36.7
11	1.65 (m)	25.5	1.64 (m)	25.6	1.64 (m)	25.6
	1.41 (br d, 14.5)		1.38 (m)		1.39 (m)	
12	1.82 (m)	28.4	1.78 (m)	28.2	1.78 (m)	28.3
	1.56 (m)		1.61 (m)		1.63 (m)	
13	—	76.5	—	77.0	—	77.0
14	2.96 (d, 16.8)	42.7	3.05 (d, 17.0)	44.2	2.98 (d, 17.1)	44.2
	2.81 (d, 16.8)		2.61 (d, 17.0)		2.57 (d, 17.1)	
15	—	175.4	—	174.0	—	174.2
16	4.29 (d, 8.9)	79.5	4.31 (d, 8.8)	76.9	4.34 (d, 8.8)	77.0
	4.13 (d, 8.9)		4.25 (d, 8.8)		4.29 (d, 8.8)	
17	1.34 (s)	21.0	1.27 (s)	20.8	1.25 (s)	20.7
18	4.73 (dd, 3.5, 11.8)	61.6	4.72 (br d, 12.6)	61.6	4.68 (br s)	61.7
	4.68 (dd, 4.0, 11.8)		4.69 (br d, 12.6)			
20	0.69 (s)	17.7	0.68 (s)	17.6	0.69 (s)	17.6
1'	—	167.0	—	166.9	—	166.8
2'	—	129.0	—	129.1	—	129.2
3'	7.01 (m)	137.9	7.01 (m)	137.9	7.05 (m)	138.1
4'	1.51 (br d, 7.1)	14.1	1.51 (br dd, 1.0, 7.0)	14.2	1.58 (br d, 7.1)	14.3
5'	1.85 (br t, 1.3)	12.2	1.85 (br s)	12.2	1.92 (br s)	12.3
1"	—	167.9	—	167.9	—	176.7
2"	—	128.7	—	128.8	2.61 (sept, 7.0)	34.4
3"	7.05 (m)	138.2	7.07 (m)	138.2	1.18 (d, 7.0)	19.3
4"	1.51 (br d, 7.1)	14.2	1.52 (br dd, 1.0, 7.1)	14.2	1.13 (d, 7.0)	18.9
5"	1.86 (br t, 1.3)	12.2	1.88 (br s)	12.2		—

[a]δ ppm (mult., *J* in Hz), 500 MHz. [b]δ ppm, 125 MHz.

3.4.13. Compounds **68** and **69**

Compounds **68** and **69** were found to possess the same molecular formula $C_{25}H_{34}O_8$. The ^{1}H and ^{13}C NMR spectra of **68** and **69** showed the presence of the same functional groups described below; two tertiary methyls, seven sp^3 methylenes, two sp^3 oxymethylenes, one sp^3 methine, one sp^3 oxymethine, two sp^3 quaternary carbons, three oxygen-bearing sp^3 quaternary carbons, one tigloyl group and two carbonyl carbons. These data implied that **68** and **69** are a pair of C-13 epimers of *neo*-clerodane type diterpenoid with a 13-*spiro*-15,16-γ-lactone moiety. The ^{1}H-^{1}H COSY and HMBC correlations shown in Figure 3.31

indicated the existence of the partial structures of B, C and D-rings as seen in **62**. The presence of a 18,19-γ-lactone moiety was elucidated from the ^{1}H-^{1}H COSY correlations of H_2-2−H_2-3, together with the HMBC correlations of H_2-18 with C-3, C-4, C-5 and C-19, and of H-10 with C-5 with C-18. The location of the tigloyl group was assigned at C-4 in each case, from the chemical shift of C-4 and the long range coupling between 6-OH and H-6 observed in the ^{1}H-^{1}H COSY spectrum (Fig. 3.31). This was further confirmed by observation of deuterium-induced shift of C-6 (Δδ 0.11 ppm) measured in CD_3OD and CD_3OH [61]. The chair conformation of A-ring and the *cis*-fusion of A/E ring were determined from the ROESY correlations of H-10 with H-2ax, H-3ax with H-1ax, and of H-18 with H_2-3. The configuration of C-13 of **68** was assigned as *R** from the ROESY correlations of Me-17 with H_2-14, while the ROESY correlation between Me-17 and H_2-16 revealed the *S** configuration of C-13 of **69** (Fig. 3.32). Thus, the structures of **68** and **69** were characterized as shown Fig. 3.33.

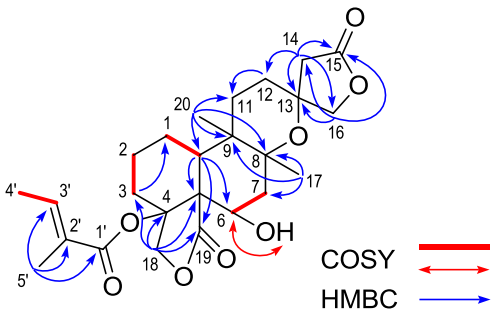

Figure 3.31. Key 2D NMR correlations of **68** and **69**.

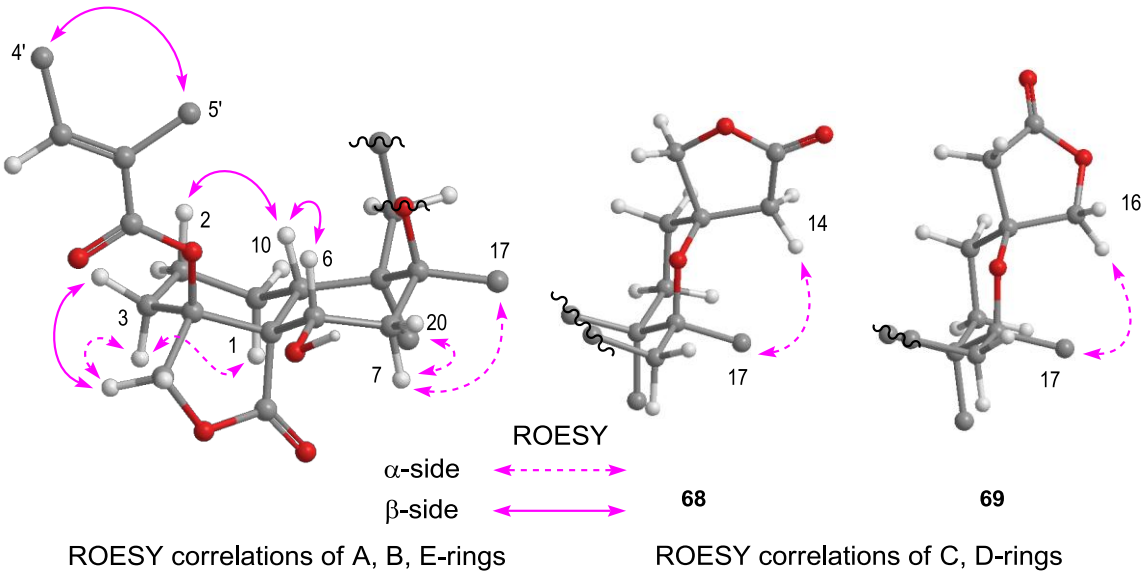

Figure 3.32. Key ROESY correlations of **68** and **69**.

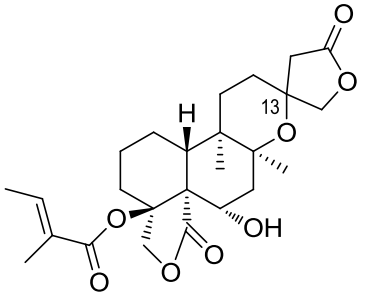

Figure 3.33. The structures of **68** and **69**.

Table 3.12. ^{1}H and ^{13}C NMR data of **68** and **69** in pyridine-d_5.

	68		**69**	
Position	^{1}H[a]	^{13}C[b]	^{1}H[a]	^{13}C[b]
1 (equatorial)	1.56 (m)	23.7	1.57 (m)	23.5
(axial)	1.25 (m)		1.23 (m)	
2 (equatorial)	1.58 (m)	22.8	1.59 (m)	22.9
(axial)	1.42 (m)		1.44 (m)	
3	2.62 (d, 15.1)	34.7	2.63 (br d, 15.1)	34.1
	1.80 (ddd, 4.1, 12.8, 15.1)		1.81 (ddd, 4.4, 12.8, 15.1)	
4	—	83.0	—	82.7
5	—	59.1	—	58.9
6	4.93 (m)	66.2	4.93 (m)	66.1
7	2.50 (dd, 12.1, 13.1)	42.8	2.50 (dd, 12.0, 13.5)	42.6
	1.82 (dd, 4.2, 13.1)		2.02 (dd, 3.8, 13.5)	
8	—	80.1	—	79.6
9	—	37.1	—	36.9
10	2.34 (dd, 1.9, 12.3)	37.5	2.35 (dd, 1.9, 12.3)	37.3
11	1.63 (m)	27.4	1.60 (m)	27.2
12	1.74 (m)	29.1	1.72 (m)	28.4
	1.60 (m)		1.65 (ddd, 2.9, 4.0, 14.3)	
13	—	76.6	—	76.8
14	2.95 (d, 16.9)	42.2	2.95 (d, 16.7)	44.5
	2.88 (d, 16.9)		2.71 (d, 16.7)	
15	—	175.5	—	174.3
16	4.27 (d, 8.5)	79.7	4.37 (d, 8.9)	76.9
	4.25 (d, 8.5)		4.31 (d, 8.9)	
17	1.22 (s)	24.9	1.16 (s)	24.6
18	5.48 (d, 8.1)	75.9	5.49 (d, 8.1)	75.7
	4.75 (d, 8.1)		4.76 (d, 8.1)	
19	—	174.4	—	174.2
20	1.31 (s)	21.7	1.30 (s)	21.4
6-OH	7.15 (br s)		7.21 (d, 5.8)	
1'	—	166.3	—	166.3
2'	—	129.0	—	129.0
3'	6.90 (m)	138.4	6.92 (m)	138.4
4'	1.57 (br dd, 1.0, 7.1)	14.1	1.58 (br dd, 1.1, 7.1)	13.9
5'	1.72 (br s)	12.1	1.70 (br t, 1.1)	11.9

[a] δ ppm (mult., *J* in Hz), 500 MHz. [b] δ ppm, 125 MHz.

3.3.14. The absolute configurations of **44-47**, **51**, **52**, **56**, **57**, **65** and **66**

The absolute configurations of **44-47**, **51**, **52**, **56**, **57**, **65** and **66** were determined by CD excitation chirality method. The 6α,7β-ditigloyloxy system showed a first negative cotton and a second positive cotton as shown in Fig. 3.34. This Cotton pattern was identical with those of *neo*-clerodanes possessing 6*R*,7*S*-dibenzoyloxy system [62-64]. Therefore, the absolute structures of **44-47**, **51**, **52**, **56**, **57**, **65** and **66** were characterized as shown in Fig. 3.35.

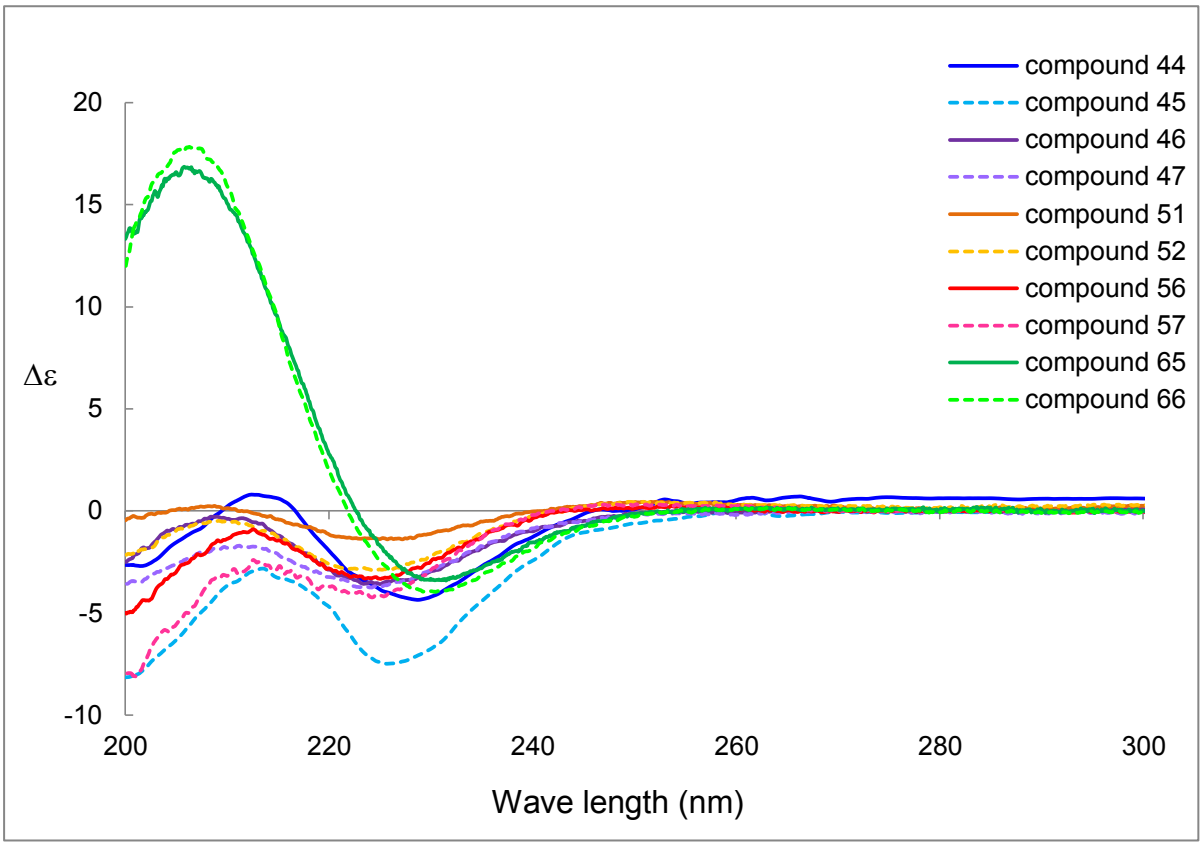

Figure 3.34. CD spectra of compounds **44-47**, **51**, **52**, **56**, **57**, **65** and **66**.

3.5. Cytotoxicity assay

Compounds **39-41**, **43-47**, **50-52**, **55-57**, **59**, **61** and **62** were evaluated for their cytotoxicity against four human cancer cell lines (KB; human epidermoid carcinoma of the nasopharynx, A549; human lung carcinoma, HeLa; human uterine carcinoma, MCF7; breast carcinoma). Two sesterterpenoids (**39** and **40**) showed moderate cytotoxicity against four cancer cell lines with IC_{50} value ranging from 13.6 to 37.6 μg/mL. In contrast, diterpenoids exhibited weak or no cytotoxicity, although some acylated *neo*-clerodane-type diterpenoids with a 13-*spiro*-15,16-γ-lactone structure isolated from *Scutellaria* plants were reported as potent cytotoxic compounds against several human cancer cell lines [47, 51]. Although the essential structural feature for the cytotoxic acylated *neo*-clerodane-type diterpenoids with a

13-*spiro*-15,16-γ-lactone is unclear, they possess oxygen functions at C-6, C-7 and C-11, benzoyl and/or nicotinyl groups connected to some of these positions, and a double bond in the A-ring moiety. The structural differences between those and the compounds isolated from *S.coleifolia* were the absence of the oxygen function at C-11 as well as the presence of the tigloyl group(s) instead of benzoyl and/or nicotinyl groups.

Table 3.13. Cytotoxicity (IC_{50}[a] in μg/mL) of compounds **39**-**41**, **43**-**47**, **50**-**52**, **55**-**57**, **59**, **61** and **62**[b] against four human cancer cell lines.

	KB	MCF7	A549	HeLa
39	14.8 ± 1.35	16.1 ± 1.12	32.5 ± 0.98	13.6 ± 0.29
40	15.6 ± 0.56	17.4 ± 2.02	37.6 ± 1.75	26.0 ± 0.76
41	> 100	> 100	61.0 ± 5.60	> 100
45	> 100	73.1 ± 4.85	> 100	> 100
46	> 100	36.2 ± 2.46	> 100	> 100
47	> 100	80.3 ± 7.09	> 100	> 100
51	> 100	78.9 ± 6.22	> 100	> 100
52	> 100	82.5 ± 6.07	> 100	> 100
55	> 100	67.8 ± 4.59	> 100	> 100
daunorubicin	1.26±0.06	1.62±0.13	9.76 ± 0.17	1.80 ± 0.06

[a] Data are mean ± SE from three or four experiments.
[b] **43**, **44**, **50**, **56**, **57**, **59**, **61**, **62** were not cytotoxic against all the tested cell lines at the tested concentration.

3.6. Conclusion

The chemical investigation on the aerial parts of *S.coleifolia* led to the isolation of two new sesterterpenoids (**39** and **40**), three 19-*nor*-*neo*-clerodane type diterpenoids (**65**-**67**) and twenty-six *neo*-clerodane-type diterpenoids (**41**-**64**, **68** and **69**) together with six known compounds. The structures of new compounds were elucidated by the analyses of spectroscopic data. Compounds **39** and **40** were sesterterpenoids with a β-methyl-α,β-unsaturated-γ-lactone moiety, structurally similar to manoalide derivatives. Although manoalide derivatives were isolated from marine sponges [59], it was the first examples of manoalide derivatives isolated from higher plant. In addition, ten pairs of C-13 epimers of *neo*-clerodanes were obtained from this plant, in which 13*S** epimer was predominant in most cases. Our study showed that *S. coleifolia* contained a variety of highly oxygenated *neo*-clerodane-type diterpenoids and its composition was quite complex.

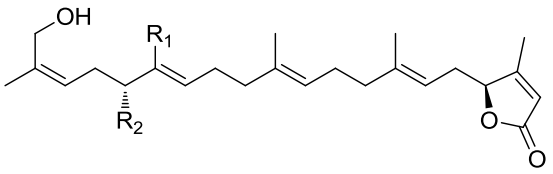

	R_1	R_2	
39	CH_3	OH	(partial racemic mixture)
40	CH_2OH	H	(partial racemic mixture)

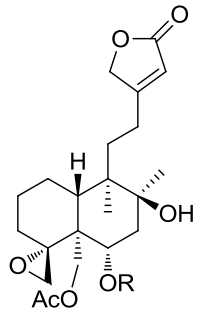

	R
41	tigloyl
42	2-methylbutyryl

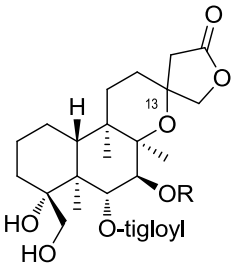

	R	C-13
43	isobutyryl	*S**
44	tigloyl	*R*
45	tigloyl	*S*

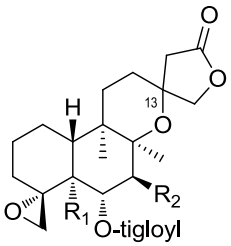

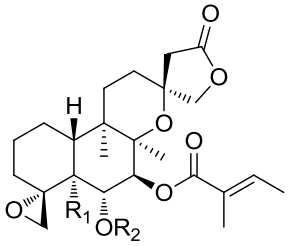

	R_1	R_2
63	CH_3	Ac
64	CH_2OH	2-methylbutyryl

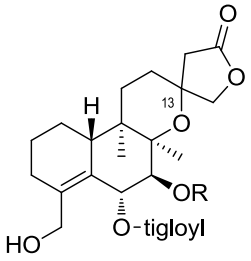

	R	C-13
65	tigloyl	*R*
66	tigloyl	*S*
67	isobutyryl	*S**

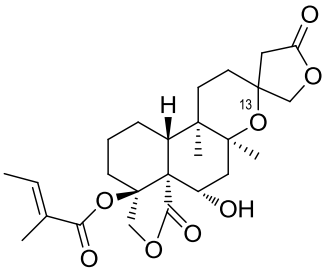

	C-13
68	*R**
69	*S**

	R_1	R_2	C-13
46	CH_3	O-tigloyl	*R*
47	CH_3	O-tigloyl	*S*
48	CH_3	O-Ac	*R**
49	CH_3	O-Ac	*S**
50	CH_3	O-isobutyryl	*S**
51	CHO	O-tigloyl	*R*
52	CHO	O-tigloyl	*S*
53	CHO	O-Ac	*R**
54	CHO	O-Ac	*S**
55	CHO	O-isobutyryl	*S**
56	CH_2OH	O-tigloyl	*R*
57	CH_2OH	O-tigloyl	*S*
58	CH_2OH	O-Ac	*R**
59	CH_2OH	O-Ac	*S**
60	CH_2OH	O-isobutyryl	*R**
61	CH_2OH	O-isobutyryl	*S**
62	COOH	H	*R**

Figure 3.35. New compounds isolated from the aerial parts of *S.coleifolia*.

Chapter 4
Summary and General Conclusions

This research was focused on searching new drug leads from the plant resources. The chemical constituents of two Meliaceous plants (*Dysoxylum cumingianum* C. DC. and *Azadirachta indica* A. Juss) and one Lamiaceous plant (*Scutellaria coleifolia* Levl.) were explored, resulting in the isolation and characterization of forty-five new compounds together with twenty-nine known compounds.

Chemical study on the 90% MeOH-soluble fraction of the leaves of *D. cumingianum* led to the isolation of ten new compounds, including six new triterpenoid, one triterpenoid glucoside, one stigmastane and two pregnanes, along with fifteen known compounds. Cytotoxicity of twelve isolated compounds (**1**-**3**, **11**, **13**-**16**, **17**, **20** and **22**-**24**) against three human cancer cell lines (KB, KB-C2 and MCF7) was evaluated. Compounds **1**, **2**, **11** and **20** showed significant enhanced cytotoxicity in the presence of 2.5 μM colchicine, indicating that they might have some MDR-reversal effect.

Four new triterpenoids, together with eight known compounds were isolated from the MeOH extract of the fruits of *A. indica*. Their structures were determined by extensive spectroscopic analyses and chemical conversion. Cytotoxic activity against two cancer cell lines (KB and MCF7) and an MDR cancer cell line (KB-C2) was evaluated for compounds **27**, **30**-**32**, and meliasenin T (**33**). Among tested compounds, meliasenin S (**30**) demonstrated moderate cytotoxic activity against KB-C2 cell in the presence of 2.5 μM colchicine, although meliasenin S itself was not cytotoxic any cancer cell lines. This result suggested that compound **30** might possess an MDR-reversal activity.

Chemical investigation on the EtOAc-soluble fraction of the aerial parts of *S. coleifolia* resulted in the isolation and structure elucidation of thirty-one new compounds, including two sesterterpenoids (**39** and **40**), three 19-*nor*-*neo*-clerodanes (**65**-**67**) and twenty-six *neo*-clerodanes (**41**-**64**, **68** and **69**), as well as six known compounds. Two sesterterpenoids were structurally correlated with manoalide derivatives isolated from marine sponge. This study provided the first example of manoalide derivatives isolated from higher plant. Furthermore, a lot of *neo*-clerodanes were also found to be contained this plant and its composition was found to be complicated. In cytotoxicity assay, compounds **39** and **40** were showed moderate cytotoxicity against tested cancer cell lines (KB, MCF7, A549 and HeLa) with IC_{50} value ranging from 13.6 to 37.6 μg/mL.

Chapter 5
Experimental Section

5.1. General experimental procedures

Optical rotations were measured with a JASCO DIP-370 digital polarimeter. MS were obtained on Waters LCT PREMIER 2695 and API QSTAR time-of-flight spectrometer. 1D and 2D NMR spectra were measured on Bruker AVANCE-500, ANVANCE-400, DRX-500 and AM-400 instruments using TMS (0.03%, v/v) as an internal standard. CD spectra were recorded on JASCO CD-J600 and CD-J1500 spectropolarimeter (JASCO). UV spectra were recorded on a Beckman DU-650 spectrophotometer. IR spectra were measured with a JASCO FT-IR-4200. Column chromatography was performed with silica gel 60N (63-210 μm, Kanto Kagaku, Japan), silica gel (200-300 mesh; Qingdao Marine Chemical, Inc., People's Republic of China), Sephadex LH-20 (25-100 μm; GE Health Care, U.K.), MCI-gel CHP 20P (75-150 μm; Mitsubishi Chemical, Japan), YMC-pack ODS-A (S-50 μm; YMC Co., Ltd., Japan), Lichroprep RP-18 gel (40-63 μm; Merck, Germany), and Toyopearl HW-40C (TOSOH). Preparative HPLC was performed on either JASCO apparatus, HITACHI apparatus, Agilent apparatus or Shimadzu apparatus equipped with CAPCELL PACK C18 SG120 (250 × 20 mm; 5 μm; Shiseido), CAPCELL PACK UG120 (250 × 20 mm; 3 μm; Shiseido), COSMOSIL $5C_{18}$-MS-II (250 × 20 mm; 5 μm; Nacalai Tesque), COSMOSIL Cholester (250 × 20 mm; 5 μm; Nacalai Tesque), COSMOSIL πNAP (250 × 20 mm; 5 μm; Nacalai Tesque)], GPC (Gel-Permeation Chromatography) [Asahi pack GS-310 2G (MeOH, SHOWA DENKO)], Mightysil RP-18GP (20 mm×250 m; 5 μm; Kanto Kagaku), or Zorbax SB-C_{18} (9.4 mm×250 mm; 5 μm; Agilent Technologies). TLC was conducted on precoated silica gel 60 F_{254} (Merck), and spots were detected by UV illumination and by spraying cerium sulfate reagent followed by heating.

5.2. Experimental procedure of chapter 1

5.2.1. Plant material

The leaves of *Dysoxylum cumingianum* were collected in Lanyu, Taiwan, in February 1990. Identification was carried out by Professor I-S. Chen of Kaohsiung Medical University, Taiwan. The voucher specimen was deposited at Kaohsiung Medical University's College of Pharmacy herbarium.

5.2.2. Extraction and isolation

Air-dried leaves of *D. cumingianum* (8.7 kg) were extracted with MeOH (3×20 L) at room temperature. After concentration, an aliquot (580 g) was partitioned between $CHCl_3$ and H_2O. The $CHCl_3$-soluble fraction was further partitioned with *n*-hexane and MeOH-H_2O (9:1, v/v) to give *n*-hexane-soluble fraction (50 g) and 90% MeOH-soluble fraction (228.5 g). The 90% MeOH-soluble fraction was separated by repeated column chromatography as shown in charts 1.1 and 1.2 to give twenty-five compounds.

Chart 1.1

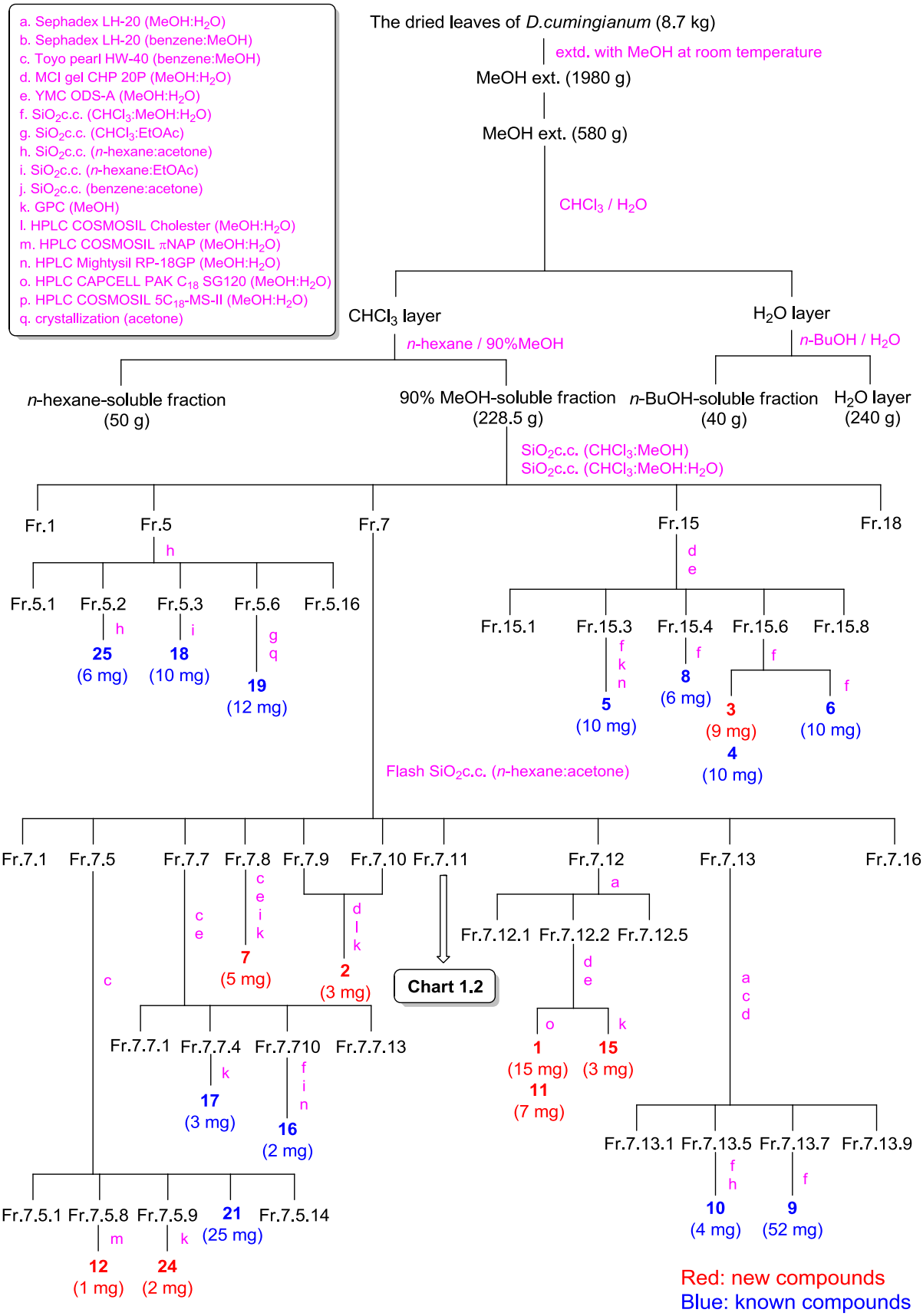
a. Sephadex LH-20 (MeOH:H2O)
b. Sephadex LH-20 (benzene:MeOH)
c. Toyo pearl HW-40 (benzene:MeOH)
d. MCI gel CHP 20P (MeOH:H2O)
e. YMC ODS-A (MeOH:H2O)
f. SiO2c.c. (CHCl3:MeOH:H2O)
g. SiO2c.c. (CHCl3:EtOAc)
h. SiO2c.c. (n-hexane:acetone)
i. SiO2c.c. (n-hexane:EtOAc)
j. SiO2c.c. (benzene:acetone)
k. GPC (MeOH)
l. HPLC COSMOSIL Cholester (MeOH:H2O)
m. HPLC COSMOSIL πNAP (MeOH:H2O)
n. HPLC Mightysil RP-18GP (MeOH:H2O)
o. HPLC CAPCELL PAK C18 SG120 (MeOH:H2O)
p. HPLC COSMOSIL 5C18-MS-II (MeOH:H2O)
q. crystallization (acetone)
The dried leaves of D.cumingianum (8.7 kg)
extd. with MeOH at room temperature
MeOH ext. (1980 g)
MeOH ext. (580 g)
CHCl3 / H2O
CHCl3 layer
H2O layer
n-hexane / 90%MeOH
n-BuOH / H2O
n-hexane-soluble fraction (50 g)
90% MeOH-soluble fraction (228.5 g)
n-BuOH-soluble fraction (40 g)
H2O layer (240 g)
SiO2c.c. (CHCl3:MeOH)
SiO2c.c. (CHCl3:MeOH:H2O)
Fr.1
Fr.5
Fr.7
Fr.15
Fr.18
Fr.5.1
Fr.5.2
Fr.5.3
Fr.5.6
Fr.5.16
25 (6 mg)
18 (10 mg)
19 (12 mg)
Fr.15.1
Fr.15.3
Fr.15.4
Fr.15.6
Fr.15.8
5 (10 mg)
8 (6 mg)
3 (9 mg)
4 (10 mg)
6 (10 mg)
Flash SiO2c.c. (n-hexane:acetone)
Fr.7.1
Fr.7.5
Fr.7.7
Fr.7.8
Fr.7.9
Fr.7.10
Fr.7.11
Fr.7.12
Fr.7.13
Fr.7.16
7 (5 mg)
2 (3 mg)
Chart 1.2
Fr.7.12.1
Fr.7.12.2
Fr.7.12.5
1 (15 mg)
15 (3 mg)
11 (7 mg)
Fr.7.7.1
Fr.7.7.4
Fr.7.710
Fr.7.7.13
17 (3 mg)
16 (2 mg)
Fr.7.13.1
Fr.7.13.5
Fr.7.13.7
Fr.7.13.9
10 (4 mg)
9 (52 mg)
Fr.7.5.1
Fr.7.5.8
Fr.7.5.9
21 (25 mg)
Fr.7.5.14
12 (1 mg)
24 (2 mg)
Red: new compounds
Blue: known compounds

Chart 1.2

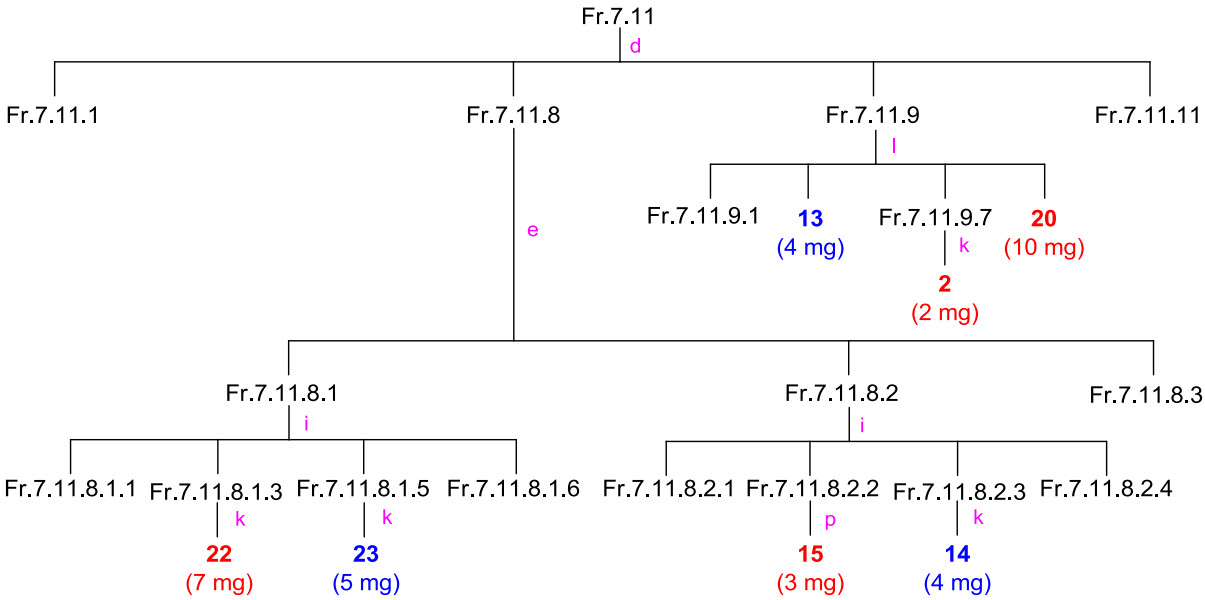

5.2.3. Compound **1** (= cumingianol A)

Amorphous powder; $[\alpha]_D^{19}$ −20.1 (*c* 0.76, MeOH); ^{1}H NMR data (pyridine-d_5+D_2O): see Table 1.1; ^{13}C NMR data (pyridine-d_5+D_2O): see Table 1.2; HRESIMS: *m/z* 557.3803 $[M+Na]^+$ (calcd for $C_{32}H_{54}O_6Na$, 557.3818).

5.2.4. Compound **2** (= cumingianol B)

Amorphous powder; $[\alpha]_D^{29}$ −18.4 (*c* 0.21, MeOH); ^{1}H NMR data (pyridine-d_5+D_2O): see Table 1.1; ^{13}C NMR data (pyridine-d_5+D_2O): see Table 1.2; HRESIMS: *m/z* 557.3818 $[M+Na]^+$ (calcd for $C_{32}H_{54}O_6Na$, 557.3818).

5.2.5. Compound **3** (= cumingianoside R)

Amorphous powder; $[\alpha]_D^{18}$ −43.3 (*c* 0.55, MeOH); ^{1}H NMR data (pyridine-d_5+D_2O): see Table 1.1; ^{13}C NMR data (pyridine-d_5+D_2O): see Table 1.2; HRESIMS: *m/z* 691.4398 $[M+Na]^+$ (calcd for $C_{37}H_{64}O_{10}Na$, 691.4397).

5.2.6. Acetylation of compound **3**

Compound **3** (5 mg) was treated with Ac_2O (1 mL) and dry pyridine (1 mL) at room temperature overnight. After workup as usual, the mixture was chromatographed on silica gel [toluene-acetone (20:1 → 12:1)] to furnish a heptaacetate (4 mg), whose spectral data was identical with those of cumingianoside C peracetate [3].

5.2.7. Compound **7** (= cumingianol C)

Amorphous powder; $[\alpha]_D^{20}$ –19.4 (*c* 0.34, MeOH); ^{1}H NMR data (pyridine-d_5+D_2O): see Table 1.1; ^{13}C NMR data (pyridine-d_5+D_2O): see Table 1.2; HRESIMS: *m/z* 539.3704 $[M+Na]^+$ (calcd for $C_{32}H_{52}O_5Na$, 539.3712).

5.2.8. Compound **11** (= cumingianol D)

Amorphous powder; $[\alpha]_D^{19}$ –20.8 (*c* 0.75, MeOH); ^{1}H NMR data (pyridine-d_5+D_2O): see Table 1.1; ^{13}C NMR data (pyridine-d_5+D_2O): see Table 1.2; HRESIMS: *m/z* 557.3814 $[M+Na]^+$ (calcd for $C_{32}H_{54}O_6Na$, 557.3818).

5.2.9. Compound **12** (= cumingianol E)

Amorphous powder; $[\alpha]_D^{28}$ –76.9 (*c* 0.11, MeOH); ^{1}H NMR data (pyridine-d_5+D_2O) see Table 1.1; ^{13}C NMR data (pyridine-d_5+D_2O): see Table 1.2; HRESIMS: *m/z* 557.3845 $[M+Na]^+$ (calcd for $C_{32}H_{54}O_6Na$, 557.3818).

5.2.10. Compound **15** (= cumingianol F)

Amorphous powder; $[\alpha]_D^{28}$ –49.2 (*c* 0.37, MeOH); ^{1}H NMR data (pyridine-d_5+D_2O) see Table 1.1; ^{13}C NMR data (pyridine-d_5+D_2O): see Table 1.2; HRESIMS: *m/z* 557.3842 $[M+Na]^+$ (calcd for $C_{32}H_{54}O_6Na$, 557.3818).

5.2.11. Compound **20** (= dyscusin A)

Amorphous powder; $[\alpha]_D^{28}$ –28.4 (*c* 0.85, pyridine); ^{1}H NMR (500 MHz, in pyridine-d_5+D_2O): δ_H 5.70 (1H, dd, *J* = 2.0, 5.0 Hz, H-6), 4.56 (1H, d, *J* = 3.7 Hz, H-4), 4.41 (1H, dd, *J* = 4.3, 10.2 Hz, H-21a), 4.15 (1H, dd, *J* = 10.2 Hz, H-21b), 4.13 (1H, br d, *J* = 10.0 Hz, H-22), 3.87 (1H, dt, *J* = 3.7, 11.5 Hz, H-3), 1.45 (3H, s, Me-19), 1.36 (1H, m, H-17), 1.02 (3H, d, *J* = 6.8 Hz, Me-26), 0.97 (3H, t, *J* = 7.4 Hz, Me-29), 0.91 (3H, d *J* = 6.8 Hz, Me-27), 0.74 (3H, s, Me-18); ^{13}C NMR (125 MHz, in pyridine-d_5+D_2O): δ_C 144.7 (C-5), 126.5 (C-6), 78.1 (C-4), 73.0 (C-3), 72.3 (C-22), 63.0 (C-21), 56.8 (C-14), 50.8 (C-9), 49.8 (C-17), 49.1 (C-20), 42.7 (C-13), 41.8 (C-24), 39.5 (C-12), 38.2 (C-1), 36.7 (C-10), 32.4 (C-7), 32.4 (C-8), 31.8 (C-23), 29.4 (C-25), 28.0 (C-16), 26.4 (C-2), 24.5 (C-15), 24.0 (C-28), 21.3 (C-19), 21.0 (C-11), 20.7 (C-26), 18.1 (C-27), 12.3 (C-29), 12.1 (C-18); HRESIMS: *m/z* 485.3607 $[M+Na]^+$ (calcd for $C_{29}H_{50}O_4Na$, 485.3601).

5.2.12. Compound **22** (= dyscusin B)

White amorphous powder; $[\alpha]_D^{28}$ −157.4 (*c* 0.67, MeOH); ^1H and ^{13}C NMR data (pyridine-d_5+D_2O): see Table 1.3; HRESIMS: *m/z* 355.2260 $[M+Na]^+$ (calcd for $C_{21}H_{32}O_3Na$, 355.2249).

5.2.13 Compound **24** (= dyscusin C)

White amorphous powder; $[\alpha]_D^{30}$ +13.6 (*c* 0.21, MeOH); ^1H and ^{13}C NMR data (pyridine-d_5+D_2O): see Table 1.3; HRESIMS: *m/z* 333.2417 $[M+H]^+$ (calcd for $C_{21}H_{33}O_3$, 333.2406).

5.3. Experimental procedure of chapter 2

5.3.1. Plant material

The fruits of *Azadirachta indica* were collected at Jahangirnagar University, Savar, Dhala, Bangladesh in August 2007. The plant was identified by Dr. F. A. Ahmed of Jahangirnagar University. Herbarium specimens (DACB34192) are deposited in Bangladesh National Herbarium.

5.3.2. Extraction and isolation

The dried fruits of *A. indica* (2.4 kg) were powdered and extracted with MeOH for 1 day at room temperature nine times. After concentration, the MeOH extract (235 g) was successively partitioned with *n*-hexane, EtOAc and H_2O. The *n*-hexane-soluble fraction and EtOAc-soluble fraction were repeatedly separated by column chromatography (See chart 2.1) to give twelve compounds.

Chart 2.1

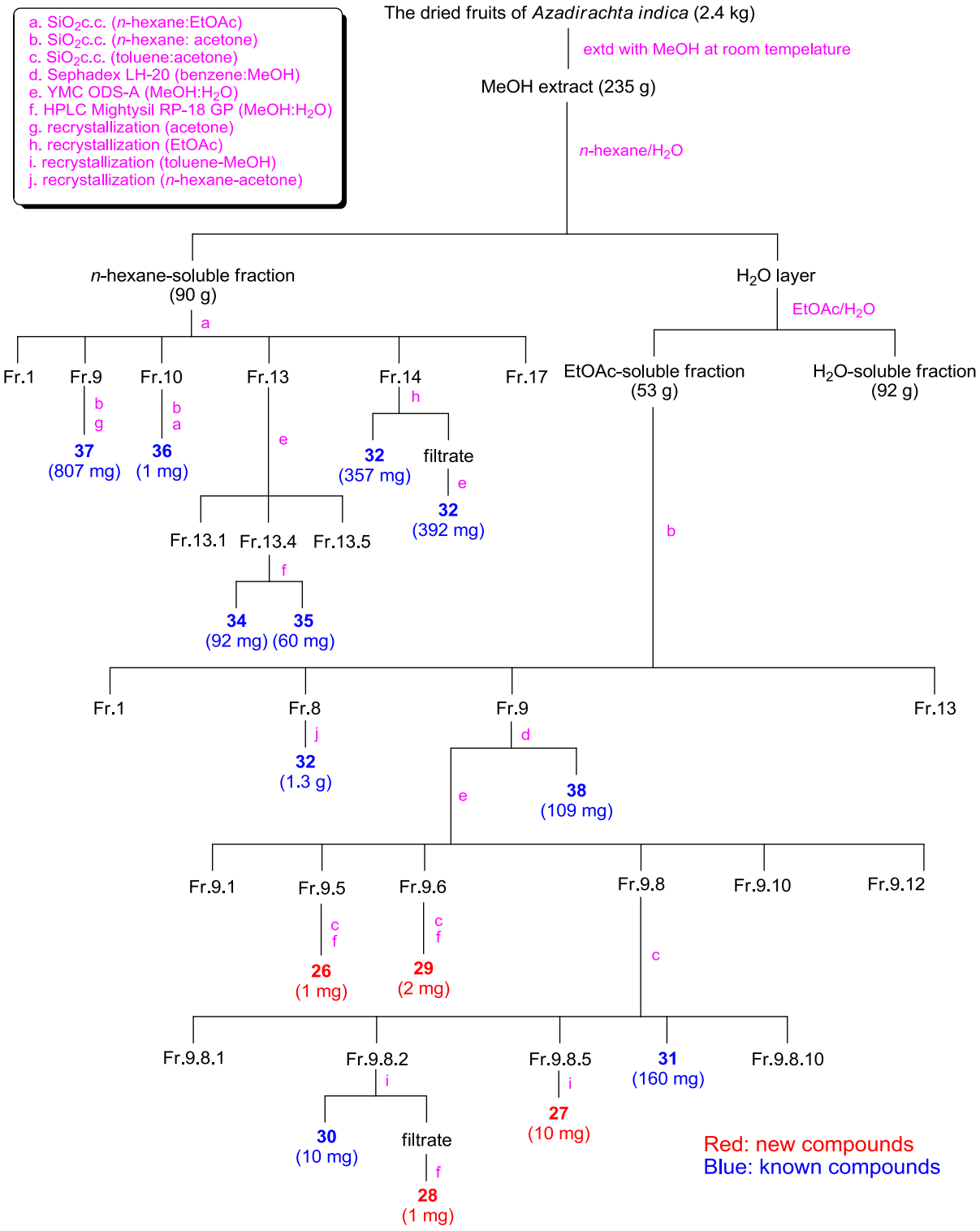

5.3.3. Compound **26** (= indicalilacol A)

White amorphous powder; $[\alpha]_D^{23}$ –26.4 (*c* 0.04, MeOH); IR (neat) ν_{max} 3566, 1716 cm^{-1}; ^1H NMR data ($CDCl_3$): see Table 2.1; ^{13}C NMR data ($CDCl_3$): see Table 2.2; HRESIMS: *m/z* 539.3372 $[M+Na]^+$ (calcd for $C_{31}H_{48}O_6Na$, 539.3349).

5.3.4. Compound **27** (= indicalilacol B)

White amorphous powder; $[\alpha]_D^{27}$ –65.9 (*c* 0.43, MeOH); IR (neat) ν_{max} 3421, 1761, 1670 cm^{-1}; ^1H NMR data ($CDCl_3$): see Table 2.1; ^{13}C NMR data ($CDCl_3$): see Table 2.2; HRESIMS: *m/z* 487.3418 $[M-H]^-$ (calcd for $C_{30}H_{47}O_5$, 487.3424).

5.3.5. Preparation of compound **27a**

A mixture of compound **27** (6.2 mg; 0.013 mmol), acetone dimethyl acetal (50 μL; 0.41 mmol) and *p*-toluenesulfonic acid (*p*-TSA) (1 mg; 0.005 mmol) in CH_2Cl_2 (10 mL) was stirred at room temperature for 18 h. The reaction mixture was diluted with $CHCl_3$, and washed with H_2O. The $CHCl_3$-soluble fraction was dried over Na_2SO_4, and concentrated under reduced pressure. The residue was chromatographed over silica gel [*n*-hexane–acetone (7:1→5:1)] to afford **27a** (6.8 mg) as off-white powder; $[\alpha]_D^{29}$ –43.4 (*c* 0.68, MeOH); ^1H NMR (500 MHz, pyridine-d_5): δ_H 5.35 (1H, d, *J* = 3.3 Hz, H-7), 4.57 (1H, ddd, *J* = 6.3, 6.3, 10.4 Hz, H-23), 3.94 (1H, d, *J* = 6.3 Hz, H-24), 1.51 (3H, s, Me-32), 1.42 (3H, s, Me-33), 1.38 (3H, s, Me-26), 1.31 (3H, s, Me-27), 1.15 (3H, s, Me-28), 1.06 (3H, s, Me-30), 0.97 (3H, s, Me-29), 0.91 (3H, s, Me-18), 0.85 (3H, s, Me-19); ^{13}C NMR (125 MHz, pyridine-d_5): δ_C 178.0 (C-21), 146.0 (C-8), 118.8 (C-7), 107.9 (C-31), 85.1(C-24), 79.8 (C-25), 76.4 (C-23), 75.2 (C-3), 51.0 (C-14), 49.1 (C-9), 47.7 (C-17), 45.0 (C-5), 44.0 (C-13), 41.0 (C-20), 37.9 (C-4), 35.2 (C-10), 34.1 (C-15), 31.8 (C-1), 31.7 (C-12), 30.8 (C-22), 28.7 (C-32), 28.7 (C-28), 27.5 (C-30), 27.4 (C-26), 27.3 (C-33), 26.5 (C-2), 25.1 (C-16), 24.4 (C-6), 23.8 (C-27), 23.2 (C-18), 22.1 (C-29), 17.8 (C-11), 13.3 (C-19); HRESIMS: *m/z* 551.3705 $[M+Na]^+$ (calcd for $C_{33}H_{52}O_5Na$, 551.3712).

5.3.6. Oxidation of **27a**

Compound **27a** (6.8 mg; 0.013 mmol) was treated with pyridinium chlorochromate (PCC) (5.6 mg; 0.026 mmol) in CH_2Cl_2 (15 mL) at room temperature for 2.5 h. After removal of PCC by filtration, the filtrate was concentrated under reduced pressure. The residue was applied to a silica gel CC [*n*-hexane–acetone (7:1→6:1)] to give a product (**27b**, 3.9 mg), which was shown to be identical with 21-oxo-melianodiol 24,25-acetonide by spectral comparisons.

5.3.7. Compound **28** (= indicalilacol C)

White amorphous powder; $[\alpha]_D^{15}$ –67.7 (*c* 0.07, MeOH); UV (MeOH) λ_{max} (log ε) 238 (3.69) nm; IR (neat) ν_{max} 3446, 1684 cm^{-1}; ^1H NMR data (pyridine-d_5): see Table 2.1; ^{13}C NMR data (pyridine-d_5): see Table 2.2; HRESIMS: *m/z* 525.3570 $[M+Na]^+$ (calcd for

$C_{31}H_{50}O_5Na$, 525.3556).

5.3.8. Compound **29** (= indicalilacol D)

White amorphous powder; $[\alpha]_D^{26}$ –49.3 (*c* 0.18, MeOH); IR (neat) ν_{max} 3503, 1776, 1705 cm^{-1}; ^1H NMR data ($CDCl_3$): see Table 2.1; ^{13}C NMR data ($CDCl_3$): see Table 2.2; HRESIMS: *m/z* 507.3078 $[M+Na]^+$ (calcd for $C_{30}H_{44}O_5Na$, 507.3086).

5.3.9. Compound **31**

White amorphous powder; ^1H NMR (500 MHz, $CDCl_3$): δ_H 5.29 (1H, br s, H-7), 5.26 (1H, br s, H-21), 4.50 (1H, m, H-23), 3.26 (1H, dd, *J* = 4.0, 11.2 Hz, H-3), 3.18 (1H, br s, H-24), 1.30 (3H, s, Me-26), 1.28 (3H, s, Me-27), 1.01 (3H, s, Me-30), 0.99 (3H, s, Me-28), 0.88 (3H, s, Me-29), 0.86 (3H, s, Me-18), 0.77 (3H, s, Me-19); ^{13}C NMR data ($CDCl_3$): see Table 2.2.

5.3.10. Preparation of 21-oxo-melianodiol 24,25-acetonide (**27b**)

A mixture of melianodiol (**32**) (20 mg; 0.041 mmol) and Fetizon's reagent [45, 46] (390 mg; 0.684 mmol) in benzene (10 mL) was refluxed for 24 h with stirring. After removal of Fetizon's reagent by filtration, the filtrate was concentrated under reduced pressure. The residue was further reacted with acetone dimethyl acetal (30 μL; 0.25 mmol) and *p*-toluenesulfonic acid (1 mg; 0.005 mmol) in CH_2Cl_2 (10 mL) for 10 h with stirring. The reaction mixture was worked up as described above. The residue was subjected to silica gel column chromatography [$CHCl_3$–MeOH (1:0→80:1)] to give 21-oxo-melianodiol 24,25-acetonide (6.0 mg), as a white amorphous powder; $[\alpha]_D^{28}$ –77.8 (*c* 0.51, $CHCl_3$); ^1H NMR (500 MHz, pyridine-d_5): δ_H 5.31 (1H, d, *J* = 3.0 Hz, H-7), 4.59 (1H, ddd, *J* = 6.2, 6.2, 10.3 Hz, H-23), 3.95 (1H, d, *J* = 6.2 Hz, H-24), 1.52 (3H, s, Me-32), 1.43 (3H, s, Me-33), 1.39 (3H, s, Me-26), 1.32 (3H, s, Me-27), 1.10 (3H, s, Me-28), 1.05 (3H, s, Me-30), 1.04 (3H, s, Me-29), 0.99 (3H, s, Me-18), 0.92 (3H, s, Me-19); ^{13}C NMR (125 MHz, pyridine-d_5): δ_C 215.2 (C-3), 178.0 (C-21), 145.7 (C-8), 118.4 (C-7), 107.9 (C-31), 85.2 (C-24), 79.8 (C-25), 76.5 (C-23), 52.5 (C-5), 50.9 (C-14), 48.5 (C-9), 47.8 (C-17), 47.8 (C-4), 44.0 (C-13), 41.1 (C-20), 38.3 (C-1), 35.2 (C-10), 35.0 (C-2), 34.1 (C-15), 31.6 (C-12), 30.9 (C-22), 28.7 (C-32), 27.5 (C-30), 27.4 (C-26), 27.3 (C-33), 25.2 (C-16), 24.8 (C-28), 24.6 (C-6), 23.8 (C-27), 23.3 (C-18), 21.4 (C-29), 17.9 (C-11), 12.6 (C-19); HRESIMS: *m/z* 549.3577 $[M+Na]^+$ (calcd for $C_{33}H_{50}O_5Na$, 549.3556).

5.3.11. Reduction of melianodiol (**32**)

Melianodiol (**32**) (50 mg: 0.103 mmol) was reacted with $NaBH_4$ (11.6 mg: 0.307 mmol) in EtOH (10 mL) for 3 h at room temperature. After removal of the solvent, the reaction mixture was purified by silica gel chromatography [$CHCl_3$-MeOH (1:0→9:1)] to give a product (**32a**, 13.4 mg), which was identical with meliantriol (**31**).

5.3.12. Preparation of meliasenin T (**33**)

A mixture of compound **31** (23 mg: 0.048 mmol) and *p*-toluene sulfonic acid (1 mg: 0.006 mmol) in MeOH (3mL) was stirred for 1 h at room temperature. The reaction mixture was purified by HPLC Migthysil RP-18 GP [MeOH:H_2O (4:1) flow rate 5.0 mL/min, RI, t_R 60 min (**30**), 86 min (**33**)] to yield **30** (4.8 mg) and **33** (4.7 mg).

5.4. Experimental procedure of chapter 3

5.4.1. Plant material

The aerial parts of *S*. *coleifolia* were collected at Muli county, Sichuan Province, People's Republic of China in August 2011. This plant was identified by Prof. Xi-Wen Li (Kunming Institute of Botany), and a herbarium specimen (KIB 20110811) was deposited at the Herbarium of the Kunming Institute of Botany, Chinese Academy of Sciences.

5.4.2. Extraction and isolation

The aerial parts of *S*. *coleifolia* (3.0 kg) were extracted with 70% aqueous acetone (15 L) 3 times at room temperature for 72 h each time. The extract was concentrated under reduced pressure, and the residue was successively partitioned with EtOAc, *n*-BuOH and H_2O. The EtOAc-soluble fraction (130 g) was separated by repeated column chromatography as shown in charts 3.1 and 3.2 to yield thirty-seven compounds.

Chart 3.1

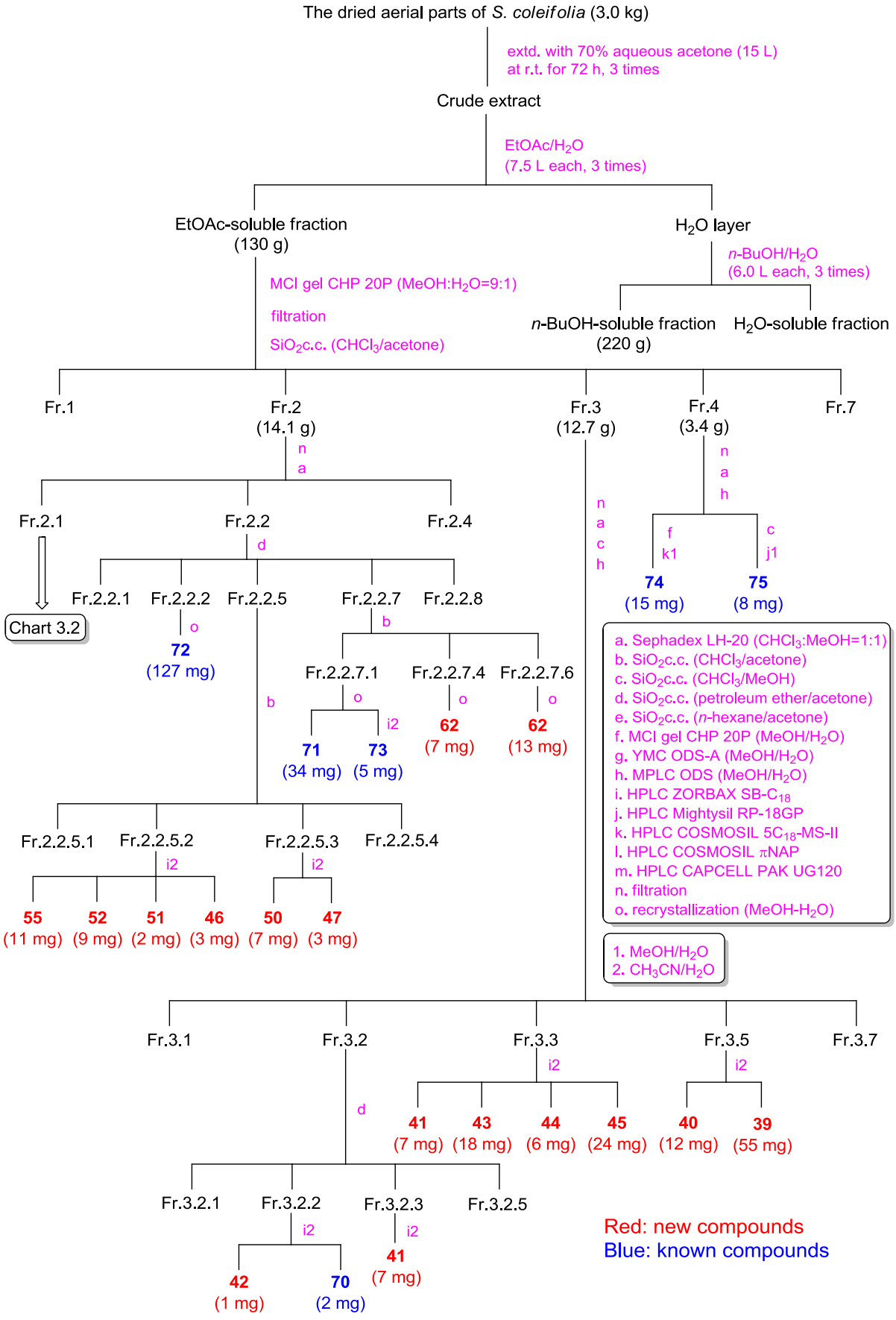
The dried aerial parts of S. coleifolia (3.0 kg)
extd. with 70% aqueous acetone (15 L) at r.t. for 72 h, 3 times
Crude extract
EtOAc/H2O (7.5 L each, 3 times)
EtOAc-soluble fraction (130 g)
H2O layer
n-BuOH/H2O (6.0 L each, 3 times)
MCI gel CHP 20P (MeOH:H2O=9:1)
filtration
SiO2c.c. (CHCl3/acetone)
n-BuOH-soluble fraction (220 g)
H2O-soluble fraction
Fr.1
Fr.2 (14.1 g)
Fr.3 (12.7 g)
Fr.4 (3.4 g)
Fr.7
Fr.2.1
Fr.2.2
Fr.2.4
Fr.2.2.1
Fr.2.2.2
Fr.2.2.5
Fr.2.2.7
Fr.2.2.8
Chart 3.2
72 (127 mg)
Fr.2.2.7.1
Fr.2.2.7.4
Fr.2.2.7.6
71 (34 mg)
73 (5 mg)
62 (7 mg)
62 (13 mg)
74 (15 mg)
75 (8 mg)
Fr.2.2.5.1
Fr.2.2.5.2
Fr.2.2.5.3
Fr.2.2.5.4
55 (11 mg)
52 (9 mg)
51 (2 mg)
46 (3 mg)
50 (7 mg)
47 (3 mg)
a. Sephadex LH-20 (CHCl3:MeOH=1:1)
b. SiO2c.c. (CHCl3/acetone)
c. SiO2c.c. (CHCl3/MeOH)
d. SiO2c.c. (petroleum ether/acetone)
e. SiO2c.c. (n-hexane/acetone)
f. MCI gel CHP 20P (MeOH/H2O)
g. YMC ODS-A (MeOH/H2O)
h. MPLC ODS (MeOH/H2O)
i. HPLC ZORBAX SB-C18
j. HPLC Mightysil RP-18GP
k. HPLC COSMOSIL 5C18-MS-II
l. HPLC COSMOSIL πNAP
m. HPLC CAPCELL PAK UG120
n. filtration
o. recrystallization (MeOH-H2O)
1. MeOH/H2O
2. CH3CN/H2O
Fr.3.1
Fr.3.2
Fr.3.3
Fr.3.5
Fr.3.7
41 (7 mg)
43 (18 mg)
44 (6 mg)
45 (24 mg)
40 (12 mg)
39 (55 mg)
Fr.3.2.1
Fr.3.2.2
Fr.3.2.3
Fr.3.2.5
42 (1 mg)
70 (2 mg)
41 (7 mg)
Red: new compounds
Blue: known compounds

Chart 3.2

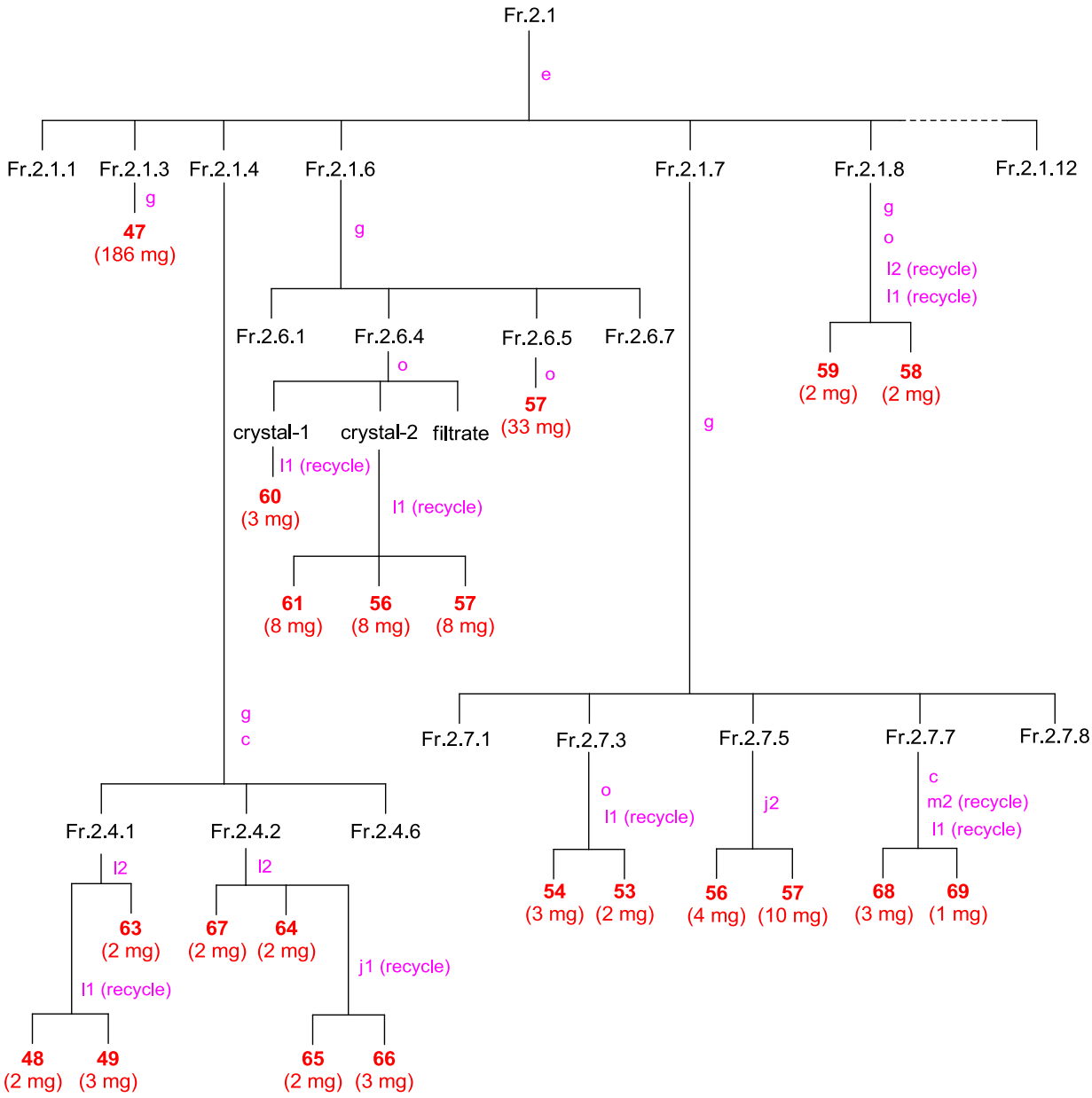

5.4.3. Compound **39** (= coleifolide B)

Colorless oil; $[\alpha]_D^{17}$ +14.7 (*c* 3.04, $CHCl_3$); CD (EtOH; 1.2×10^{-4} M, Δε) λ_{max} 209 (+10.2). ^1H and ^{13}C NMR data (pyridine-d_5): see Table 3.1; HRESIMS: *m/z* 425.2657 $[M+Na]^+$ (calcd for $C_{25}H_{38}O_4Na$, 425.2667).

5.4.4. Preparation of **39a**

Compound **39** (6 mg, 14 μmol) was reacted with pivaloyl chloride (50 μL, 0.414 mmol) in pyridine (2 mL) under ice cooling for 10 min. After removal of the solvent, the reaction mixture was subjected to chromatography over silica gel [*n*-hexane:acetone (8:1→5:1)] to

afford **39a** (4.8 mg, 70 %). Colorless oil; $[\alpha]_D^{19}$ +11.0 (*c* 0.12, $CHCl_3$); ^{1}H NMR (500 MHz, pyridine-d_5): δ_H 6.18 (1H, d, *J* = 2.5 Hz, 16-OH), 5.90 (1H, quint, *J* = 1.5 Hz, H-2), 5.71 (1H, t, *J* = 7.5 Hz, H-18), 5.64 (1H, t, *J* = 7.0 Hz, H-14), 5.20 (1H, tq, *J* = 1.1, 6.9 Hz, H-10), 5.17 (1H, tq, *J* = 1.1, 7.1 Hz, H-6), 4.95 (1H, t, *J* = 5.4 Hz, H-4), 4.87 (1H, d, *J* = 12.3 Hz, H-20a), 4.81 (1H, d, *J* = 12.3 Hz, H-20b), 4.35 (1H, t, *J* = 6.4 Hz, H-16), 2.68 (1H, m, H-17a), 2.64 (1H, m, H-5a), 2.61 (1H, m, H-17b), 2.30 (1H, dt, *J* = 7.1, 15.0 Hz, H-5b), 2.22 (2H, br dd, *J* = 7.0, 15.0 Hz, H_2-13), 2.11 (2H, m, H_2-9), 2.08 (2H, m, H_2-8), 2.03 (2H, m, H_2-12), 1.88 (3H, d, *J* = 1.5 Hz, Me-25), 1.82 (3H, s, Me-22), 1.80 (3H, d, *J* = 1.1 Hz, Me-28), 1.61 (3H, s, Me-24), 1.61 (3H, s, Me-23), 1.21 (9H, s, pivaloyl $C(Me)_3$); ^{13}C NMR (125 MHz, pyridine-d_5): δ_C 178.0 (pivaloyl –OCOC$(Me)_3$), 173.1 (C-1), 169.1 (C-3), 139.5 (C-7), 138.6 (C-15), 135.2 (C-11), 131.6 (C-19), 128.0 (C-18), 125.2 (C-14), 124.5 (C-12), 117.3 (C-2), 117.2 (C-6), 84.3 (C-4), 77.0 (C-16), 63.5 (C-20), 39.9 (C-8), 39.8 (C-12), 38.9 (pivaloyl –OCOC$(Me)_3$), 34.8 (C-17), 30.5 (C-5), 27.3 (3C, pivaloyl –OCOC$(Me)_3$), 26.8 (C-9), 26.6 (C-13), 21.5 (C-21), 16.4 (C-24), 16.1 (C-23), 13.6 (C-25), 12.0 (C-22); HRESIMS: *m/z* 509.3266 $[M+Na]^+$ (calcd for $C_{30}H_{46}O_5Na$, 509.3243).

5.4.5. Preparation of (*R*)- or (*S*)-2NMA ester of **39a**

A mixture of **39a** (1 mg, 2.1 μmol), DMAP (1.2 mg, 10 μmol), EDC (3.0 mg, 15.6 μmol) and (*R*)- or (*S*)-2-NMA (2.1 mg, 10 μmol) in CH_2Cl_2 (2 mL) was stirred at room temperature for 24 h. The reaction mixture was directly purified by preparative TLC (*n*-hexane:EtOAc = 2:1), giving (*R*)- or (*S*)-2NMA ester of **39a** (each 0.8 mg, 57%).

(*R*)-2NMA ester of **39a**: ^{1}H NMR (500 MHz, pyridine-d_5): δ_H 5.890 (1H, m, H-2), 5.477 (1H, dd, *J* = 6.1, 7.6 Hz, H-16), 5.406 (1H, t, *J* = 7.1 Hz, H-18), 5.375 (1H, t, *J* = 7.2 Hz, H-14), 5.171 (1H, m, H-6), 5.048 (1H, t, *J* = 6.9 Hz, H-10), 4.944 (1H, m, H-4), 4.838 (1H, d, *J* = 12.5 Hz, H-20a), 4.752 (1H, d, *J* = 12.5 Hz, H-20b), 2.691 (1H, m, H-17a), 2.638 (1H, m, H-5a), 2.551 (1H, m, H-17b), 2.299 (1H, m, H-5b), 2.078 (2H, m, H_2-9), 2.013 (2H, *m*, H_2-8), 1.931 (2H, m, H_2-13), 1.865 (3H, d, *J* = 1.4 Hz, Me-25), 1.794 (2H, t, *J* =7.7 Hz, H_2-12), 1.729 (3H, s, Me-21), 1.615 (3H, s, Me-24), 1.483 (3H, s, Me-22), 1.467 (3H, s, Me-23); HRESIMS: *m/z* 707.3959 $[M+Na]^+$ (calcd for $C_{43}H_{56}O_7Na$, 707.3924).

(*S*)-2NMA ester of **39a**: ^{1}H NMR (500 MHz, pyridine-d_5): δ_H 5.897 (1H, m, H-2), 5.594 (1H, t, *J* = 7.0 Hz, H-14), 5.450 (1H, dd, *J* = 5.7, 8.0 Hz, H-16), 5.180 (1H, m, H-6), 5.161 (1H, m, H-18), 5.145 (1H, m, H-10), 4.946 (1H, m, H-4), 4.716 (1H, d, *J* = 12.3 Hz, H-20a), 4.534 (1H, d, *J* =12.3 Hz, H-20), 2.621 (1H, m, H-5a), 2.580 (1H, dt, *J* = 8.0, 15.1 Hz, H_a-17a), 2.470 (1H, dt, *J* = 5.7, 15.1 Hz, H-17b), 2.106 (2H, m, H_2-13), 2.096 (2H, m, H_2-9), 2.021 (2H, m, H_2-8), 1.969 (2H, t, *J* = 7.8 Hz, H_2-12), 1.871 (3H, d, *J* = 1.5 Hz, Me-25),

1.677 (3H, s, Me-22), 1.622 (3H, s, Me-24), 1.548 (3H, s, Me-23), 1.526 (3H, s, Me-20); HRESIMS: *m/z* 707.3942 $[M+Na]^+$ (calcd for $C_{43}H_{56}O_7Na$, 707.3924).

5.4.6. Preparation of (*R*)-MPA ester of **39a**

A mixture of **39a** (2.1 mg, 4.3 μmol), DMAP (1.2 mg, 10 μmol), EDC (3.8 mg, 20 μmol), and (*R*)-MPA (3.3 mg, 20 μmol) in CH_2Cl_2 (2 mL) was stirred at room temperature for 21 h. The reaction mixture was purified by preparative TLC (*n*-hexane:EtOAc = 2:1) to yield (*R*)-MPA ester of **39a** (0.9 mg, 33%). HRESIMS: *m/z* 657.3793 $[M+Na]^+$ (calcd for $C_{39}H_{54}O_7Na$, 657.3767).

5.4.7. Compound **40** (= coleifolide A)

Pale yellow oil; $[\alpha]_D^{17}$ +7.4 (*c* 0.50, $CHCl_3$); CD (EtOH; 1.2×10^{-4} M, Δε) λ_{max} 209 (+9.0); ^1H and ^{13}C NMR data (pyridine-d_5): see Table 3.1; HRESIMS: *m/z* 425.2665 $[M+Na]^+$ (calcd for $C_{25}H_{38}O_4Na$, 425.2667).

5.4.8. Compound **41**

Amorphous powder; $[\alpha]_D^{20}$ +37.5 (*c* 0.98, $CHCl_3$); ^1H and ^{13}C NMR data (pyridine-d_5): see Table 3.2; HRESIMS: *m/z* 513.2464 [M+Na]+ (calcd for $C_{27}H_{38}O_8Na$, 513.2464).

5.4.9. Compound **42**

Amorphous powder; $[\alpha]_D^{19}$ +7.0 (*c* 0.2, $CHCl_3$); ^1H and ^{13}C NMR data (pyridine-d_5): see Table 3.2; HRESIMS: *m/z* 515.2635 $[M+Na]^+$ (calcd for $C_{27}H_{40}O_8Na$, 515.2620).

5.4.10. Compound **43**

Amorphous powder; $[\alpha]_D^{16}$ –30.6 (*c* 1.08, $CHCl_3$); ^1H and ^{13}C NMR data (pyridine-d_5): see Table 3.3; HRESIMS *m/z* 559.2896 $[M+Na]^+$ (calcd for $C_{29}H_{44}O_9Na$, 559.2883).

5.4.11. Compound **44**

Amorphous powder; $[\alpha]_D^{20}$ –113.1 (*c* 0.58, $CHCl_3$); CD (EtOH, *c* 1.8×10^{-4} M; Δε) λ_{max} 229 (–4.4), 212 (+0.8); ^1H and ^{13}C NMR data (pyridine-d_5): see Table 3.3; HRESIMS: *m/z* 571.2870 $[M+Na]^+$ (calcd for $C_{30}H_{44}O_9Na$, 571.2883).

5.4.12. Compound **45**

Amorphous powder; $[\alpha]_D^{18}$ –33.4 (*c* 2.75, $CHCl_3$); CD (EtOH, *c* 1.8×10^{-4} M; Δε) λ_{max} 226 (–7.5), 214 (–2.8); ^1H and ^{13}C NMR data (pyridine-d_5): see Table 3.3; HRESIMS: *m/z*

571.2880 $[M+Na]^+$ (calcd for $C_{30}H_{44}O_9Na$, 571.2883).

5.4.13. Compound **46**

Amorphous powder; $[\alpha]_D^{19}$ –64.6 (*c* 0.31, $CHCl_3$); CD (EtOH, *c* 1.9×10^{-4} M; Δε) λ_{max} 225 (–3.6), 209 (–0.3); ^1H NMR data (pyridine-d_5): see Table 3.4; ^{13}C NMR data (pyridine-d_5): see Table 3.5; HRESIMS: *m/z* 553.2776 $[M+Na]^+$ (calcd for $C_{30}H_{42}O_8Na$, 553.2777).

5.4.14. Compound **47**

Amorphous powder; $[\alpha]_D^{20}$ –95.4 (*c* 0.3, $CHCl_3$); CD (EtOH, *c* 1.9×10^{-4} M; Δε) λ_{max} 224 (–3.6), 209 (–1.7); ^1H NMR data (pyridine-d_5): see Table 3.4; ^{13}C NMR data (pyridine-d_5): see Table 3.5; HRESIMS: *m/z* 553.2764 $[M+Na]^+$ (calcd for $C_{30}H_{42}O_8Na$, 553.2777).

5.4.15. Compound **48**

Amorphous powder; $[\alpha]_D^{18}$ –29.6 (*c* 0.17, MeOH); ^1H NMR data (pyridine-d_5): see Table 3.4; ^{13}C NMR data (pyridine-d_5): see Table 3.5; HRESIMS: *m/z* 529.2191 $[M+K]^+$ (calcd for $C_{27}H_{38}O_8K$, 529.2204).

5.4.16. Compound **49**

Amorphous powder; $[\alpha]_D^{21}$ –57.7 (*c* 0.34, MeOH); ^1H NMR data (pyridine-d_5): see Table 3.4; ^{13}C NMR data (pyridine-d_5): see Table 3.5; HRESIMS: *m/z* 529.2186 $[M+K]^+$ (calcd for $C_{27}H_{38}O_8K$, 529.2204).

5.4.17. Compound **50**

Amorphous powder; $[\alpha]_D^{21}$ –38.9 (*c* 0.65, $CHCl_3$); ^1H NMR data (pyridine-d_5): see Table 3.4; ^{13}C NMR data (pyridine-d_5): see Table 3.5; HRESIMS: *m/z* 541.2770 $[M+Na]^+$ (calcd for $C_{29}H_{42}O_8Na$, 541.2777).

5.4.18. Compound **51**

Amorphous powder; $[\alpha]_D^{21}$ –63.3 (*c* 0.24, $CHCl_3$); CD (EtOH, *c* 1.9×10^{-4} M; Δε) λ_{max} 226 (–1.4), 209 (+0.3); ^1H NMR data (pyridine-d_5): see Table 3.6; ^{13}C NMR data (pyridine-d_5): see Table 3.7; HRESIMS: *m/z* 567.2576 $[M+Na]^+$ (calcd for $C_{30}H_{40}O_9Na$, 567.2570).

5.4.19. Compound **52**

Amorphous powder; $[\alpha]_D^{21}$ –64.0 (*c* 0.9, $CHCl_3$); CD (EtOH, *c* 1.9×10^{-4} M; Δε) λ_{max} 225

(–2.3), 209 (–0.5); ^{1}H NMR data (pyridine-d_5): see Table 3.6; ^{13}C NMR data (pyridine-d_5): see Table 3.7; HRESIMS: *m/z* 567.2579 $[M+Na]^+$ (calcd for $C_{30}H_{40}O_9Na$, 567.2570).

5.4.20. Compound **53**

Amorphous powder; $[\alpha]_D^{18}$ –23.3 (*c* 0.24, MeOH); ^{1}H NMR data (pyridine-d_5): see Table 3.6; ^{13}C NMR data (pyridine-d_5): see Table 3.7; HRESIMS: *m/z* 543.1984 $[M+K]^+$ (calcd for $C_{27}H_{36}O_9K$, 543.1996).

5.4.21. Compound **54**

Amorphous powder; $[\alpha]_D^{21}$ –34.6 (*c* 0.3, MeOH); ^{1}H NMR data (pyridine-d_5): see Table 3.6; ^{13}C NMR data (pyridine-d_5): see Table 3.7; HRESIMS: *m/z* 543.2007 $[M+K]^+$ (calcd for $C_{27}H_{36}O_9K$, 543.1996).

5.4.22. Compound **55**

Amorphous powder; $[\alpha]_D^{21}$ –11.1 (*c* 1.1, $CHCl_3$); ^{1}H NMR data (pyridine-d_5): see Table 3.6; ^{13}C NMR data (pyridine-d_5): see Table 3.7; HRESIMS: *m/z* 555.2565 $[M+Na]^+$ (calcd for $C_{29}H_{40}O_9Na$, 555.2570).

5.4.23. Compound **56**

Amorphous powder; $[\alpha]_D^{21}$ –28.4 (*c* 0.87, MeOH); CD (EtOH, *c* 1.8×10^{-4} M; Δε) λ_{max} 225 (–3.3), 213 (–0.9); ^{1}H NMR data (pyridine-d_5): see Table 3.8; ^{13}C NMR data (pyridine-d_5): see Table 3.9; HRESIMS: *m/z* 569.2715 $[M+Na]^+$ (calcd for $C_{30}H_{42}O_9Na$, 569.2727).

5.4.24. Compound **57**

Amorphous powder; $[\alpha]_D^{21}$ –64.5 (*c* 0.96, MeOH); CD (EtOH, *c* 1.8×10^{-4} M; Δε) λ_{max} 224 (–4.2), 213 (–2.4); ^{1}H NMR data (pyridine-d_5): see Table 3.8; ^{13}C NMR data (pyridine-d_5): see Table 3.9; HRESIMS: *m/z* 547.2899 $[M+H]^+$ (calcd for $C_{30}H_{43}O_9$, 547.2907).

5.4.25. Compound **58**

Amorphous powder; $[\alpha]_D^{21}$ –32.2 (*c* 0.28, MeOH); ^{1}H NMR data (pyridine-d_5): see Table 3.8; ^{13}C NMR data (pyridine-d_5): see Table 3.9; HRESIMS: *m/z* 529.2394 $[M+Na]^+$ (calcd for $C_{27}H_{38}O_9Na$, 529.2414).

5.4.26. Compound **59**

Amorphous powder; $[\alpha]_D^{19}$ –41.0 (*c* 0.5, MeOH); ^{1}H NMR data (pyridine-d_5): see Table 3.8; ^{13}C NMR data (pyridine-d_5): see Table 3.9; HRESIMS: *m/z* 507.2597 $[M+H]^+$ (calcd for $C_{27}H_{39}O_9$, 507.2594).

5.4.27. Compound **60**

Amorphous powder; $[\alpha]_D^{16}$ –14.8 (*c* 0.25, MeOH); ^{1}H NMR data (pyridine-d_5): see Table 3.8; ^{13}C NMR data (pyridine-d_5): see Table 3.9; HRESIMS: *m/z* 557.2733 $[M+Na]^+$ (calcd for $C_{29}H_{42}O_9Na$, 557.2727).

5.4.28. Compound **61**

Amorphous powder; $[\alpha]_D^{20}$ –32.1 (*c* 0.87, MeOH); ^{1}H NMR data (pyridine-d_5): see Table 3.8; ^{13}C NMR data (pyridine-d_5): see Table 3.9; HRESIMS: *m/z* 557.2748 $[M+Na]^+$ (calcd for $C_{29}H_{42}O_9Na$, 557.2727).

5.4.29. Compound **62**

Amorphous powder; $[\alpha]_D^{21}$ –19.3 (*c* 0.61, $CHCl_3$); ^{1}H and ^{13}C NMR data (pyridine-d_5): see Table 3.10; HRESIMS: *m/z* 485.2148 $[M+Na]^+$ (calcd for $C_{25}H_{34}O_8Na$, 485.2151).

5.4.30. Compound **63**

Amorphous powder; $[\alpha]_D^{22}$ –70.8 (*c* 0.16, MeOH); ^{1}H and ^{13}C NMR data (pyridine-d_5): see Table 3.10; HRESIMS: *m/z* 513.2460 $[M+Na]^+$ (calcd for $C_{27}H_{38}O_8Na$, 513.2464).

5.4.31. Compound **64**

Amorphous powder; $[\alpha]_D^{22}$ –53.9 (*c* 0.22, MeOH); ^{1}H and ^{13}C NMR data (pyridine-d_5): see Table 3.10; HRESIMS: *m/z* 571.2872 $[M+Na]^+$ (calcd for $C_{30}H_{44}O_9Na$, 571.2883).

5.4.32. Compound **65**

Amorphous powder; $[\alpha]_D^{19}$ +38.7 (*c* 0.15, MeOH); CD (EtOH, *c* 1.9×10^{-4} M; $\Delta\varepsilon$) λ_{max} 231 (–3.4), 206 (+16.8); ^{1}H and ^{13}C NMR data (pyridine-d_5): see Table 3.11; HRESIMS: *m/z* 555.2340 $[M+K]^+$ (calcd for $C_{29}H_{40}O_8K$, 555.2360).

5.4.33. Compound **66**

Amorphous powder; $[\alpha]_D^{21}$ +10.1 (*c* 0.29, MeOH); CD (EtOH, *c* 1.9×10^{-4} M; $\Delta\varepsilon$) λ_{max} 230 (–3.9), 206 (+17.8); ^{1}H and ^{13}C NMR data (pyridine-d_5): see Table 3.11; HRESIMS: *m/z*

539.2604 $[M+Na]^+$ (calcd for $C_{29}H_{40}O_8Na$, 539.2621).

5.4.34. Compound **67**

Amorphous powder; $[\alpha]_D^{20}$ +32.0 (*c* 0.24, MeOH); ^1H and ^{13}C NMR data (pyridine-d_5): see Table 3.11; HRESIMS: *m/z* 527.2631 $[M+Na]^+$ (calcd for $C_{28}H_{40}O_8Na$, 527.2621).

5.4.35. Compound **68**

Amorphous powder; $[\alpha]_D^{20}$ +20.0 (*c* 0.28, MeOH); ^1H and ^{13}C NMR data (pyridine-d_5): see Table 3.12; HRESIMS: *m/z* 485.2150 $[M+Na]^+$ (calcd for $C_{25}H_{34}O_8Na$, 485.2151).

5.4.36. Compound **69**

Amorphous powder; $[\alpha]_D^{22}$ +32.4 (*c* 0.11, MeOH); ^1H and ^{13}C NMR data (pyridine-d_5): see Table 3.12; HRESIMS: *m/z* 485.2149 $[M+Na]^+$ (calcd for $C_{25}H_{34}O_8Na$, 485.2151).

5.5. Biological evaluation

5.5.1. Cell lines and cultures

KB (human epidermoid carcinoma of the nasopharynx) cells, MCF7 (breast carcinoma), A549 cells (human lung carcinoma) and HeLa cells (human uterine carcinoma) were obtained from the RIKEN Bioresource Center (RIKEN). Multidrug-resistant human epidermoid carcinoma KB-C2 cells were kindly provided by Prof. Shin-ichi Akiyama (Kagoshima University, Japan). KB cells, A549 cells and HeLa cells were cultured in Dulbecco's modified Eagle's medium (DMEM) with 10% fetal bovine serum (FBS). KB-C2 cells were maintained in DMEM medium in the presence of 10% FBS and 5 μM colchicine. MCF7 cells were cultured in RPMI1640 supplemented with 10% FBS. All cells were incubated at 37ºC in a humidified atmosphere with 5% CO_2–95% air

5.5.2. Cytotoxicity assay

Cells were seeded at each density (5×10^4 cells/well for KB and KB-C2, 5×10^4 cells/well for MCF7, or 10×10^4 cells/well for A549 and HeLa) in 96-well plate and pre-incubated for 24 h. Test samples were dissolved in small amount of DMSO and diluted in the appropriate culture medium (final concentration of DMSO < 0.5%). After removal of pre-incubated culture medium, 100μL of medium containing various concentration (0.1, 0.5, 2, 2.5, 5, 10, 50 and 100 μg/mL) of test compound were added and further incubated for 48 h. Cell viability was determined by 3-(4,5-dimethylthiazole-2-yl)-2,5-diphenyltetrazolium bromide (MTT) colorimetric assay [65]. IC_{50} values (concentration in μg/mL required to inhibit cell

viability by 50%) were calculated using the concentration-inhibition curve. Cytotoxic activities are shown as mean ± SE from three or four experiments.

Acknowledgements

First, I would like to express my sincere gratitude to my supervisor, Prof. Yoshiki Kashiwada, for his helpful support and considerable encouragement in my research.

I owe my heartfelt gratitude to ex-professor Yoshihisa Takaishi (Vice President of the University of Tokushima) for his kind guidance and construction advice.

I am deeply grateful to Prof. Han-Dong Sun for giving me the opportunity to study in his laboratory and supporting my study and life in China.

Special thanks also to Dr. Wie-Lie Xiao and Dr. Jian-Xin Pu, Ms. Xue Du and Ms. Ming-Hong Zhang for their helpful and invaluable guidance, assistances and support my work and life in China.

I would like to offer my special thanks to all of the students of Professor Sun's laboratory, especially, Dr. Wei-Guang Wang and Mr. Yi-Ming Shi, for their cordial support and deep friendship.

I am indebt to Mr. Syuji Kitaike, Mr. Hitoshi Iida (Central Instrument Room) and Mr. Kiyoshi Imabayashi (Medicinal herb garden) for their kind assistances.

This work was supported by Otsuka Yoshimitsu Scholarship.

I would like to express my greatest appreciation to all the people of the Laboratory of Pharmacognosy, especially Dr. Juan Xiong, Dr. Fakhruddin Ali Ahmed, Dr. Sang-Yong Kim, Dr. Hisako Sasaki, Miss Yuka Omichi, Mr. Yosuke Shinozaki, Miss Emiko Shibayama, Mr. Tomohiko Sekita, Mr. Masatoshi Taniguchi, Mr. Noriyuki Watanabe, Mr. Yasuhiro Joko, Mr. Shin Kitaoka, Miss Kaori Sado, Mr. Yoshihiro Suyama and Miss Saki Ichikawa and so on, for meaningful discussion, their huge help, considerable encouragement and wonderful days.

Finally, I would like to my cordial gratitude to my parents, Toshio Kurimoto and Yasuyo Kurimoto, for their tremendous support and warm encouragement to date.

References and notes

[1] Newman, D.J.; Cragg, G.M. *J*. *Nat*. *Prod*. **2012**, *75*, 311-335.

[2] Seinney, D.C.; Anthony, J. *Nat*. *Rev*. *Drug Discovery* **2011**, *10*, 507-519

[3] Li, H.L.; Liu, T.S.; Huang, T.C.; Koyama, T.; DeVol, C.E. "Flora of Taiwan", Epoch Publishing Co., Ltd., Taipei Taiwan, **1977**, *3*, 547.

[4] Kashiwada, Y.; Fujioka, T.; Chang, J.-J.; Chen, I.-S.; Mihashi, K.; Lee, K.-H. *J*. *Org*. *Chem*. **1992**, *57*, 6946-6953.

[5] Fujioka, T.; Sakurai, A.; Mihashi, K.; Kashiwada, Y.; Chen, I.-S.; Lee, K.-H. *Chem*. *Pharm*. *Bull*. **1997**, *45*, 68-74.

[6] Fujioka, T.; Sakurai, A.; Mihashi, K.; Kashiwada, Y.; Chen, I.-S.; Lee, K.-H. *Chem*. *Pharm*. *Bull*. **1997**, *45*, 202-206.

[7] Kashiwada, Y.; Fujioka, T.; Mihashi, K.; Chen, I-.S.; Katayama, H.; Ikeshiro, Y.; Lee, K.H. *J*. *Nat*. *Prod*. **1997**, *60*, 1105-1114.

[8] Xie, B.-J., Yang, S.-P., Chen, H.-D., Yue, J.-M. *J*. *Nat*. *Prod*. **2007**, *70*, 1532-1535.

[9] Jolad, S.D.; Hoffman, J.J.; Schram, K.H.; Cole, J.R. *J*. *Org*. *Chem*. **1981**, *46*, 4085-4088.

[10] Hisham, A.; Ajitha, B.M.D.; Fujimoto, Y.; Hara, N.; Shimada, H. *Magn*. *Reson*. *Chem*. **1996**, *34*, 146-150.

[11] Su, B-.N.; Chai, H.; Mi, Q.; Riswan, S.; Kardono, L.B.S.; Afriastini, J.J.; Santarsiero, B.D.; Mesecar, A.D.; Fransworth, N.R.; Cordell, G.A.; Swanson, S.M.; Kinghorn, A.D. *Bioorg*. *Med*. *Chem*. **2006**, *14*, 960-972.

[12] Xu, Y.J., Imiyabir, Z.; Lai, Y.H.; Vittal J.J.; Goh, S.H. *ACGC Chemical Research Communications* **2001**, *13*, 37-41.

[13] Rogers, L.L., Zeng, L., McLaughlin, J.L. *J*. *Org*. *Chem*. **1998**, *63*, 3781-3785.

[14] Fraga, B.M.; González, P.; Hernández, M.G.; Suárez, S. *Tetrahedron* **1999**, *55*, 1781-1792.

[15] Breen, G.J.; Ritche, E.; Sidwell, W.T.L.; Taylor, W.C. *Aust*. *J*. *Chem*. **1966**, *19*, 455-481.

[16] Chan, W.R.; Taylor, D.R.; Yee, T.H. *J*. *Chem*. *Soc*. *C : Organic*. **1971**, *15*, 2662-2667.

[17] Lyons, C.W.; Taylor, D.R. *J*. *Chem*. *Soc*., *Chem*. *Commun*. **1975**, *13*, 517-518.

[18] Kashiwada, Y.; Fujioka, T.; Mihashi, K.; Marubayashi, N.; Mizuki, K.; Chen I.-S.; Lee, K.-H. *J*. *Nat*. *Prod*. **1995**, *58*, 495-503.

[19] Inada, A.; Murata, H.; Inatomi, Y.; Nakanishi, T.; Darnaedi, D. *Phytochemistry* **1997**, *45*, 1225-1228.

[20] Biswas, K.; Chattopadhyay, I.; Banerjee, R.K.; Bandyopadhyay, U. *Curr. Sci*. **2002**, *82*, 1336-1345.

[21] Paul, R.; Prasad, M.; Sah, N. K. *Canc*. *Biol*. *Ther.* **2011**, *12*, 467-476.

[22] Atawodi, S.E.; Atawodi, J.C. *Phytochem*. *Rev*. **2009**, *8*, 601-620.

[23] Siddiqui, S. *Curr*. *Sci*. **1942**, *11*, 278-279.

[24] Koul, O.; Isman, M.B.; Ketkar, C.M. *Can*. *J*. *Bot*. **1990**, *68*, 1-11.

[25] Champagne, D. E.; Koul, O.; Isman, M.B.; Scudder, G.G.E.; Towers, G.H.N. *Phytochemistry* **1992**, *31*, 377-394.

[26] Siddiqui, B.S.; Ghiasuddin, S.F.; Siddiqui. S. *Phytochemistry* **1992**, *31*, 4275-4278.

[27] Siddiqui, B.S.; Rasheed, M.; Ghiasuddin, S.F.; Naqvi, S.N.H.; Tariq, R.M. *Tetrahedron* **2000**, *56*, 3547-3551.

[28] Chianese, G.; Yerbanga, S.R.; Lucantoni, L.; Habluetzel, A.; Basilico, N.; Taramelli, D.; Fattorusso, E.; Taglialatela-Scafati, O. *J*. *Nat*. *Prod*. **2010**, *73*, 1448-1452.

[29] Butterworth, J.H.; Morgan, E.D. *J*. *Chem*. *Soc*., *Chem*. *Commun*. **1968**, 23-24.

[30] Govindachari, T.R. *Curr. Sci*. **1992**, *63*, 117-122.

[31] Siddiqui, S.; Mahmood, T.; Faizi, S.; Siddiqui, B.S. *J*. *Chem*. *Soc*., *Perkin Trans*.*1* **1987**, 1429-32.

[32] Siddiqui, S.;Siddiqui, B.S.; Faizi, S.; Mahmood, T. *J*. *Chem*. *Soc*. *Pak*. **1986**, *8*, 341-347.

[33] Siddiqui, S.; Faizi, S.; Mahmood, T.; Siddiqui, B.S. *J*. *Chem*. *Soc*., *Perkin Trans*.*1* **1986**, 1021-1025.

[34] Siddiqui, S.; Siddiqui, B.S.; Faizi, S. *Planta Med*. **1985**, *51*, 478-480.

[35] Siddiqui, S.; Mahmood, T.; Siddiqui, B.S.; Faizi, S. *Pak*. *J*. *Sci*. *Ind*. *Res*. **1985**, *28*, 1-4.

[36] Siddiqui, S.; Faizi, S.; Siddiqui, B.S. *Heterocycles* **1984**, *22*, 295-298.

[37] Siddiqui, S.; Faizi, S.; Siddiqui, B.S.; Ghiasuddin *J*. *Nat*. *Prod*. **1992**, *55*, 303-310.

[38] Lavie, D.; Jain, M.K.; Shpan-Gabrielith, S.R. *Chem*. *Comm*. **1967**, 910-911.

[39] Hu, J-.F.; Fan, H.; Wang, L-.J.; Wu, S-.B.; Zhao, Y. *Phytochemistry Lett*. **2011**, *4*, 292-297.

[40] Puripattanavong, J.; Weber, S.; Brecht, V.; Frahm, A.W. *Planta Med*. **2000**, *66*, 740-745.

[41] Xu, G-.H.; Kim, J-.A.; Kim, S-.Y.; Ryu, J-.C.; Kim, Y-.S.; Jung, S-.H.; Kim, M-.K.; Lee, S-.H. *Chem*. *Pharm*. *Bull*. **2008**, *56*, 839-842.

[42] Biavatti, M.W.; Vieira, P.C.; da Silva, M.F.G.F.; Fernandes, J.B.; Albuquerque, S. *J*. *Nat*. *Prod*. **2002**, *65*, 562-565.

[43] Nakanishi, T.; Inada, A.; Lavie, D. *Chem*. *Pharm*. *Bull*. **1986**, *34*, 100-104.

[44] Yaguchi, Y.; Sakurai, N.; Nagai, M.; Inoue, T. *Chem*. *Pharm*. *Bull*. **1988**, *36*, 1419-1424.

[45] Fetizon, M.; Golfier, M. *C*. *R*. *Acad*. *Sc*. *Paris*. *Serie C*. **1968**, *267*, 900-903.

[46] Balogh, V.; Fetizon, M.; Golfier, M. *J*. *Org*. *Chem*. **1971**, *36*, 1339-1341.

[47] Shang, X.; He, X.; He, X.; Li, M.; Zhang, R.; Fan, P.; Zhang, Q.; Jia, Z. *J*. *Ethnopahrmacology* **2010**, *128*, 279-313.

[48] Ministry of Health and Welfare of Japan, The Japanese Pharmacopoeia, 16th ed. 2011, Tokyo (in Japanese).

[49] Pharmacopeia Commission, Ministry of Public Health, Pharmacopeia of the People's Republic in China. Part 1, **2000**, Beijing (in Chinese).

[50] Awad, R.; Arnason, J.T.; Trudeau, V.; Bergeron, C.; Budzinski, J.W.; Foster, B.C. *Phytomedicine* **2003**, *10*, 640-649.

[51] Wang, T.S.; Wang, S.Q.; Xiao, D.L. *J*. *Med*. *Plants Res*. **2012**, *6*, 4259-4275.

[52] Sun, H-.D.; Qiu, S-.X.; Lobkovsky, E.B.; Lin, L-.Z.; Fransworth, N.R.; Clardy, J.; Fong, H.H.S. *Tetrahedron* **2001**, *57*, 65-70.

[53] Rodríguez, B.; Jimeno, M.L. *Magn*. *Reson*. *Chem*. **2004**, *42*, 605-616.

[54] SDBS, http://sdbs.db.aist.go.jp/sdbs/cgi-bin/direct_frame_top.cgi

[55] Jarvis, B.B.; Pena, N.B.; Cömezóglu, N.; Rao, M.M. *Phytochemistry* **1986**, *25*, 533-535.

[56] Abe, F.; Nagao, T.; Okabe, H. *Biol*. *Pharm*. *Bull*. **2002**, *25*, 920-922.

[57] Kusumi, T.; Yabuuchi, T.; Takahashi, H.; Ooi, T. *J*. *Synth*. *Org*. *Chem*. *Jpn*. **2005**, *63*, 1102-1114.

[58] Kobayashi, M.; Okamoto, T.; Hayashi, K.; Yokoyama, N.; Sasaki, T.; Kitagawa, I. *Chem*. *Pharm*. *Bull*. **1994**, *42*, 265-270.

[59] Piao, S.J.; Zhang, H.J.; Lu, H.Y.; Yang, F.; Jiao, W.H.; Yi, Y. H.; Chen, W.S.; Lin, H.W. *J*. *Nat*. *Prod*. **2011**, *74*, 1248-1254.

[60] Raccuglia, R.A.; Bellone, G.; Loziene, K.; Piozzi, F.; Rosselli, S.; Maggi, A.; Bruno, M.; Simmonds, M.S.J. *Phytochemistry* **2010**, *71*, 2087-2091.

[61] Abe, S.; Tanaka, N.; Kobayashi, J.; *J*. *Nat*. *Prod*. **2012**, *75*, 484-488.

[62] Miyaichi, Y.; Kizu, H.; Yamaguchi, Y,; Tomimori, T. *Yakugaku Zasshi* **1994**, *114*, 264-271.

[63] Hussein, A.A.; de la Torre, M.C.; Jimeno, M-.L.; Rodríguez, B.; Bruno, M.; Piozzi, F.; Servettaz, O. *Phytochemistry* **1996**, *43*, 835-837.

[64] Rodríguez, B.; de la Torre, M.C.; Jimeno, M-.L.; Bruno, M.; Vassallo, N.; Bondì, M.L.; Piozzi, F.; Servettaz, O. *J*. *Nat*. *Prod*. **1997**, *60*, 348-355.

[65] Mosmann, T. *J*. *Immunol*. *Methods*, **1983**, *65*, 55-63.